Boston University Theses & Dissertations

2024

Hematopoiesis in the lung: from development to adulthood

BOSTON UNIVERSITY

SCHOOL OF MEDICINE

Dissertation

HEMATOPOIESIS IN THE LUNG: FROM DEVELOPMENT TO ADULTHOOD

By

ANTHONY KOK WAI YEUNG

B.S., University of California Los Angeles, 2012

Submitted in partial fulfillment of the

requirements for the degree of

Doctor of Philosophy

2022

Approved by

First Reader ____

George J. Murphy, Ph.D.

Associate Professor of Medicine

Second Reader ____

Finn J. Hawkins, M.B. B.Ch.

Assistant Professor of Medicine

DEDICATION

I dedicate this work to my parents, who have always supported me in pursuit of my dreams and passions; and to my dog, Parker, for whom I work tirelessly to provide the best life a good boy can have.

ACKNOWLEDGEMENTS

To my mentors – I am eternally grateful to each and every one of you for building me up to be the budding scientist I am today. To my PI, Dr. George Murphy, your passion for science and mentorship is perfectly balanced with your drive to first and foremost be a conscientious citizen. Your incredible selflessness, compassion, and endless devotion to others is a trait that I so deeply admire. I hope that I can carry on your legacy and make you proud someday. To my mini-PI, Dr. Kim Vanuytsel, whom I will forever and always be the biggest fan of. Together with George, you taught me what it truly means to perform science with great care and precision. You so generously offered so much of your knowledge and expertise to help shepherd me towards success. To the MD/PhD program co-directors, Dr. Trinkaus-Randall and Dr. Borkan, for first putting your faith in my ability to succeed on this physician scientist path and for continually supporting me on this long and arduous journey. To Dr. Anna Engler, Dr. Camille Edwards, Dr. Rhiannon Werder, and Dr. Anna Belkina for blessing me with so much of your scientific and medical knowledge. To my former mentors Dr. Reggie Edgerton and Dr. Guillermo Garcia-Alias for recognizing my potential and opening my eyes to this career path. To my committee, Dr. Lee Quinton, Dr. Andrew Larry Frelinger, Dr. Katya Ravid and Dr. Finn Hawkins, thank you all for all the insight you have provided and for being so supportive of me during this process.

To my friends and colleagues – I am so lucky to have the best labmates I could ever ask for. Rich, Greg, Sara, Sabrina, Todd, Alex, Charith, Vikram, Mira, Yvonne – you are the reason I walked into lab with a smile on my face every day. I will miss our legendary Murphy Lab lunches. To Neelou, my grad school partner in crime, we are simultaneously polar opposites yet perfectly matched to make this absurd dynamic duo (plus Brian makes a chaotic triumvirate). I will always cherish our bond and cannot wait to see where this journey takes us. To Brian, Allison and all the other Glitter/Egg med school buddies, each of you have enriched my life with so much joy. To Dhithya, Chaleena, Joanna, Jackie, Sarah and all my other west coast (best coast) buddies, you all keep me grounded and remind me of what pure unabashed happiness feels like.

To all the mice and sample donors who made this research and my thesis work possible, I am grateful for your contributions to science and my training.

To my family – my mom, dad, and 2 brothers, thank you for your unconditional love. You are the steady bridge of support I need to achieve the goals I have set for myself. To my dog, Parker, whom I welcomed into my life at the beginning of my PhD training, arguably the best decision I made during my time here. You have brought so much love and comfort into my life and the lives of everyone around us.

HEMATOPOIESIS IN THE LUNG: FROM DEVELOPMENT TO ADULTHOOD

ANTHONY KOK WAI YEUNG

Boston University School of Medicine

Ph.D. degree requirements completed in 2022

Dual M.D./Ph.D. degrees expected in 2024

Major Professor: George J. Murphy, Ph.D., Associate Professor of Medicine

ABSTRACT

Megakaryocytes (MK) are responsible for platelet biogenesis, which is thought to occur canonically in the adult bone marrow (BM) and in the fetal liver during development. However, emerging evidence highlights the lung as a previously underappreciated residence for MKs that may significantly contribute to circulating platelet mass. While a diversity of cells specific to the BM are known to promote the maturation and trafficking of MKs, little investigation into the impact of the lung niche on the development and function of MKs has been done. Here, we describe the application of single cell RNA sequencing (scRNA-Seq) coupled with histological, ploidy and flow cytometric analyses to profile primary MKs derived from syngeneic mouse lung and hematopoietic tissues. Transcriptional profiling demonstrated that lung MKs have a unique signature distinct from their hematopoietic counterparts with lung MKs displaying enrichment for maturation markers, potentially indicating a propensity for more efficient platelet production.

Reciprocally, fetal lung MKs also showed the robust expression of cytokines and growth factors known to promote lung development. Lastly, lung MKs possess an enrichment profile skewed towards roles in immunity and inflammation. These findings highlight the existence of a lung-specific MK phenotype and support the notion that the lung plays an independent role in the development and functional maturation of MKs.

In addition to MKs, the lung houses many resident hematopoietic cells, including hematopoietic stem and progenitor cells (HSPCs). The existence of lung HSPCs suggests that the differentiation and development of lung resident hematopoietic cells may occur in-situ. To investigate the potential role the lung has in instructing site specific hematopoiesis, we employed explant cultures of murine and human fetal lungs. This displayed adherent endothelial cells transitioning into floating hematopoietic cells, suggesting that the fetal lung is a source of hemogenic endothelial cells that have the functional capacity to undergo endothelial to hematopoietic transition (EHT) to produce HSPCs. Flow cytometric and functional assessment of fetal lung explants showed the production of HSPCs that expressed key EHT and pre-HSPC markers. Expression profiles revealed by scRNA-Seq and small molecule modulation demonstrated that fetal lung EHT is reliant on canonical EHT signaling pathways. These findings suggest that functional HECs are present in the fetal lung, thus establishing this location as a potential extramedullary site of de-novo hematopoiesis. Overall, these findings suggest that the lung may have a greater role in instructing tissue specific hematopoiesis and/or overall hematopoietic development.

TABLE OF CONTENTS

LIST OF TABLES

LIST OF FIGURES

LIST OF ABBREVIATIONS

AGM..Aorta-Gonad-Mesonephros

Ang1...Angiopoietin-1

ARDS...Acute Respiratory Distress Syndrome

bFGF..Basic Fibroblast Growth Factor

BM..Bone Marrow

BSA...Bovine Serum Albumin

CFU...Colony Forming Unit

E..Embryonic Day

ECM..Extracellular Matrix

EHT...Endothelial to Hematopoietic Transition

EMP...Erythro-Myeloid Progenitor

FLT3L...FMS-Related Tyrosine Kinase Ligand

HBSS..Hanks' Balanced Salt Solution

HEC...Hemogenic Endothelial Cell

HPC...Hematopoietic Progenitor Cell

HSC...Hematopoietic Stem Cell

HSPC...Hematopoietic Stem and Progenitor Cell

IGF-1..Insulin-Like Growth Factor 1

IL6..Interleukin-6

ILCs...Innate Lymphoid Cell

LSK...$Lin^-/Sca^+/Kit^+$

MFI..Median Fluorescence Intensity

MK..Megakaryocyte

MMP14...Membrane-Type Metalloproteinase 14

NKs...Natural Killer Cell

NKX2.1...NK2 Homeobox 1

PBS...Phosphate Buffer Solution

PCA..Principal Component Analysis

PDGF...Platelet Derived Growth Factor

PDPN..Podoplanin

PSC..Pluripotent Stem Cells

RBC...Red Blood Cell

SCF..Stem Cell Factor

scRNA-Seq...Single-Cell RNA Sequencing

SDF1...Stromal-Cell-Derived Factor-1

TGFβ1...Transforming Growth Factor Beta 1

TLR..Toll Like Receptor

TPO...Thrombopoietin

UMAP ....Uniform Manifold Approximation and Projection

VECAD..Vascular Endothelial Cadherin

VEGF...Vascular Endothelial Growth Factor

VEGFA...Vascular Endothelial Growth Factor A

WK..Week

YAP..Yes Activated Protein

CHAPTER ONE: INTRODUCTION

Platelets and Megakaryocytes: Functions and Diversity

Platelets are non-nucleated cells about 2-3μm in diameter and are essential in coagulation[1]. They are derived from multinucleated megakaryocytes (MKs), which in contrast are very large, ranging from 30-100μm in diameter in humans[2,3]. Platelets are the second most abundant peripheral blood cell type, second only to erythrocytes[4]. A normal human peripheral blood platelet count typically ranges from 150,000 to 400,000 platelets per microliter of blood. In stark contrast to the abundance of platelets, MKs make up just 0.05% of the adult human bone marrow and they are even less commonly found in circulating blood. This small number of MKs is capable of producing a large number of platelets due to their ability to undergo endomitosis whereby MKs increase their size and double their nucleic content as high as 128N[3].

Considering the essential role of platelets in both aberrant and normal hemostasis, platelet counts and other platelet function tests have become a standard part of many clinical workups. It logically follows that a low platelet count, thrombocytopenia, and a high platelet count, thrombocytosis, would place a patient at an increased risk for bleeding complications and coagulopathies, respectively. However, thrombocytosis most commonly presents as reactive thrombocytosis in which an elevated platelet count is secondary to an underlying concern, often an infection, severe tissue trauma, malignancy, or inflammatory disorder[5]. In this setting, anticoagulative therapy is typically not recommended as the thrombocytosis is self-limiting and often does not increase a patient's risk for thrombotic events[5]. Some clinical studies even suggest that thrombocytosis is a positive prognostic indicator, while thrombocytopenia is a negative indicator[6–9]. These clinical findings suggest that platelets and their regulation may have more coordinated roles in the resolution of various pathologies. Working towards the goal of understanding the full potential of platelets is rooted in developing greater insight into their roles beyond hemostasis.

Platelets have been demonstrated to carry out a variety of functions. Upon tissue damage, platelets are recruited to the site of injury and upon activation will release their stored granules. These granules are enriched with various cytokines that in addition to promoting coagulation and aggregation will promote the repair process via distinct mechanisms[10,11]: Angiogenesis is supported through the release of many factors including vascular endothelial growth factor (VEGF), angiopoietin-1 (Ang1), and basic fibroblast growth factor (bFGF); Mesenchymal cell proliferation is promoted via release of cytokines like platelet derived growth factor (PDGF) and insulin-like growth factor 1 (IGF-1); Immune cell recruitment to aid in repair is induced via release and expression of inflammatory markers such as P-selectin and CD40L. Beyond the setting of tissue repair, platelets themselves have the capacity to act as immune cells in the context of both innate and adaptive immunity[12]. Platelets express various immune cell receptors and proteins such as various toll-like receptors, defensins and complement proteins. Platelets can also promote the activation and differentiation of T-cells and antigen presenting cells.

While these diverse platelet functions have been described, previous work suggests that they may not be ubiquitous across all platelets nor physiological status. Subsets of platelets based on size, density and volume have been described and suggested to confer functional differences, such as changes in ability to aggregate or coagulate[13–17]. A subset of platelets can express MHCI in response to an infectious stimuli to promote T-cell activation[18,19]. At steady state, surface expression of TLR2 and TLR4 is only found on a fraction of platelets[20]. More TLRs can be found stored within platelets and are recruited to the surface only in certain inflammatory conditions. More TLR2^{+} and TLR4^{+} platelets are found in patients with acute coronary syndrome and atrial fibrillation, suggesting these conditions may enhance their recruitment and/or expression[21,22]. However, patients with sepsis saw no significant increase in TLR expression[23]. This suggests there are subsets of platelets primed to respond to specific pathological cues. How platelets develop these unique phenotypes is not clearly understood. However, platelets are anucleated and are estimated to have about 2.20 femtograms of RNA per platelet, which is ~1000 fold lower than the average leukocyte[24]. The small amount of genomic and transcriptomic material suggests that their phenotype may be pre-determined when being produced by their parent MK.

Similar to platelets, MKs exhibit some functional diversity. 3 main subtypes of MKs have been described: platelet producing, hematopoietic stem cell (HSC) maintaining and immune. MKs have been demonstrated to support HSC homeostasis by promoting their quiescence at steady state and HSC regeneration after radioablative or chemotherapeutic injury[25,26]. A subset of MKs with low ploidy are skewed towards immune functions, exhibiting a monocyte-like phenotype with a capacity to engulf bacteria and present antigen to activate T-cells[27]. These MK subtypes preferentially reside in different locales of the BM niche[27]: Platelet producing MKs are most closely associated with the sinusoids; HSC maintaining MKs are closely associated with HSCs and are relatively much farther away from vessels; immune MKs are small, low ploidy and distant from BM sinusoids. Though often discussed in the context of the BM, MK subsets are suggested to first arise during embryonic development as evidenced by sequencing analyses of yolk sac and fetal liver derived MKs[28]. Whether these unique subtypes result in differential platelets is not known. However, an individual MK does have the capacity to coordinate the development of its own platelets. MKs can differentially sort angiogenic factors into alpha granules, which results in the production of heterogeneous platelet subsets[29–31]. In-vitro studies have also shown that MKs can process antigen on MHC class I molecules and subsequently transfer them to proplatelets[32]. Another means of introducing diversity involves emperipolesis, wherein MKs engulf a cell, primarily neutrophils, into a vacuole and exchange membrane content[33]. The engulfed cell egresses fully intact and the newly acquired membranous content is retained by the MK, which can be transferred to platelet progeny[34].

While the underlying mechanisms that result in MK and platelet heterogeneity are not well understood, these findings collectively demonstrate the diverse capabilities of MKs to interact and adapt to different environmental cues. To this end, understanding the cellular microenvironment of MKs is a critical field of research. Interestingly, many recent studies have highlighted a previously underappreciated relationship between MKs/platelets and the lung, suggesting the lung may have a unique capacity to influence megakaryopoiesis.

Lung Megakaryocytes: Fact or Fiction?

The presence of MKs in the lung was first described in 1893 by Aschoff[35]. Histological evaluation across 50 autopsies showed that MKs are found most frequently in the lung compared to the spleen, kidney, liver, and heart[36]. Work from others confirmed the increased presence of MKs specifically in the lung[37–41]. However, the majority of these findings were observed post-mortem in patients who suffered from a terminal illness, including various lung and blood pathologies. This is important to take into consideration since a hyperinflammatory state can result in a leukemoid reaction and cause hypercoagulability[42,43]. Some noted that the frequency of MKs found in the lung were significantly greater than expected to be incidentally found in the setting of leukocytosis[38]. However, this still left many unanswered questions about the lung MK landscape under steady state conditions.

Studies involving mammalian models helped to shed more light on lung MK biology. In 1937, Howell and Donahue would describe histological evidence of MKs in the lung actively producing platelets[44]. They also demonstrated in cats that blood exiting the pulmonary vasculature had a greater number of platelets, suggesting that thrombopoiesis may occur in the lung. In 1965, Kaufman et al. demonstrated in dogs that MKs traversing the venous circulation can enter the lungs to produce platelets[45]. Later, similar findings were described in human studies in which MK and platelet numbers were compared in blood sampled from the central arterial and venous vessels in patients who had undergone cardiac catheterization[46,47]. Assessments based on these studies and others resulted in a wide range of platelet contribution estimates ranging from as low as 7% to one study suggesting that all platelets are derived from the lung[48]. To date, no consensus on this estimate exists.

Despite these findings, skepticism around the existence of lung MKs as a distinct cellular population remained for many reasons. For instance, physiological stress from surgery results in an increased number of circulating MKs in humans, a finding also noted by Kaufman et al. in their dog studies[45,49]. This is important to consider as many of the studies previously described required significant surgical manipulation in order to access the lung vasculature. MKs are also very large cells averaging about 30µm in diameter, which is relatively large considering capillary diameters average around 5-10µm[50–52]. Additionally, the inherent role of MKs/platelets in coagulation requires the expression of many surface receptors involved in their adherence to endothelial cells[53]. These features make MKs a prime candidate to become unintentionally lodged in a rich capillary network like that of the lung. This is also observed in the setting of cell transplant studies wherein many cell types can become incidentally lodged in the lung after venous transfusion due to a "first-pass effect"[54]. One should note that the propensity of MKs to become lodged in the lung could have developed intentionally due to some unknown evolutionary advantage. Nevertheless, these concerns continued to persist and were further exacerbated by the difficulty of manipulating and isolating MKs, their rarity, and the historical lack of tools to overcome these barriers.

In 2017, a tremendous leap of progress was made in the investigation of lung MKs. Combining Cre-recombinase based lineage tracing with 2-photon microscopy, Lefrançais and Ortiz-Muñoz et al. utilized fluorescent intravital imaging to demonstrate that lung MKs give rise to platelets in the murine lung[55]. This was direct evidence that platelet biogenesis can occur in the lung under steady state conditions. They also quantified the average amount of platelets an individual lung MK can produce, and extrapolated this to the total lung volume. Based on this mathematical model, they estimated that about 50% of all circulating platelets are derived from lung MKs. Through the use of bulk RNA-sequencing, lung MKs were also suggested to have a profile skewed towards immune functions. This suggests that lung MKs may confer a distinct phenotype to lung-derived platelets. While this has yet to be proven, many studies have demonstrated that platelets can have a significant impact on lung physiology.

Several studies have demonstrated that platelets play a distinct role in both normal and aberrant pulmonary biology. During embryonic development, the localized release of TGFβ1 from platelets in the lung promotes the differentiation of myofibroblasts which are responsible for depositing elastin in the lung[56]. Notably, the disruption of this process results in neonatal lethality, demonstrating the critical role of platelets in normal lung development. In a pneumonectomy model of lung regeneration, platelet derived stromal-cell-derived factor-1 (SDF1/CXCl12) induces the release of membrane-type metalloproteinase MMP14 from pulmonary endothelial cells, which promotes alveolar regeneration[57]. Platelets were also demonstrated to protect the lung epithelium against severe injury by preventing cell death in the setting of Pseudomonas aeruginosa infection in mice[58]. Clinical evidence also suggests that platelets may have a protective role in the setting of acute respiratory distress syndrome (ARDS)[59]. Multiple studies assessing platelet counts in critically ill patients with ARDS suggest that thrombocytopenia may be an indicator for worse prognosis[60–62]. Beyond their protective functions, platelets have also been implicated in the progression of inflammatory and autoimmune disorders such as pulmonary fibrosis and systemic lupus erythematosus[63–65].

While many studies have implicated platelets as an important contributor to lung biology, the physiological significance of MKs residing in the lung requires further investigation. However, MKs capable of thrombogenesis is a significant addition to an already impressive list of lung resident hematopoietic populations.

Hematopoietic Residents of the Lung

Due to the lung's primary role in respiration, the lung is constantly at risk of environmental exposures. As such, the majority of resident blood cells in the lung are immune cells[66]. Within the innate immune compartment are 2 macrophage subtypes. Alveolar macrophages are localized to the surface of the alveolar epithelium; in addition to being a first line of defense, alveolar macrophages are critical in maintaining tissue homeostasis by clearing debris and regulating surfactant[67–69]. Interstitial macrophages are found within the lung parenchyma; they are important in the innate immune response and are also involved in regulating the pulmonary immune cell population to prevent hyperreactive inflammation, asthma and fibrosis[70–72]. In addition to macrophages, innate lymphoid cells (ILCs) and natural killer cells (NKs) are also involved in pathogen clearance as well as tissue repair post-injury[73]. The adaptive immune response in the lung begins with lung resident dendritic cells, which migrate to the mediastinal lymph nodes to promote the expansion and activation of T- and B-cells[74]. A chemotactic gradient promotes the migration of these cells to the lung to mount an immune response and results in the establishment of memory T- and B-cells[75–77]. These experienced lymphocytes can remain in the lung to respond to subsequent infections.

While memory lymphocytes are established in the lung in response to pathogenic exposure, the origins of other lung resident blood cells are either varied or unknown. Macrophage populations are thought to arise from 3 distinct sites of development: yolk sac, fetal liver and BM[78,79]. Notably, each subpopulation seems to preferentially occupy distinct spaces within the lung[78,80]. ILCs have been described as “sedentary”, with around 95% of ILCs found to remain resident in the lung and primarily maintained via self-renewal[81]. This suggests that lung ILCs are recruited to the lung during development and are not maintained by an external pool of circulating progenitors[73]. However, lineage studies are required to fully investigate the developmental origins of ILCs. In contrast, lung NKs and

DCs are suggested to be largely replenished from circulation[66,82]. The origins of lung MKs are unknown, although they are found both intra- and extravascularly in the lung.

Overall, the origin of lung hematopoietic populations is complex and varied. Furthermore, many of these studies did not take into consideration the existence of lung HSPCs, which were more recently described to be present in both fetal and adult lungs. In addition to phenotyping lung MKs, Lefrançais and Ortiz-Muñoz et al. demonstrated that multipotent HSPCs can be found extravascularly in the lung[55]. They furthermore demonstrated that transplantation of healthy lungs into severely thrombocytopenic c-MPL knockout mice can result in long-term reconstitution of platelets. Significant chimerism in leukocyte populations was also observed post-transplantation, suggesting that the adult murine lung is a source of functionally competent HSPCs. Fetal lungs derived from embryonic day 16 mice (E16) are also a source of HSPCs capable of long term engraftment[83]. While the origin of lung HSPCs is currently unknown, the presence of HSPCs in both the adult and fetal lung raises many interesting questions regarding the lung's influence on hematopoiesis. While lung HSPCs have the capacity to reconstitute the blood, their role in the establishment and/or maintenance of lung hematopoietic populations and overall hematopoiesis is not known. Furthermore, the hematopoietic niche is known to be important in the functionalization of local blood cells[84–86], thus the role of the lung in instructing local blood development is another important avenue of investigation.

Hypothesis and Specific Aims

We hypothesize that symbiotic interactions between MKs, hematopoietic progenitors, and the lung microenvironment aid in the development and functionalization of lung specific MKs and HSPCs.

Aim 1: Profile lung-MKs and construct a cellular map of the lung-MK niche.

Aim 2: Investigate the development of lung HSPCs and their origins.

CHAPTER TWO: LUNG MEGAKARYOCYTES DISPLAY DISTINCT TRANSCRIPTIONAL AND PHENOTYPIC PROPERTIES

Disclaimer: Portions of the text from this chapter were adapted from the following publication: Yeung, A. K., Villacorta-Martin, C., Hon, S., Rock, J. R. & Murphy, G. J. Lung megakaryocytes display distinct transcriptional and phenotypic properties. Blood Advances 4, 6204–6217 (2020). A.K.Y. performed experimental design, data collection, data analysis, interpretation of data and manuscript preparation. C.V.M. performed the bioinformatic/computational analysis and supported the experimental design and manuscript preparation. S.H. and J.R.R. performed/supported data collection. G.J.M. performed experimental design, data collection, data analysis, interpretation of data and manuscript preparation.

INTRODUCTION

Megakaryocytes (MKs) and the platelets they produce are essential for clot formation, but both are also involved in critical biological processes including development, inflammation, and regeneration[87–90]. The majority of platelet biogenesis is thought to occur canonically in the adult bone marrow (BM) and in the fetal liver during development[90]. As such, our current understanding of MK development stems predominantly from the investigation of these tissues. The presence of MKs in the lung was first described in 1893, and emerging evidence further highlights the lung as a previously underappreciated residence for MKs that may significantly contribute to circulating platelet mass[35,44,46,48,91–

[96]. Interest in lung-MKs was reinvigorated with the application of intravital 2-photon microscopy to the lungs of live mice showing de-novo platelet production and immobile MKs residing in the lung interstitium[55]. However, approximations of the absolute number of platelets being generated in the lung remains heavily debated. Residency in the lung suggests MKs are interacting with a diversity of cells that differ widely from those found in the BM. Various cells specific to the BM niche, including osteoblasts and mesenchymal stromal cells, are known to promote the maturation and trafficking of MKs to carry out platelet production[97–105]. Beyond this, the BM niche induces MKs to adopt a myriad of other functions, including BM homeostasis and viral immunity[87,106,107].

We therefore hypothesized that MK maturation in the context of the lung niche induces localized MKs to adopt a lung-specific phenotype and functional profile. The need to better understand megakaryopoiesis in this context is further highlighted by recent work demonstrating the diverse, lung-specific influence of platelets. The multi-faceted role of platelets in the lung in both health and disease includes support of embryonic pulmonary development, protection against bacterial exotoxin-induced damage to the lung epithelium, and promotion of pulmonary fibrosis[56–58,65,108]. Whether these platelets are sourced from MKs found and functionalized in the lung or BM is currently not known.

The role of platelets in inflammation and immunity is well described and continues to be a critical point of interest due to implications for human health[64,89,109,110]. While MKs alone are known to express functional toll like receptors (TLR) and produce inflammatory cytokines, our knowledge of the MK immune profile largely stems from in-vitro studies, limiting our understanding of the significance of in-vivo MKs in immunity[87]. Furthermore, involvement of BM-MKs in immunity is primarily only appreciable upon stimulation by a stressor, such as infection or sepsis[107,111–113]. In contrast, recent evidence suggests that under homeostatic conditions, lung-MKs may possess a transcriptional signature skewed towards innate immune functions[15]. Lung-MKs also have demonstrated responsiveness to pulmonary insults including bacterial pneumonia and bleomycin[55,114].

Importantly, the methodologies utilized in previous studies have significant limitations concerning the tracking and isolation of lung-MKs. These include the use of promiscuous markers of the MK-lineage[115–117], a lineage tracing model with significant off-target recombination in immune-cell populations[118,119] , as well as the use of bulk sequencing methodologies that do not allow for the identification and investigation of individual cells.

MKs are rare cells making up just 0.1% of the mouse BM, and there is a paucity of useful reagents/markers to isolate and study MK development. This led us to choose single-cell RNA Sequencing (scRNA-Seq) to transcriptionally profile lung-MKs at single cell resolution[120,121]. Furthermore, in order to profile MKs at different stages of development, we assessed both fetal and adult MKs. Flow cytometry in combination with scRNA-Seq analyses demonstrated that the majority of lung-MKs are terminally mature and possess a transcriptional and phenotypic profile that suggests they are primed for efficient platelet production. This analysis also confirmed the notion that lung-MKs have a phenotype skewed towards immunity and inflammation. These findings demonstrate the existence of a unique lung-MK phenotype and support the hypothesis that the lung microenvironment plays a critical role in the development and functionalization of MKs. The immune phenotype displayed by lung-MKs also introduces the potential role of MKs as an integral component in the immune landscape of the lung.

MATERIALS AND METHODS

Mice

10-week old and timed-pregnant C57/BL6 mice were purchased from Jackson Laboratories. All animal housing and experimental procedures were approved by the Boston University School of Medicine Institutional Animal Care and Use Committee (BUSM IACUC).

Tissue isolation and processing

Fetal tissue processing: 20 embryonic day 13 (E13) fetal mice were isolated from 3 timed-pregnant mice. The fetal liver and lung were isolated from surrounding tissue by blunt dissection and set aside in a solution of 10% characterized fetal bovine serum in Hanks' balanced salt solution (HBSS, Gibco). Using a 5mL syringe fitted with a 16-gauge needle, the fetal liver was drawn up and expelled several times to dissociate the tissue. Digested livers were filtered through a 70µm cell strainer before being resuspended in 3mL of red blood cell (RBC) lysis buffer (Sigma) for 5 minutes at 37^{o}C. For all samples, 70µm strainers were used for filtering to best accommodate the large size of MKs, which in mice average about 30µm in diameter and can be as large as 60µm[1,122]. Post-RBC lysis, cells were washed, filtered and resuspended in sort buffer (PBS with 2% RNase/DNase free BSA, Millipore). Fetal lungs were minced gently with a scalpel and placed into a digestion buffer consisting of the following: HBSS, 2.4U/mL Dispase II (Roche), 0.1% Collagenase A (Roche), and 2.5mM $CaCl_2$ (Fluka). 4mL of digestion buffer per 5 embryonic lungs was used. This digest mixture was placed on a rocker at 37^{o}C for 1-hour. Post digestion, lung samples were filtered and resuspended in RBC lysis for 1 min at 37^{o}C, then washed, filtered and resuspended in sort buffer.

Adult tissue processing: Week 10 adult C57/BL6 mice (5 Total: 3 Female and 2 Male) were anesthetized with isoflurane and euthanized by cervical dislocation. Using scissors, the abdomen was opened, and the renal and abdominal artery were cut. A thoracotomy was performed to expose the heart and lungs, and mice were perfused via the right ventricle with 5mL of PBS. Post-perfusion, lungs were removed and minced with a scalpel before being placed in a digest buffer containing the following: HBSS, 1mg/mL DNase I (Sigma), 0.5mg/mL LiberaseTM (Sigma), and 1mg/mL Elastase (Worthington). 6mL of digestion buffer per adult lung were used. This digest mixture was placed on a rocker at 37^{o}C for 30-minutes. Post digestion, lung samples were pipetted up and down with a 5mL serological pipette to dissociate tissue, filtered and resuspended in 3mL of RBC lysis for 5 min at 37^{o}C. BM was isolated from the femur and tibia as previously described[123]. In short, skin and muscle were dissected away from the femur and tibias bilaterally. Bones were crushed by mortar and pestle to expose the marrow then flushed with PBS. BM isolates were filtered and resuspended in RBC lysis then washed, filtered and resuspended in sort buffer.

Tissue Histology

Adult mice were euthanized and transcardially perfused as described above. Post-perfusion, lungs were removed and inflated via the trachea with 4% paraformaldehyde to fix inflate lungs. Fetal lungs could not be perfused and were thus placed directly into fixative. Lungs were fixed and cryoprotected overnight in sucrose and paraformaldehyde. Fixed tissue was then embedded and frozen in Optimum Cutting Temperature embedding medium. 5-6µm tissue sections were made using a cryostat and placed on slides. Sections were rinsed with PBS prior to permeabilizing and blocking in a solution of 0.4% Triton X-100 and 10% NDS. Sections were stained overnight using the following primary antibodies: rat-anti-mouse-CD41 (1:100, MWReg30, Biolegend), Armenian hamster-anti-mouse-CD42d (1:100, 1C2, Biolegend), rabbit-anti-TTF1/NKX2.1 (1:200, EP1584Y, abcam), Syrian hamster-anti-pdpn (1:100, 8.1.1, eBioscience), goat-anti-mouse-VECAD (1:100). Sections were subsequently stained with the appropriate secondary antibodies from JacksonImmuno all at 1:400 dilution: donkey-anti-rat Alexa Fluor 488, donkey-anti-rabbit Alexa Fluor 647, goat-anti-Syrian hamster Alexa Fluor 647, donkey-anti-Armenian hamster Cyanine3, donkey-anti-goat Cyanine3. Sections were counterstained with Hoechst, cover slipped and imaged on the Zeiss LSM 710-Live Duo Confocal. Post-image processing was performed using ImageJ (NIH).

Flow cytometry

A solution of 1% BSA in PBS, 5mM EDTA was used for staining and washing cells. Isolated cells were resuspended with the appropriate antibodies and stained on ice for 30 minutes. Fc-Receptor block treatment was performed using an anti-mouse CD16/32 antibody (BioLegend, Clone: 93) for 10 minutes prior to fluorescent staining. Flow cytometry was conducted on a Stratedigm S1000EXI, and FlowJo_v10.6.2 (FlowJo, LLC) software was used for analysis. Antibodies used: CD41a-BV421 (MWReg30, Biolegend), CD41a-PE (MWReg30, Biolegend), CD41a-APC (MWReg30, Biolegend), CD42d-APC (1C2, eBioscience), CD42d-PE (1C2, eBioscience), CD42d-Alexa Fluor 488 (1C2, eBioscience), CD284/TLR4-APC (SA15-21, biolegend), CD282/TLR2-APC (QA16A01, biolegend), I-A/I-E/MHCII-APC (M5/114.15.2, biolegend), CD74-Alexa Fluor 647 (In1, Biolegend).

Ploidy Assay

Pelleted cells from a BSA gradient were isolated and stained with CD41a-APC for 30 minutes on ice. Stained cells were subsequently washed and resuspended in a solution of 0.5mg/mL propidium iodide, 10% NP40, and 1% BSA in PBS then immediately analyzed by flow cytometry.

BSA Enrichment

To enrich for MKs, isolated bulk primary cells were resuspended in HBSS and gently placed on a 1.5%/3% BSA density gradient for 30 minutes at room temperature as previously described[124]. Staining of enriched MKs was adapted based on previously described methods[125].

Single cell RNA sequencing

Cell sorting for scRNA-Seq

Cell sorting was conducted on a Beckman MoFlo Coulter Astrios. Isolated primary cells were stained with CD41a-APC and resuspended in sort buffer (2% BSA in PBS) containing Calcein Blue AM (1:1000). Live-singlets and the top 1% of CD41a-APC$^+$ events were sorted into sort buffer. Cells counts and viability after sorting was confirmed by hemocytometer using trypan blue.

10x Chromium

Isolated cells were single cell captured using the 10X Genomics Chromium platform and prepared using the Single Cell 3' v3 kit. Library preparation and sequencing was done at the Boston University Microarray and Sequencing Resource (BUMSR) Core using the Illumina NextSeq 500 instrument.

Bioinformatic analysis

Reads were demultiplexed and aligned to the mouse genome assembly (GRCm38, Ensembl) with the CellRanger pipeline v.3.0.2 (10X Genomics). Further analyses were done using Seurat v. 3.1.4[126]. After inspection of the quality control metrics, cells with more than 12% of mitochondrial content or less than 800 detected genes were excluded for downstream analyses. We normalized and scaled the UMI counts using the regularized negative binomial regression (SCTransform)[127]. Following the standard procedure in Seurat's pipeline, we performed linear dimensionality reduction (PCA), and used the top 20 principal components to compute both the UMAP[128] and the clusters (Louvain method)[129] which were computed at a range of resolutions from 1.5 to 0.05 (more to fewer clusters). Adult populations were annotated using Louvain resolution 0.75, and fetal populations were annotated using Louvain resolution 0.25. The megakaryocyte populations in adult BM and lung as well as in fetal liver and lung were then combined for subsequent analyses (**Fig. 2**). Cell cycle scores and classifications were done using the Seurat method[130]. In order to annotate our samples, the same scoring method was used to calculate the enrichment in molecular signatures derived from cell types present in a previous publication[131]. The cut-offs for independent filtering[132] prior to differential expression testing required genes: a) being detected in at least 10% of the cells of either population and b) having a natural log fold change of at least 0.25 between populations. The tests were performed using Seurat's wrapper for the MAST framework[133]. For a comparison on the performance of methods for single-cell differential expression see Soneson & Robinson et al.[134]. GEO accession: GSE152574, Token: sdmtwiagzbsnfwl.

Statistical analysis

Significance for Enrichr based pathway enrichment was determined by Fisher exact test[135,136]. Significance for pairwise scRNA-Seq gene expression comparisons was determined using the MAST framework[133]. Significance for flow cytometry assays performed in triplicate was determined by student paired t-test.

RESULTS

Adult lung-MKs are localized to the alveolar interstitium of the distal lung, and fetal lung-MKs are found both intra- and extra-vascularly.

To better understand the location and the potential cellular interactions that may promote the development of a lung-MK phenotype, immunofluorescent microscopy was performed on cryosections of fetal and adult mouse lungs to visualize the niche of lung-MKs. Adult lung-MKs are preferentially localized to the distal lung within the interstitial space between adjacent alveoli (**Fig 2.1. A-C**). Additionally, multinucleated MKs were often found in close proximity to distal lung epithelial cells expressing NKX2.1 and podoplanin, which typically mark type 2 and type 1 alveolar epithelial cells, respectively. Fetal lung-MKs are found in the developing lung both intra- and extra-vascularly (**Fig 2.1. D, E**). Platelets were notably less abundant in fetal lung sections.

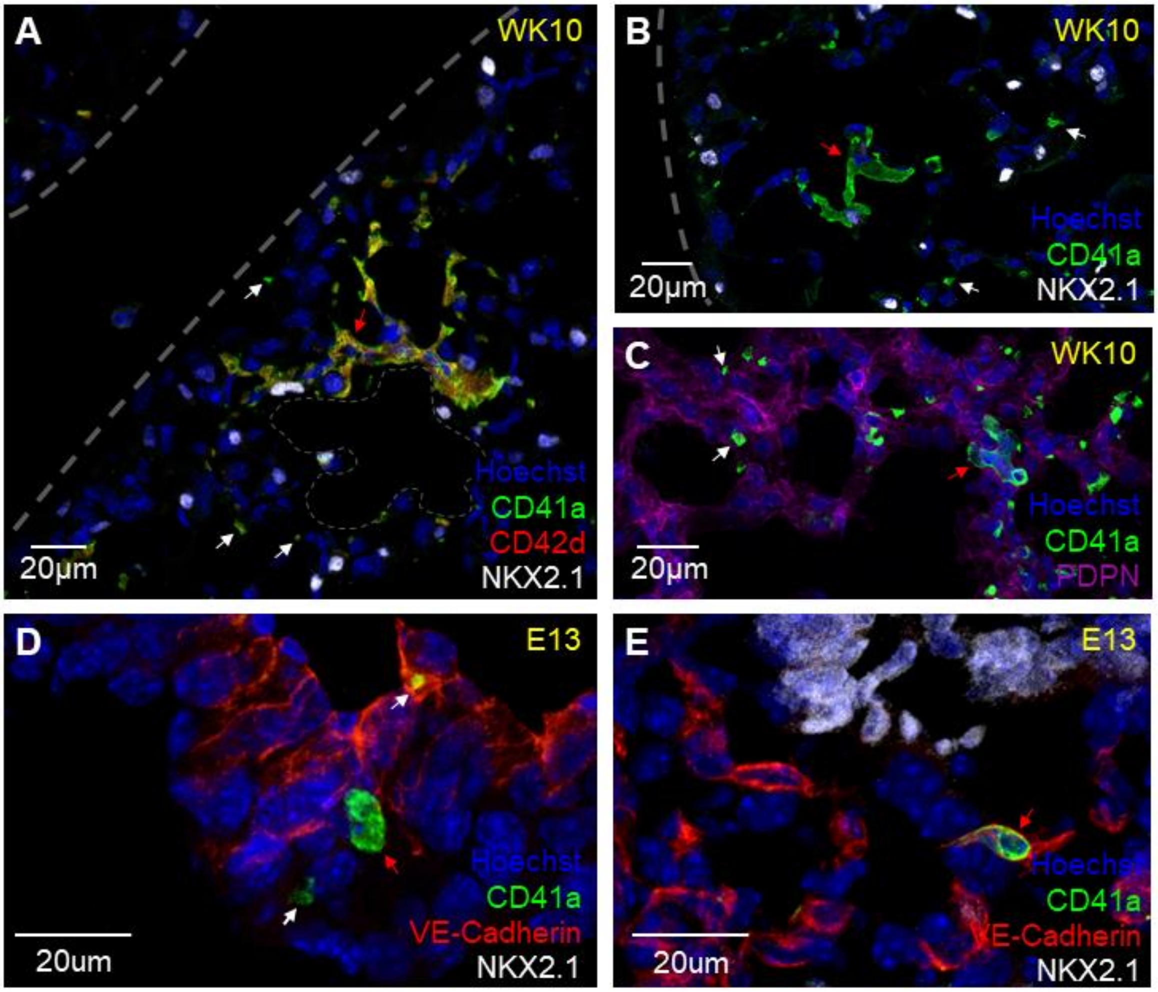

Figure 2.1 Adult lung-MKs are localized to the alveolar interstitium of the distal lung, and fetal lung-MKs are found both intra- and extra-vascularly. (A-C) Immunofluorescent staining of 5-6μm fixed-frozen WK10 adult mouse lung sections stained for markers of MKs (CD41a and CD42d), lung epithelial cells (NKX2.1), alveolar type 1 epithelial cells (PDPN), and nuclei (Hoechst). Lung borders and an alveolar airspace are outlined in gray dashed lines. Multinucleated adult lung-MKs were preferentially localized to the interstitium of the alveolar septum between neighboring alveoli. (D, E) Immunofluorescent staining of 5-6μm fixed-frozen E13 fetal mouse lung sections stained for VE-Cadherin (endothelial cell marker), CD41a, NKX2.1 and Hoechst. Fetal lung-MKs were identified in the developing lung in both extravascular (D) and intravascular (E) spaces. Platelets were notably less prevalent in the fetal lung. White and red arrows highlight platelets versus MKs, respectively.

Creation of a single-cell transcriptomic atlas of primary fetal and adult murine MKs from hematopoietic and pulmonary tissues.

The developmental trajectory of the hematopoietic and pulmonary systems involves many stages throughout embryonic and post-natal maturation[121,137,138]. To create a transcriptomic library that spans multiple stages and sites of MK development, scRNA-Seq was performed on cells isolated from fetal liver and lung, as well as adult BM and lung (**Fig. 2.2A**). Embryonic day 13 (E13) was chosen as the fetal timepoint, which is when the majority of murine hematopoietic development is occurring in the liver[124,137]. Notably, post-natal lung development continues for many weeks but begins to plateau at around week 8 in adult mice[139]. To ensure sampling of adult MKs from a developmentally stable source, week 10 (WK10) was chosen as the adult timepoint. Enrichment of MKs in all tissues was accomplished using flow cytometry to sort for CD41a^{+} cells (**Fig. 2.2B, C**). No BSA enrichment was done prior to sorting. Since CD41a is broadly expressed throughout the MK-lineage, it was chosen to ensure that MKs at various stages of development were being captured. Furthermore, based on prior publications that have assessed CD41a expression across hematopoietic cell types, we chose to gate on the top 1% of CD41a^{+} events to enhance enrichment of MK-lineage cells while still allowing for the capture of MK progenitors[115,116,140]. The gating strategy employed combined with the single cell transcriptomic profiling provides sufficient resolution to ensure accurate yet broad analysis of MKs at all development stages. Sorted MKs were also imaged to ensure that the strategy employed successfully captured nucleated MKs across a range of developmental states and not platelet aggregates (**Fig. 2.3**).

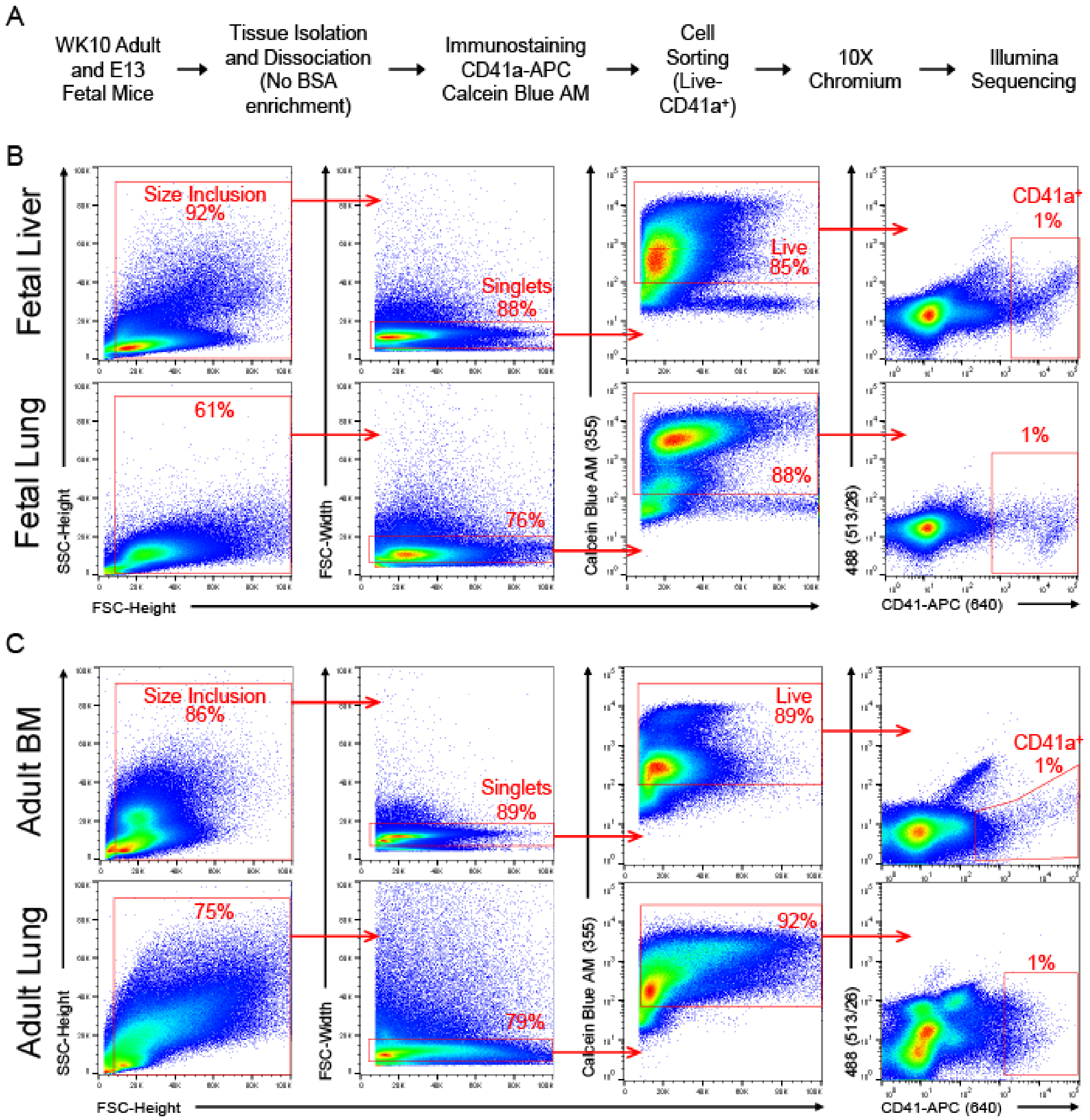

Figure 2.2. Development of a single cell transcriptomic atlas of primary murine megakaryocytes from fetal and adult mice. (A) Schematic of single cell RNA sequencing workflow. (B, C) Gating strategy utilized for flow cytometric sorting of live CD41a events. The top 1% of CD41a events were sorted for in order to preferentially enrich for MK lineage cells.

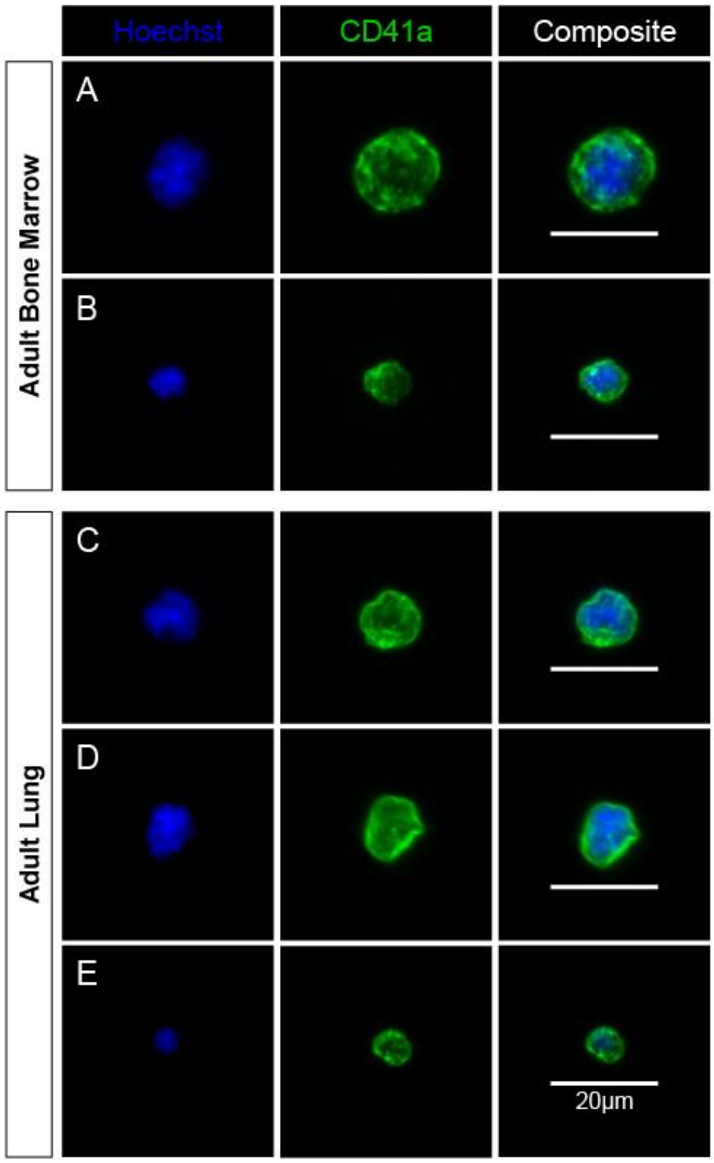

Figure 2.3. Immunofluorescent imaging of sorted MKs. Using the sorting strategy depicted in Fig. 2.2, sorted MKs were mounted onto slides and imaged using a Zeiss LSM 710 Live Duo Confocal microscope. (A E) Sorted BM and lung MKs showed membranous CD41a staining typical of putative MKs. Both tissue sources yielded larger, more mature MKs with large nuclei (A, C, D) as well as smaller MK progenitors (B, E).

Lung-MKs display a distinct transcriptional profile that is enriched for markers of maturation.

Unsupervised Uniform Manifold Approximation and Projection (UMAP) clustering was performed on sequencing datasets from fetal lungs and livers, as well as adult lungs and BM (**Fig. 2.4**, **B**). Fetal and adult MK-lineage clusters were selected based on the expression of key MK-lineage marker genes including *Fli1*, *Pf4*, and *Itga2b* (**Dashed box Fig. 2.5B, D**), and remapped (**Fig. 2.5A, C**). Fetal lung-MKs (FLu) clustered separately from fetal liver-MKs (FLiv-1 and FLiv-2) (**Fig. 2.5A**). This trend was also seen when comparing adult lung-MKs (ALu) with adult BM-MKs (ABM-1, ABM-2 and ABM-3) (**Fig. 2.5C**), highlighting the unique transcriptional profile of both fetal and adult lung-MKs. It should be noted that intra-vascular staining was not employed prior to scRNA-Seq. However, others have previously demonstrated that approximately 80% of total lung-MKs are extravascular, and our UMAP clustering resulted in 1 fetal-lung and 1 adult-lung cluster[55]. This suggests that the transcriptional profile of lung-MKs is relatively homogenous compared to BM and fetal liver MKs.

Fetal and adult MK clusters were further evaluated by performing gene expression analysis against a set of genes canonically associated with MKs at varying maturational stages (**Fig. 2.5B, D**). Fetal lung-MKs had the highest enrichment of several genes linked to MK development including *Tubb1* and *Gp1ba*, markers of functional maturation[141–143] (**Fig 2.5B**). From the adult populations, ABM-1 displayed the highest expression of MK-lineage genes, suggesting that this population represents the most mature cluster of BM resident cells (**Fig. 2.5D**). Notably, ABM-1 represents a very small fraction (4.5%) of the total MKs isolated from the BM. In contrast, the singular adult lung cluster (ALu) exhibited significantly higher expression of mature MK markers including *Tubb1* and *Gp1ba* compared to clusters ABM-2 and ABM-3. These less mature BM clusters showed significant enrichment for *Gp1bb*, a marker enriched in MK progenitor populations[144,145]. Adult lung-MKs also clustered more closely to ABM-1 (**Fig. 2.5C**), suggesting a similar maturational profile that could be indicative of priming for platelet production. Collectively, this data suggests that there is a larger proportion of terminally mature MKs residing in the fetal and adult lung as compared to the fetal liver and BM, respectively.

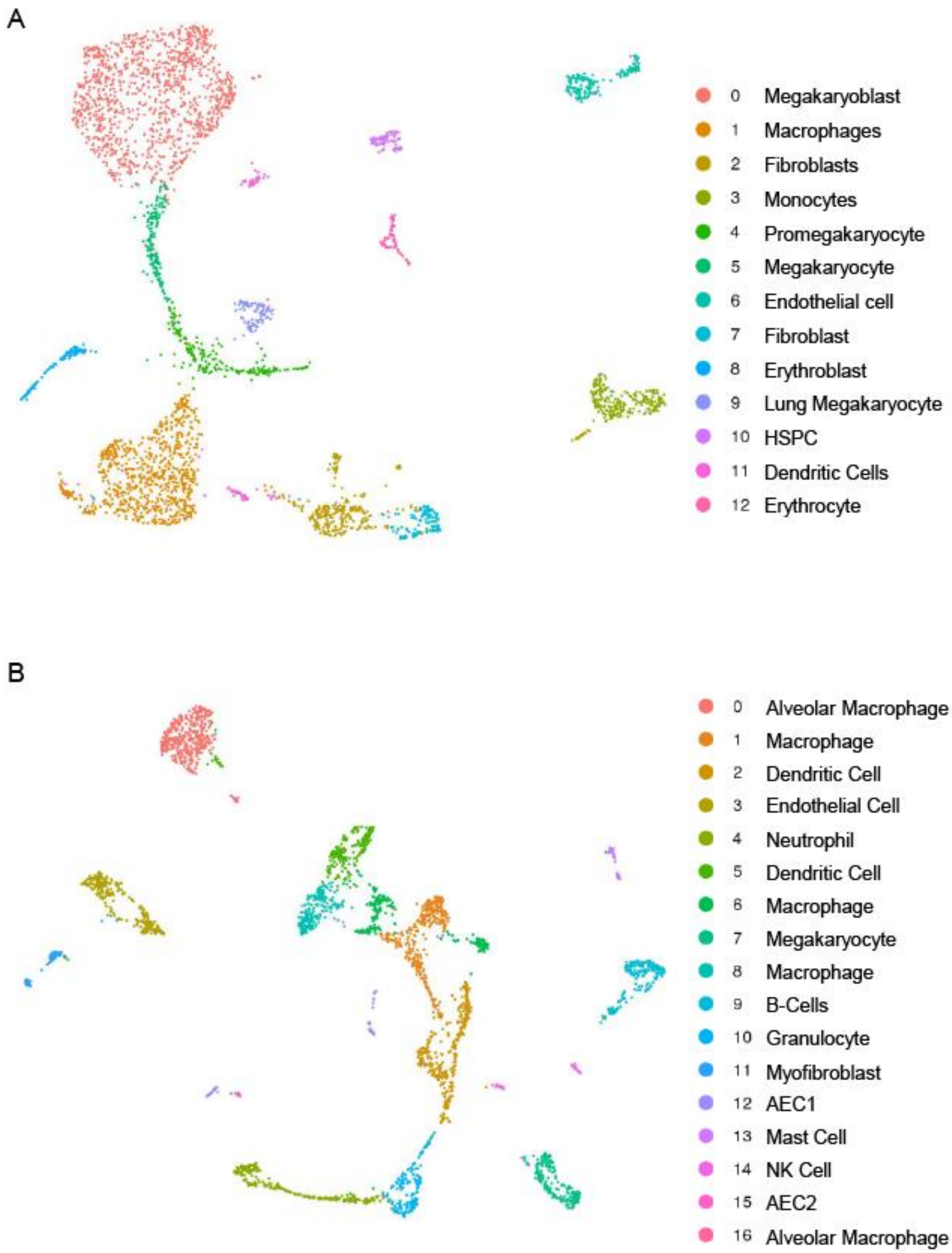

Figure 2.4. Unsupervised UMAP clustering of all sequenced cells. (A) UMAP of cells isolated from embryonic day 13 fetal livers and lungs. (B) UMAP of cells isolated from week 10 adult bone marrow and lungs.

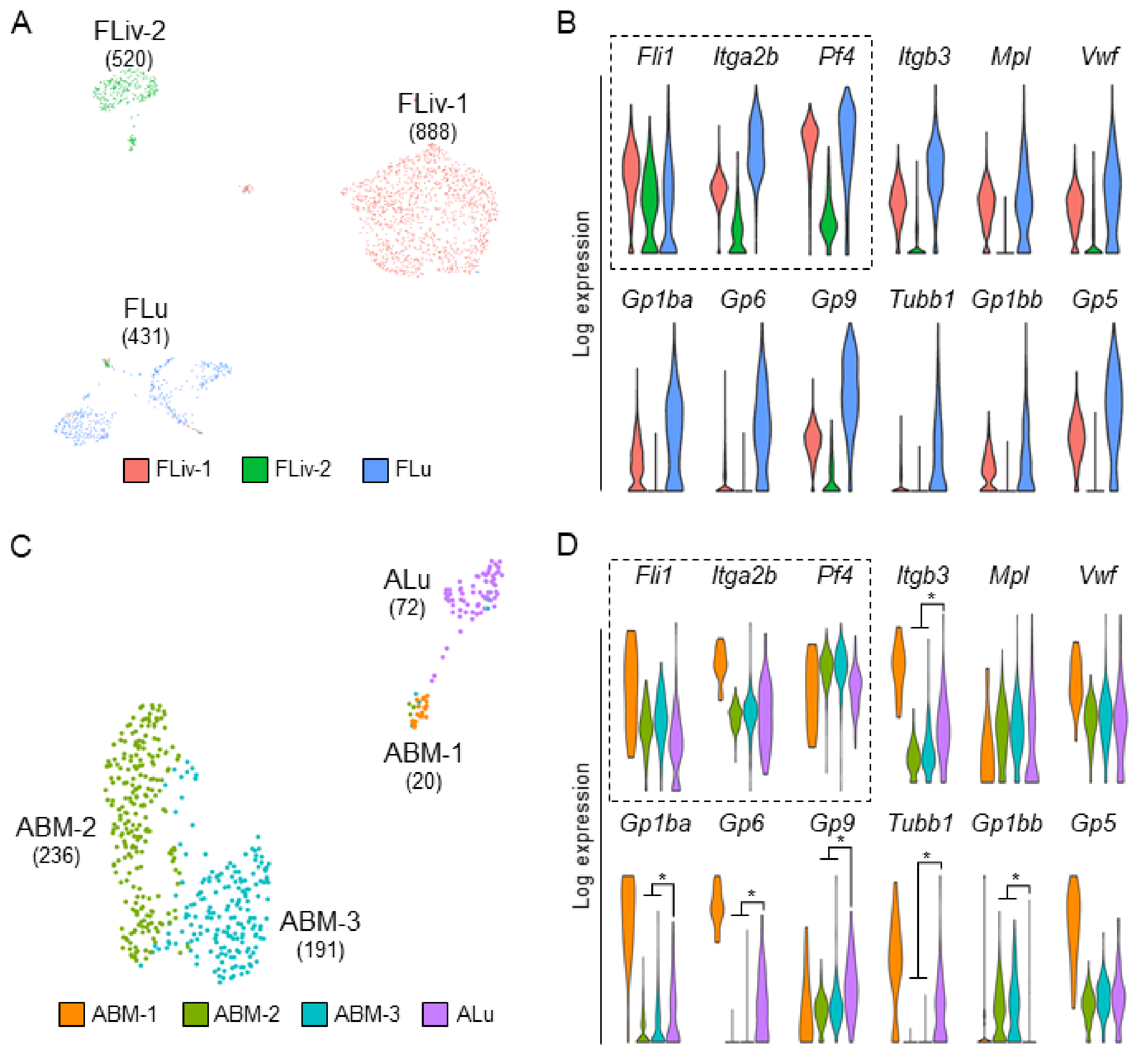

Figure 2.5. Lung-MKs are transcriptionally distinct from their hematopoietic counterparts. (A, C) UMAP clustering of MK-lineage clusters from fetal liver [FLiv-1, FLiv-2], fetal lung [FLu], adult bone marrow [ABM-1, -2, -3] and adult lung [ALu]. Fetal and adult lung-MKs clustered independently from their hematopoietic counterparts. Numbers in parentheses indicate cell counts for associated clusters. (B, D) Violin plots comparing expression of key MK genes between associated clusters. Key genes used to confirm MK lineage identity are outlined with a dashed box. Colors of violin plots in B and D correlate with their respective clusters shown in A and C, respectively. *p<0.01. Asterisks indicating significance were withheld from (B) for visual clarity.

Fetal lung-MKs display transcriptional priming for platelet and cytokine production. To further investigate the maturational development of lung-MKs, fetal MK clusters were uploaded to the KleinTools SPRING platform (https://kleintools.hms.harvard.edu/tools/spring)[146]. Visualization of fetal MK clusters with SPRING revealed a maturational trajectory of cells starting from progenitors and ending in terminally mature MKs (**Fig. 2.6A**). This trajectory plot was annotated for directionality of maturation by assessing the cell cycle phase and the intensity of expression of key lineage markers that included: *Itga2b* (CD41), *Gp1ba* (CD42b), and *Tubb1* (**Fig. 2.7A-D**). The intensity of expression of the progenitor markers *Ptprc* and *Kit* also helped determine directionality of maturation (**Fig. 2.7E, F**). 67% of the most mature clusters (**dashed box, Fig. 2.6A**) were made up of fetal lung-MKs. The top 150 genes enriched in the clusters of MKs outlined within this SPRING plot were cross referenced with the Wiki Pathways Mouse database. This analysis demonstrated an enrichment for cellular pathways important in proplatelet production, including ATP production, protein translation and cytoskeletal rearrangement (**Fig. 2.6B**). These cellular processes have been previously described to be more strongly associated with higher ploidy MKs[147]. Collectively, this suggests that fetal lung-MKs are in a more mature and metabolically active state that is primed for more efficient platelet production. Fetal-MK clusters also displayed significant upregulation of various genes coding for cytokines and growth factors that are known to be packaged into platelet granules[148–150] (**Fig. 2.6C**). Notably, fetal lung-MKs showed robust *Tgfb1* expression and lung-specific enrichment for *Igf1*, both of which have been previously demonstrated to be critical in pulmonary development[56,151–153].

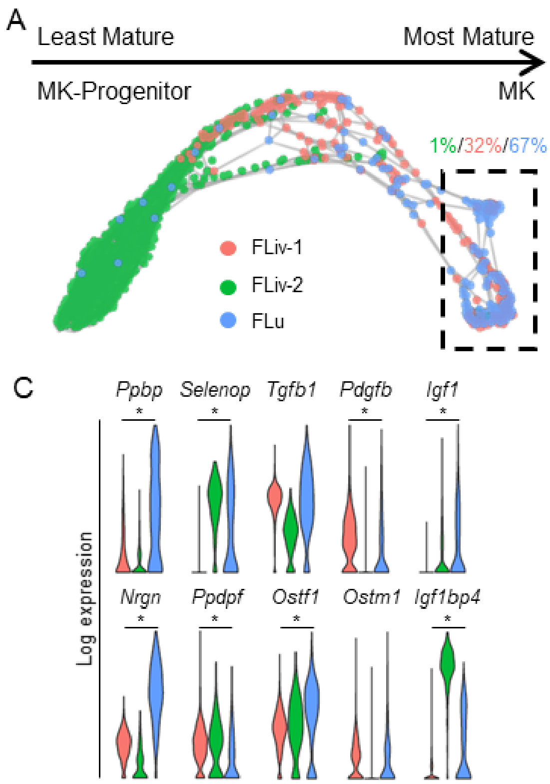

B

	WikiPathways 2019 Mouse	P-value
Lung	Cytoplasmic Ribosomal Proteins	3.06E-99
	mRNA processing	1.60E-09
	Electron Transport Chain	1.08E-03
	TNF-alpha NF-kB Signaling Pathway	2.90E-03
	G13 Signaling Pathway	3.10E-03
	Striated Muscle Contraction	4.66E-03
	Regulation of Actin Cytoskeleton	5.81E-03
	Translation Factors	6.26E-03
	Glycolysis and Gluconeogenesis	6.62E-03
	Serotonin and anxiety	7.90E-03
Liver	Keap1-Nrf2	4.79E-03
	Integrin-mediated Cell Adhesion	6.83E-03
	Insulin Signaling	7.01E-03
	EGFR1 Signaling Pathway	1.11E-02
	Kit Receptor Signaling Pathway	1.40E-02
	IL-5 Signaling Pathway	1.51E-02
	Primary Focal Segmental Glomerulosclerosis FSGS	1.69E-02
	MAPK Cascade	1.86E-02
	p38 MAPK Signaling Pathway	2.98E-02
	Nuclear Receptors	3.29E-02

Figure 2.6. Fetal lung-MKs display transcriptional priming for platelet and cytokine production. (A) SPRING plot of fetal MK-clusters. Directionality of maturation progresses from left to right and was determined based on key markers as described in Fig. 2.7. Percentages indicate which fraction of the outlined cells are represented by each respective cluster. (B) Gene set enrichment analysis of clusters outlined in a dashed box. (C) Violin plots comparing expression of various cytokines and growth factors across all fetal MK clusters. *p<0.0001

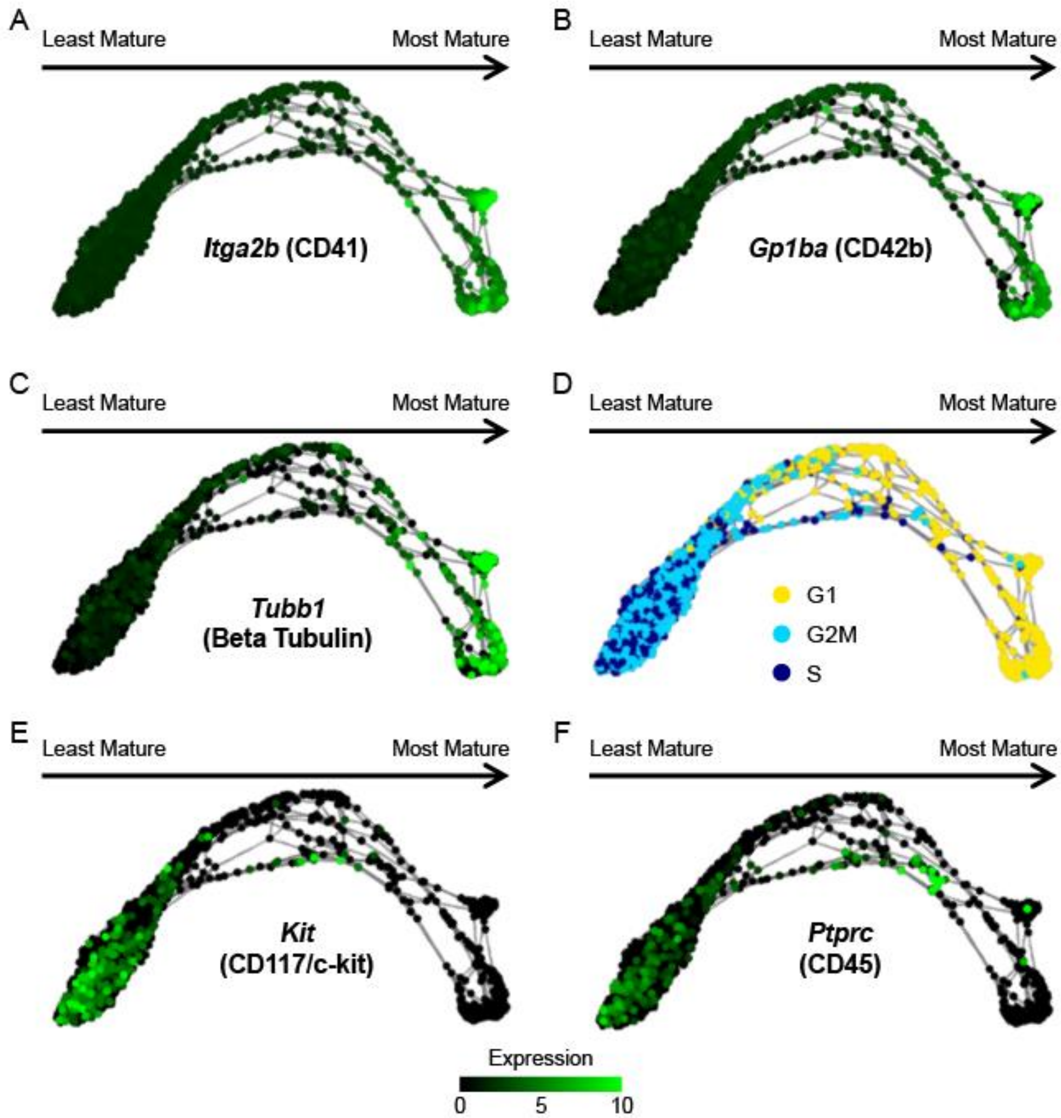

Figure 2.7. Annotation of SPRING plot directionality based on expression of maturation genes and cell cycle in fetal MK populations. (A D) This SPRING plot was annotated for directionality of maturation based on the density of cells in G1 interphase with high expression for the key maturation markers *Itga2b*, *Gp1ba*, and *Tubb1*, (E, F) as well as expression for the progenitor markers *Kit* and *Ptprc*.

Adult lung-MKs exhibit higher ploidy and express markers of maturation.

To compliment these transcriptomic studies, adult MKs were also assessed via flow cytometry for ploidy and markers of maturity. Compared to BM-derived MKs, adult lung-MKs possess a unique ploidy profile with a greater representation of high ploidy cells (**Fig. 2.8A, 2.9**). Furthermore, flow cytometry demonstrated that a significantly higher proportion of adult lung-MKs expressed the key maturational marker CD42d (**Fig. 2.8B, C**). Taken together with the scRNA-Seq analyses, these data demonstrate that the majority of adult lung MKs possess a more developmentally mature profile that may be indicative of their propensity for more efficient platelet production.

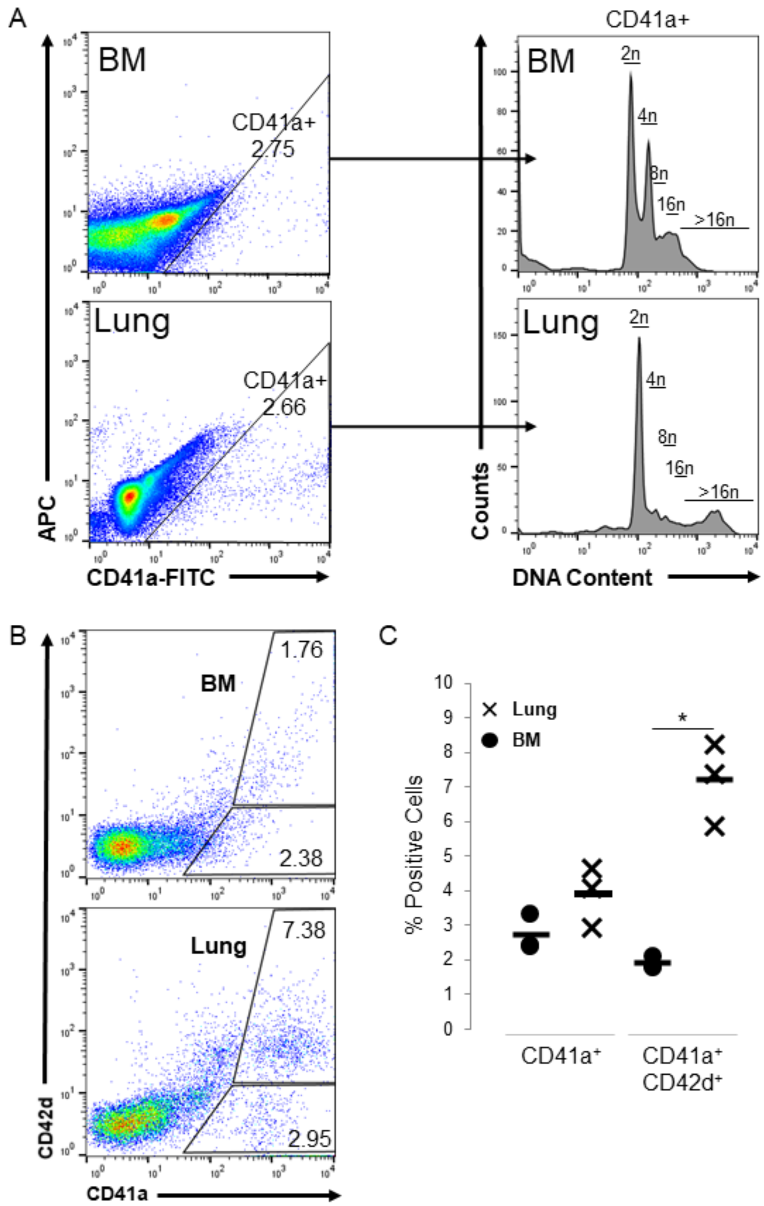

Figure 2.8. Adult lung-MKs exhibit higher ploidy and express markers of maturation. (A) Ploidy analysis of CD41a+ MKs demonstrated a greater proportion of high ploidy MKs from the lung. (B,C) Flow cytometric assessment showed a greater proportion of lung-MKs positive for the key maturation marker CD42d which was significant across 3 biological replicates. BSA enrichment was used for these experiments. Ploidy analysis without BSA enrichment was also performed and showed similar results (Fig. 2.9). Exes and dots represent individual data points, while dashes are averages. *p<0.05

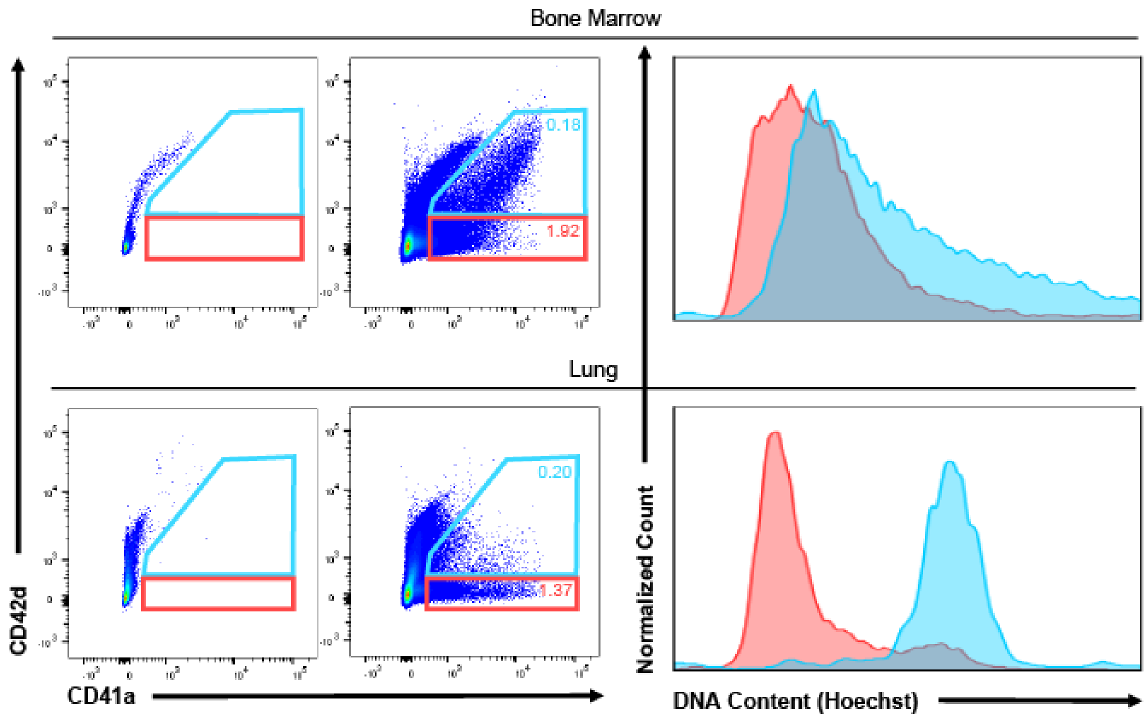

Figure 2.9. Ploidy analysis without BSA gradient. Primary cell isolates were not enriched for MKs with a BSA gradient before being stained for 30 minutes at 37° C with 15ug/mL Hoechst and 5μM Reserpine. Cell were washed and subsequently stained with CD41a APC and CD42d AF488 for 30 minutes. Propidium iodide was used for live dead cell selection. Cells were analyzed on a BD LSRII flow cytometer. This modified ploidy protocol demonstrated a higher fraction of high ploidy CD41a+/CD42d+ MKs in the lung.

Lung-MKs are skewed towards immunity and inflammation.

Differential gene expression analysis was performed on fetal and adult MK clusters as defined by UMAP (**Fig. 2.10, 2.11**). Using Enrichr analysis, the top 40 differentially expressed genes were cross referenced with the Gene Ontology Biological Process database. This analysis revealed robust enrichment for immune and inflammatory processes in fetal lung-MKs (**Fig. 2.10**). In contrast, fetal liver-derived populations were enriched for pathways related to vascular development and nuclear processes (**Fig. 2.12**). Adult lung-MKs also showed upregulation of immune and inflammatory processes (**Fig. 2.11**). Alternatively, ABM-1 showed enrichment for processes important to proplatelet production, including cytoskeletal organization and protein localization to endosomes. The gene set enriched in ABM-1 was notably more comparable to ALu versus ABM-2 and ABM-3 (**dashed box, Fig. 2.11**), further suggesting a more similar maturation profile between adult lung-MKs and ABM-1, the most mature BM-MK cluster. ABM-2 and ABM-3 demonstrated enrichment for pathways related to cell division and DNA processing, suggesting a more proliferative and immature profile (**Fig. 2.13**). Differential gene expression analyses comparing fetal lung-MKs versus adult lung-MKs revealed the enrichment of MHC class II antigen presentation genes specific to adult lung-MKs (**Fig. 2.14**).

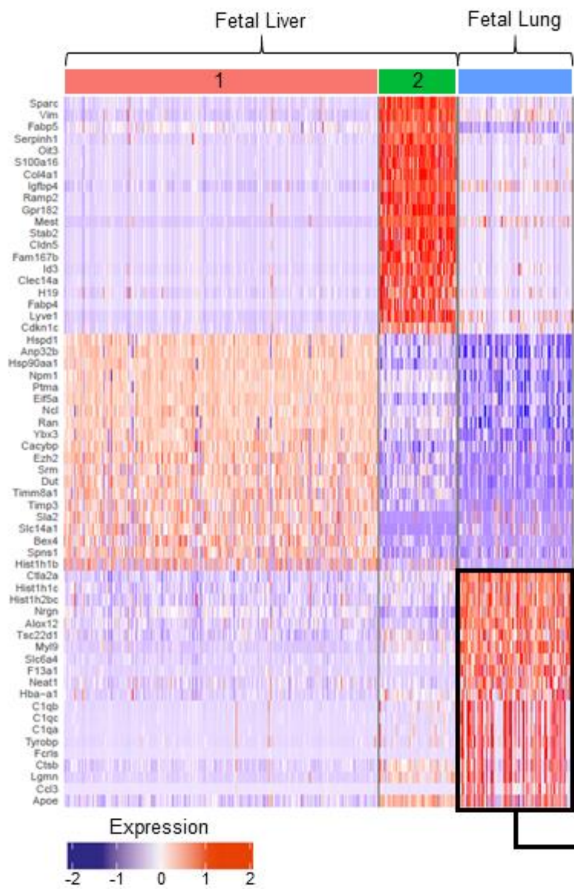

Gene Ontology Biological Process	p-Value
inflammatory response	8.2E-08
chemokine-mediated signaling pathway	1.1E-07
positive regulation of leukocyte chemotaxis	2.5E-07
regulation of natural killer cell chemotaxis	3.7E-07
cellular response to thyroid hormone stimulus	1.3E-06
response to thyroid hormone	1.7E-06
neutrophil chemotaxis	6.0E-06
cellular response to cytokine stimulus	7.1E-06
positive regulation of lymphocyte migration	7.1E-06
granulocyte chemotaxis	7.5E-06

Figure 2.10. Differential gene expression and pathway analysis demonstrate the immune phenotype of fetal lung-MKs. Heatmap and gene set enrichment analysis illustrating robust upregulation of immune/inflammatory genes in fetal lung-MKs. The top 20 differentially expressed genes associated with each cluster are listed on the left of the heatmap. The GO pathways associated with the remaining clusters are shown in Fig. 2.12.

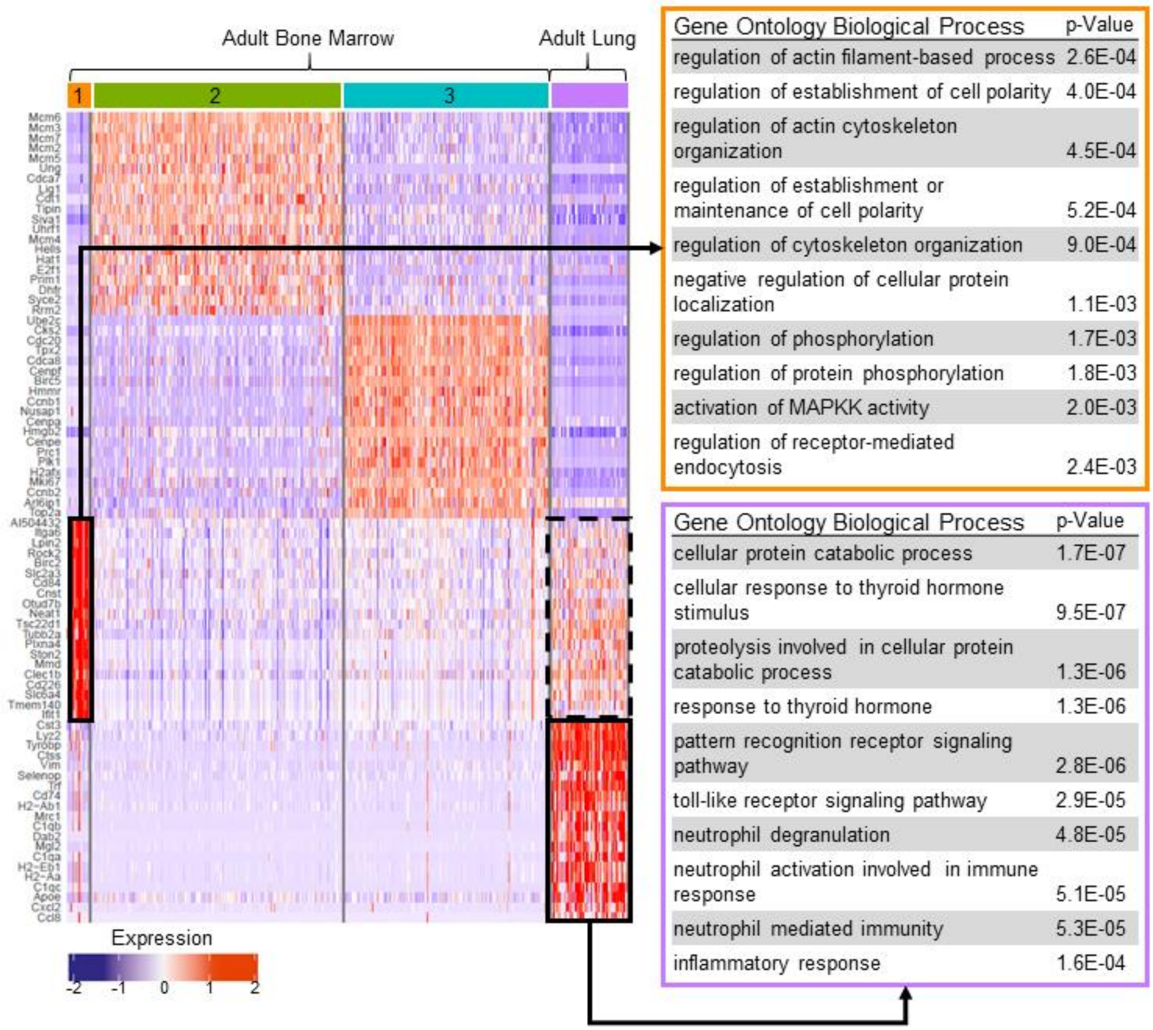

Figure 2.11. Differential gene expression and pathway analysis demonstrate the immune phenotype of adult lung-MKs. Heatmap and gene set enrichment analysis illustrating robust upregulation of immune/inflammatory genes in adult lung-MKs. Adult bone marrow cluster 1 showed enrichment for processes important in proplatelet production, which was notably also upregulated in the adult lung population outlined in a dashed black box. The top 20 differentially expressed genes associated with each cluster are listed on the left of the heatmap. The GO pathways associated with remaining clusters are shown in Fig. 2.13.

	Gene Ontology Biological Pathways	P-value
Fetal Liver 1	positive regulation of telomerase RNA localization to Cajal body (GO:1904874)	1.84E-08
	regulation of telomerase RNA localization to Cajal body (GO:1904872)	4.11E-08
	positive regulation of protein localization to Cajal body (GO:1904871)	4.12E-07
	regulation of protein localization to Cajal body (GO:1904869)	4.12E-07
	cellular macromolecule biosynthetic process (GO:0034645)	5.49E-07
	positive regulation of establishment of protein localization to telomere (GO:1904851)	6.17E-07
	regulation of establishment of protein localization to telomere (GO:0070203)	8.81E-07
	positive regulation of protein localization to chromosome, telomeric region (GO:1904816)	1.21E-06
	positive regulation of establishment of protein localization (GO:1904951)	1.61E-06
	nucleocytoplasmic transport (GO:0006913)	2.11E-06
	positive regulation of DNA biosynthetic process (GO:2000573)	4.35E-06
	mitochondrial transport (GO:0006839)	7.08E-06
	ribosomal large subunit biogenesis (GO:0042273)	7.50E-06
	nuclear transport (GO:0051169)	1.11E-05
	protein stabilization (GO:0050821)	1.26E-05
	gene expression (GO:0010467)	1.53E-05
	positive regulation of translation (GO:0045727)	1.76E-05
	positive regulation of telomere maintenance via telomerase (GO:0032212)	3.53E-05
	positive regulation of telomere maintenance via telomere lengthening (GO:1904358)	4.25E-05
	ribosomal small subunit export from nucleus (GO:0000056)	5.82E-05
Fetal Liver 2	vasculogenesis (GO:0001570)	3.77E-11
	regulation of angiogenesis (GO:0045765)	5.86E-11
	positive regulation of angiogenesis (GO:0045766)	5.36E-08
	positive regulation of vasculature development (GO:1904018)	5.68E-08
	sprouting angiogenesis (GO:0002040)	1.76E-06
	cell junction assembly (GO:0034329)	5.77E-06
	extracellular matrix organization (GO:0030198)	5.85E-06
	regulation of endothelial cell migration (GO:0010594)	1.08E-05
	cellular response to vascular endothelial growth factor stimulus (GO:0035924)	1.65E-05
	regulation of endothelial cell proliferation (GO:0001936)	1.85E-05
	negative regulation of endothelial cell proliferation (GO:0001937)	2.90E-05
	vascular smooth muscle cell differentiation (GO:0035886)	5.82E-05
	vascular smooth muscle cell development (GO:0097084)	5.82E-05
	branching morphogenesis of an epithelial tube (GO:0048754)	8.65E-05
	adherens junction organization (GO:0034332)	9.27E-05
	basement membrane organization (GO:0071711)	0.000108
	glycosaminoglycan catabolic process (GO:0006027)	0.000191
	transmembrane receptor protein serine/threonine kinase signaling pathway (GO:0007178)	0.000193
	regulation of establishment of endothelial barrier (GO:1903140)	0.000254
	muscle cell development (GO:0055001)	0.0003

Figure 2.12. Extended pathway analysis of fetal liver MKs. Pathway analysis of fetal liver MK clusters revealed enrichment for pathways related to vascular development and nuclear processes.

	Gene Ontology Biological Pathways	P-value
ABM2	DNA metabolic process (GO:0006259)	4.68E-26
	G1/S transition of mitotic cell cycle (GO:0000082)	1.02E-22
	DNA replication (GO:0006260)	7.02E-20
	cell cycle G1/S phase transition (GO:0044843)	2.18E-17
	cellular macromolecule biosynthetic process (GO:0034645)	1.67E-13
	mitotic cell cycle phase transition (GO:0044772)	4.08E-13
	nucleotide-excision repair, DNA gap filling (GO:0006297)	8.09E-10
	DNA-dependent DNA replication (GO:0006261)	1.3E-09
	error-free translesion synthesis (GO:0070987)	5.2E-08
	error-prone translesion synthesis (GO:0042276)	6.49E-08
	regulation of transcription involved in G1/S transition of mitotic cell cycle (GO:0000083)	1.99E-07
	transcription-coupled nucleotide-excision repair (GO:0006283)	3.36E-07
	nucleotide-excision repair, DNA incision, 5'-to lesion (GO:0006296)	8.64E-07
	DNA replication-dependent nucleosome organization (GO:0034723)	8.81E-07
	DNA replication-dependent nucleosome assembly (GO:0006335)	8.81E-07
	nucleotide-excision repair, DNA incision (GO:0033683)	1.19E-06
	translesion synthesis (GO:0019985)	1.45E-06
	pyrimidine deoxyribonucleotide catabolic process (GO:0009223)	1.61E-06
	postreplication repair (GO:0006301)	2.3E-06
	nucleotide-excision repair (GO:0006289)	2.37E-06
	DNA strand elongation involved in DNA replication (GO:0006271)	4.08E-06
	DNA synthesis involved in DNA repair (GO:0000731)	8.5E-06
	nucleic acid phosphodiester bond hydrolysis (GO:0090305)	1.35E-05
	DNA replication initiation (GO:0006270)	1.46E-05
	mismatch repair (GO:0006298)	3.53E-05
ABM3	mitotic nuclear division (GO:0140014)	1.98E-16
	regulation of mitotic cell cycle phase transition (GO:1901990)	1.14E-15
	mitotic sister chromatid segregation (GO:0000070)	5.14E-14
	mitotic cell cycle phase transition (GO:0044772)	4.08E-13
	anaphase-promoting complex-dependent catabolic process (GO:0031145)	2.86E-12
	regulation of mitotic cell cycle (GO:0007346)	3.12E-11
	sister chromatid segregation (GO:0000819)	3.77E-11
	regulation of ubiquitin protein ligase activity (GO:1904666)	8.05E-11
	mitotic spindle organization (GO:0007052)	1.2E-10
	positive regulation of ubiquitin protein ligase activity (GO:1904668)	2.51E-10
	microtubule cytoskeleton organization involved in mitosis (GO:1902850)	2.89E-10
	regulation of cell cycle G2/M phase transition (GO:1902749)	2.98E-10
	regulation of G2/M transition of mitotic cell cycle (GO:0010389)	4.94E-10
	G2/M transition of mitotic cell cycle (GO:0000086)	5.22E-09
	cell cycle G2/M phase transition (GO:0044839)	5.52E-09
	regulation of ubiquitin-protein ligase activity involved in mitotic cell cycle (GO:0051439)	6.13E-09
	positive regulation of ubiquitin-protein ligase activity involved in regulation of mitotic cell cycle transition (GO:0051437)	8.53E-09
	regulation of cell cycle (GO:0051726)	8.96E-09
	regulation of mitotic sister chromatid separation (GO:0010965)	1.84E-08
	protein localization to chromosome, centromeric region (GO:0071459)	1.84E-08
	positive regulation of protein ubiquitination involved in ubiquitin-dependent protein catabolic process (GO:2000060)	1.94E-08
	regulation of cell cycle process (GO:0010564)	2.38E-08
	metaphase plate congression (GO:0051310)	2.53E-08
	proteasome-mediated ubiquitin-dependent protein catabolic process (GO:0043161)	9.37E-08
	negative regulation of ubiquitin-protein ligase activity involved in mitotic cell cycle (GO:0051436)	2.92E-07

Figure 2.13. Extended pathway analysis of adult MKs. ABM 2 and ABM 3 demonstrated enrichment for pathways related to cell division and DNA processing, suggesting a more proliferative and immature profile

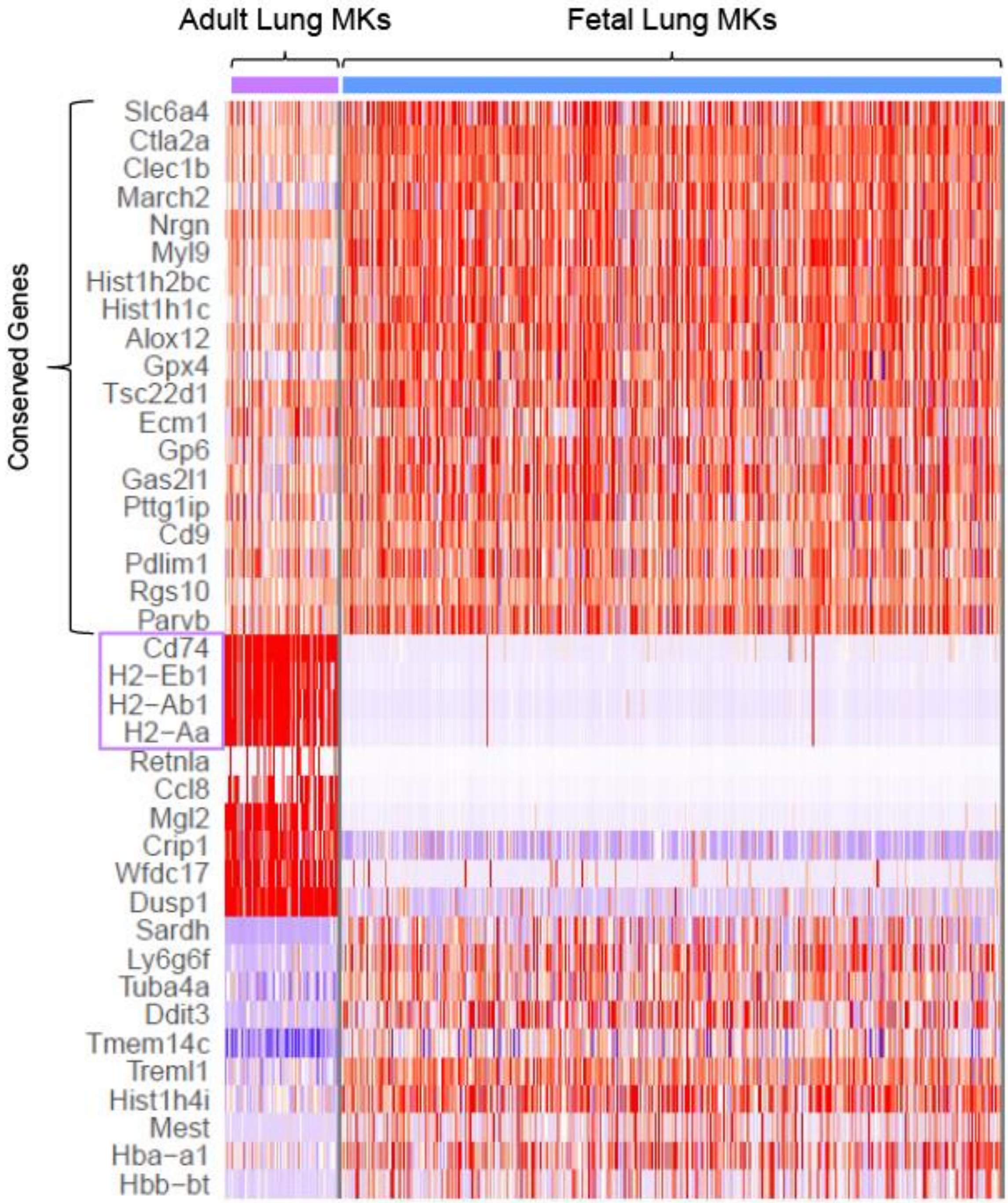

Figure 2.14. Differential gene expression analysis comparing fetal lung MKs versus adult lung MKs. The top 20 conserved genes are genes previously demonstrated to be associated with MKs, confirming the MK identity of both populations assessed. The top 4 differentially expressed genes in adult lung MKs (outlined with a purple box) are genes associated with MHC class II antigen presentation.

To further assess the immune profile of lung-MKs, gene expression analysis of various surface immune markers and chemokines was performed (**Fig. 2.15A**). Within this gene set there was a distinct pattern of expression when comparing BM and lung-MKs. Notably, lung-MKs showed significantly higher transcriptional expression of many toll-like receptors (TLR), chemokines and the immune marker *Cd74*. To assess protein level expression, flow cytometric analyses of surface immune markers were performed on CD41a^{+}/CD42d^{+} MKs (**Fig. 2.15B**). Expression of TLR2, TLR4 and MHCII was significantly higher in lung-MKs (**Fig. 2.15C**), suggesting that lung-MKs and the platelets they produce may have significant roles in microbial surveillance and antigen presentation.

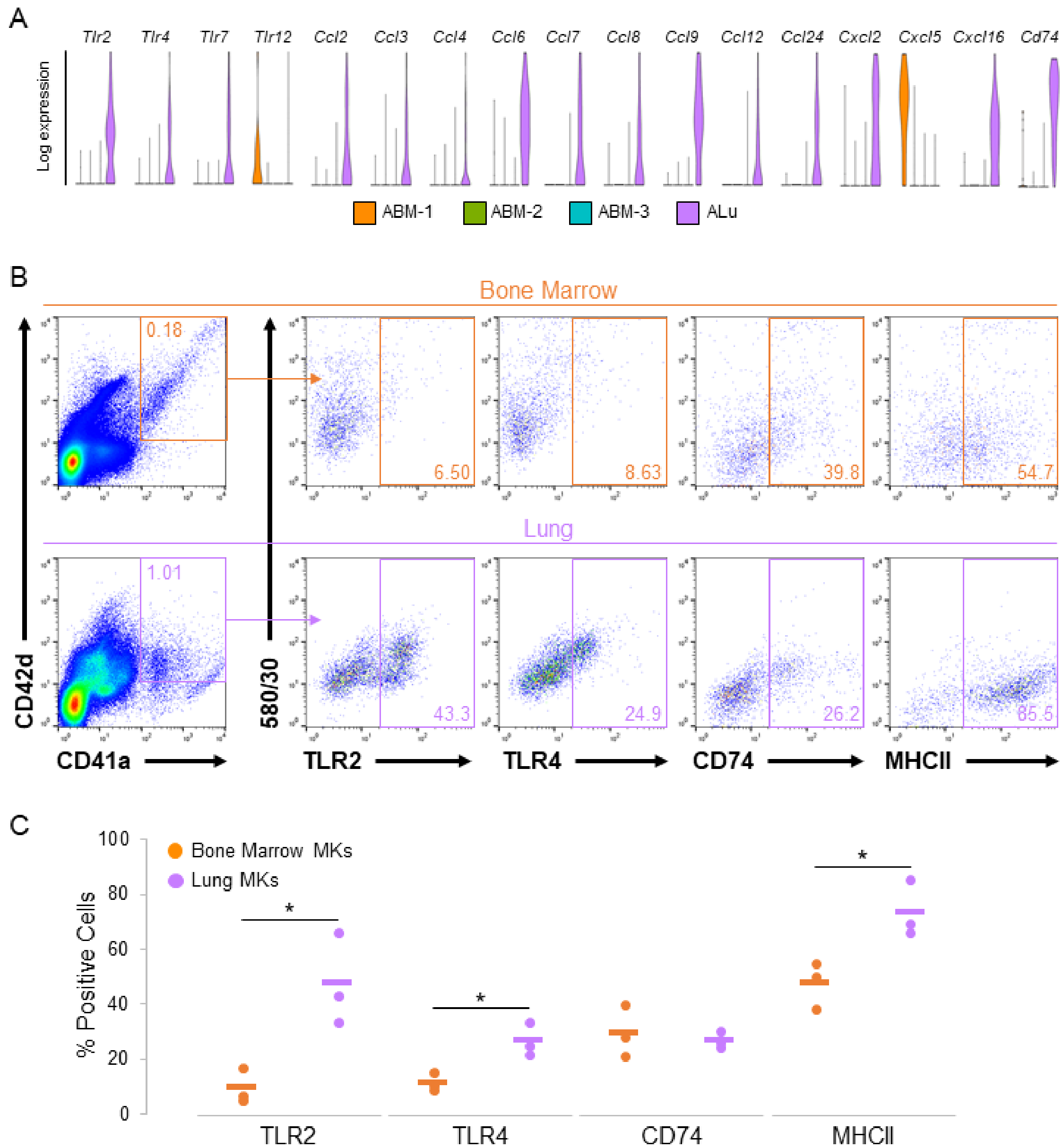

Figure 2.15. Adult Lung-MKs exhibit significant upregulation of immune markers. (A) Gene expression analysis of various toll like receptors, chemokines and the surface immune marker *Cd74* showed a distinct expression pattern with markedly more enrichment for many of these genes in lung-MKs. (B) Flow cytometric assessment of TLR2, TLR4, CD74 and MHCII was performed on CD41a+/CD42d+ MKs. (C) Percent of cells expressing these immune markers was quantified across 3 replicates, which demonstrated significantly higher expression of TLR2, TLR4 and MHCII in Lung-MKs. BSA enrichment was not used prior to immune marker analyses. *$p<0.05$

DISCUSSION

In this study, we have explored the positioning of MKs within the lung architecture which may promote the specialization of both hematopoietic and pulmonary tissue types. scRNAseq allowed us to profile individual MKs in syngeneic tissues and revealed a distinct transcriptional signature in lung-MKs. Interestingly, lung-MKs are more mature, may be primed for more efficient platelet production, and have an immune and inflammatory signature. Collectively, these findings suggest that the lung microenvironment plays a significant role in promoting the development of a lung-specific phenotype, thus further supporting the notion that the lung is a major site of MK development and functionalization.

Terminal maturation of MKs is a critical developmental process that increases a MK's capacity to efficiently produce high volumes of platelets[154,155]. During this process, MKs upregulate genes critical to the formation of proplatelets and their function in coagulation[155–158]. Lung-MKs demonstrated significant upregulation of these key maturational genes including *Tubb1* and *Gp1ba*, both of which have been previously shown to be strong indicators of late-stage maturity[141–143]. Furthermore, pathway analysis showed enrichment for processes related to ATP production, protein synthesis, and cytoskeletal rearrangement, which are of relevance to the energy intensive processes that preface platelet biogenesis[90,154]. Others have also demonstrated via scRNA-Seq that higher ploidy MKs are enriched for gene sets related to protein translation and cell metabolism[147], which aligns with the findings described above as well as the high ploidy status of lung-MKs that we have described here. Endomitotic divisions increase ploidy and cell size, which are critical for increasing protein production and expanding available cell membrane to fuel efficient platelet production[90,159]. High platelet output is further supported by turbulent blood flow, which has been suggested to be a unique feature of the lung vasculature that further supports pulmonary platelet biogenesis[160]. Upon budding off from their parent MK, platelets are carried off into circulation to carry out a variety of functions.

One key function of platelets is the transport of cytokines and growth factors to support development and regeneration[49]. Notably, other groups have demonstrated that lung specific processes are supported by factors sourced from or enriched in platelets. Platelet derived SDF1 promotes alveolar regeneration post-pneumonectomy[57]. Transforming growth factor beta 1 (TGFβ1) is critical for the early embryonic patterning of healthy lungs[56,151,161–163]. IGF1 is critical in the development of many tissues, including the lung[164–166]. Although some of these studies highlight platelets as the source of these factors, the tissue source of the platelets is currently unclear. Despite differences in maturation, our analyses of fetal-MK populations revealed robust transcriptional expression of *Tgfb1* and lung-specific enrichment of *Igf1*. This suggests that the observed differences in expression of growth factors are not solely an artifact of maturational state. Although the liver is the primary source of IGF1 during embryonic development, blood oxygenation is provided by the mother and approximately 16% of total blood flow passes through the murine pulmonary circulation[167]. We also observed a low prevalence of platelets in fetal lung sections, suggesting that this reduced blood flow restricts the passage of platelets to the developing lung. As such, fetal lung-MKs may be providing a locally enriched source of growth factors that support the development of the embryonic lung.

Recent investigation of MKs and platelets continues to reveal their previously underappreciated roles in inflammation and immunity[87–89,55,114]. By employing scRNA-Seq, we demonstrated that lung-MKs in both fetal and adult mice are indeed skewed towards an immune phenotype. Others have purported that the adoption of an immune phenotype may be a result of interactions between the non-sterile environment of the lung niche and resident MKs[55]. While this may hold true in the adult lung, embryogenesis occurs under aseptic conditions yet fetal lung-MKs still develop an immune phenotype in the absence of lung microbiota[168,169]. This suggests that the lung-MK microenvironment promotes the adoption of an immune phenotype independently of influence from interactions with foreign antigens. The physiological significance of lung-MKs being skewed toward a role in immunity remains unanswered. However, we demonstrate significant upregulation of TLR2, TLR4 and MHCII in lung-MKs, which suggests that lung-MKs and their platelet progeny may have important roles in microbial surveillance and antigen presentation. These findings were corroborated by a recent publication utilizing both scRNA-Seq and functional immune studies to demonstrate the in-vivo and ex-vivo antigen presentation capabilities specific to lung-MKs[170]. However, in contrast to our findings, this group demonstrated a lower ploidy profile in lung-MKs. The discrepancy may be due, in part, to differences in employed methodologies of cell isolation and sorting strategies. Nevertheless, the collective findings from both studies highlight the need to further investigate the unique features of this cell population.

Our findings suggest the existence of symbiosis between the lung and resident MKs. In this scenario, the lung niche supports MK development and may further functionalize resident MKs. Reciprocally, resident MKs and platelets may support the lung in processes such as microbial defense and embryonic development. Further investigation into the development of lung-MKs and their respective functional repertoire may shed light on the origin of platelets that promote or protect against the development of life-threatening lung disorders, such as lung fibrosis, acute respiratory distress syndrome and tumor progression[63,108,171–174]. This is particularly relevant in the wake of the SARS-COV-2 pandemic, in which patients presenting with both severe and mild respiratory symptoms have exhibited life threatening systemic coagulopathies including stroke, multi-organ thrombosis and disseminated intravascular coagulation[175–180]. Furthermore, multiple groups have described an increase in alveolar MKs in histopathological lung sections of SARS-COV-2 patients[181,182]. These findings, combined with the immune phenotype of lung-MKs, raise questions about the involvement of lung-MKs in the pathogenesis of SARS-COV-2 infection and other pulmonary diseases. Developing an enhanced understanding of lung-MKs will further support the continuing search for novel therapeutics to treat lung diseases and will greatly advance our understanding of the organ specific role of MKs.

CHAPTER THREE: DE-NOVO HEMATOPOIESIS FROM THE FETAL LUNG

Disclaimer: Portions of the text from this chapter were adapted from the following pre-print publication: Yeung, A. K. et al. De-Novo Hematopoiesis from the Fetal Lung. 2022.02.14.480402 (2022) doi:10.1101/2022.02.14.480402. A.K.Y. performed experimental design, data collection, data analysis, interpretation of data and manuscript preparation. G.J.M. performed and supervised experimental design, interpretation of data and manuscript preparation. C.V.M. and J.L.V. performed the bioinformatic/computational analysis and supported the experimental design and manuscript preparation. A.C.B, K.V., T.W.D., A.B.Y., V.V., G.M. and A.B.B assisted with data collection and manuscript preparation.

INTRODUCTION

Hematopoietic stem cells (HSCs) originate from a rare sub-population of arterial endothelial cells known as HECs. Making up just 1-3% of the total endothelial cell population in the aorta-gonad-mesonephros (AGM), HECs are commonly thought to be confined to a small window of gestation between embryonic days 8 to 11 (E8-11) in mice, and E27-40 in humans[183,184]. Within this time window, HECs can also be found in other hematopoietic organs and vessels including the yolk sac, placenta, and vitelline and umbilical arteries[84,185–189]. Some studies suggest that HECs may not be restricted to these hematopoietic organs and developmental window. Work from others suggests that functional HECs may also be found in the embryonic head around E10-E11 as well as the perinatal chicken and murine bone marrow (BM)[190,191]. Collectively, these studies demonstrate that our spatiotemporal understanding of HECs remains limited and raises questions about the hematopoietic potential of other organs.

Recent studies have highlighted the presence and importance of various resident blood cell populations in the lung[66]. In particular, the lung was demonstrated to be a reservoir of HSPCs, but the origins of this population of progenitors remains unknown[55,83,192]. *In-utero* mechanical stimuli have been shown to be an important environmental cue for both HEC and pulmonary development. More specifically, cyclic stretch induced activation of Yes Activated Protein (YAP) signaling in the AGM promotes EHT[193]. Interestingly, rhythmic breathing movements begin occurring around E16 in fetal mice, and mechanical stimuli has a significant impact on fetal airway and alveolar epithelial development[194–196]. Beyond mechanical signaling, cell-cell extrinsic signaling within the AGM niche is critical for EHT. The ventral wall of the dorsal aorta is the most common site of EHT due to its proximity to the underlying mesenchyme which modulates EHT via Notch, BMP4, SHH, and Wnt pathways[185,197,198]. All of these pathways are similarly very important in pulmonary fetal development[139].

Based on these parallels, we hypothesized that the fetal lung is another potential site of hemogenic endothelium with the functional capacity to produce hematopoietic progenitors. Employing fetal lung explant cultures, we demonstrate that the murine and human fetal lung are sources of putative HECs. Multipotent, fetal lung-derived HSPCs showed the canonical features of cells produced by EHT as determined by flow cytometry, single cell transcriptomics, functional assays and immunofluorescent histology. These findings highlight the fetal lung as another potential site of de-novo hematopoiesis, suggesting that the lung may have a greater role in instructing tissue specific hematopoiesis and/or overall hematopoietic development.

MATERIALS AND METHODS

Ethics Statement

All animal housing and experimental procedures were approved by the Boston University School of Medicine Institutional Animal Care and Use Committee (BUSM IACUC). Work involving human tissue samples was approved by Partners Human Research Committee (Protocol #2016P001106).

Tissue isolation and processing

Mouse

E17 timed-pregnant C57/BL6 mice were purchased from Jackson Laboratories. The fetal liver and lung were isolated from surrounding tissue by blunt dissection and set aside in a solution of 10% characterized fetal bovine serum in Hanks' balanced salt solution (HBSS, Gibco). Using a 5mL syringe fitted with a 16-gauge needle, the fetal liver and fetal lung were drawn up and expelled several times to physically dissociate the tissue. Samples were subsequently placed in a digest buffer containing HBSS, 1mg/mL DNase I (Sigma), and 0.5mg/mL LiberaseTM (Sigma). This digest mixture was placed on a rocker at 37^{o}C for

30-minutes to 1-hour. Post-digestion, lung samples were filtered and resuspended in RBC lysis for 5 min at 37^{o}C, then washed, filtered, and resuspended in HSPC medium.

Human

All fetal samples were within the age range between 19-24 weeks post-conception. Lung lobes were dissected away from the main airways and minced with a scalpel before being placed in a digest buffer containing HBSS, 1mg/mL DNase I (Sigma), and 0.5mg/mL LiberaseTM (Sigma). This digest mixture was placed on a rocker at 37^{o}C for 30-minutes to 1-hour. Post digestion, lung samples were filtered and resuspended in RBC lysis for 5 min at 37^{o}C, then washed, filtered, and resuspended in HSPC medium.

Explant Cultures

Isolated cells suspended in HSPC medium were plated onto Matrigel coated plates. HSPC medium was made up of StemPro-34 Serum Free Medium, 50 µg/ml ascorbic acid, 400 nM monothioglycerol, 100µg/ml Primocin, 2 mM L-glutamine, and the following human or murine growth factors: 50 ng/ml vascular endothelial growth factor A (VEGFA), 100 ng/ml basic fibroblast growth factor (bFGF), 100 ng/ml stem cell factor (SCF), 100 ng/ml FMS-related tyrosine kinase ligand (FLT3L), 100 ng/ml thrombopoietin (TPO), 100 ng/ml Interleukin-6 (IL6). On the third day of all cultures, media was aspirated, rinsed once with PBS, and fresh media was applied.

MethoCult Colony-Forming Unit (CFU) Assay

CFU assay was performed using the murine MethoCult GF M3434 (Stem Cell Techologies) or human MethoCult H4034 Optimum (Stem Cell Techologies) kit. Procedure was performed per manufacturer's instructions.

Tissue Histology and Cell Imaging

A small portion of the human fetal lung was fixed in 4% paraformaldehyde for 2 hours, cryoprotected in 30% sucrose and embedded in Optimum Cutting Temperature embedding medium. 10-12µm tissue sections were made using a cryostat. Sections were rinsed with PBS prior to permeabilizing and blocking in a solution of 0.4% Triton X-100 and 10% NDS. A list of antibodies used for immunofluorescence can be found under **Table 1**.

Imaging of cell cultures were performed using a Keyence BZ-X700 fluorescence microscope. Cytospins were stained using the Hema 3 Stat Pack (Fisher) and imaged using a Nikon Eclipse NiE.

Flow cytometry

All staining and washing steps were done using a solution of 1% BSA in PBS, 5mM EDTA. Single cell suspensions were stained with the appropriate master mix of antibodies on ice for 30 minutes. A table of antibodies used for analysis can be found under **Table 1**. Fc-Receptor block treatment was performed using an anti-mouse CD16/32 antibody (BioLegend, Clone: 93) or anti-human Fc receptor block (biolegend, Human TruStain FcX) for 10 minutes prior to the addition of master mix. True-Stain Monocyte Blocker (BioLegend) and Brilliant Stain Buffer Plus (BD Biosciences) were included in master mix to minimize non-specific staining. Single stain controls were processed using cells and/or beads (Invitrogen, UltraComp eBeads Plus). Flow cytometry was performed using either a BD LSRII, a Stratedigm S1000EXI or a 5-laser Cytek Aurora spectral flow cytometer. Analysis was performed using FlowJo_v10.8 (FlowJo, LLC) software.

Marker	Species	Conjugate	Clone	Vendor	Catalog. #	Dilution
CD235a	Human	PE	HIR2	BD Biosciences	555570	1:1000
CD34	Human	BV421	581	BD Biosciences	562577	1:100
CD41	Human	BV421	HIP8	Biolegend	303730	1:200
CD41	Human	Unconjugated	HIP8	BD Biosciences	BDB555465	1:100
CD42b	Human	APC	HIP1	BD Biosciences	551061	1:200
CD45	Human	APC	2D1	Biolegend	368512	1:200
CD45	Human	PE-Cy7	2D1	Biolegend	368532	1:200
EPCR (CD201)	Human	APC	RCR-401	Biolegend	351906	1:100
GPI80	Human	PE	3H9	MBL	D087-5	1:50
KDR	Human	PE	89106	BD Biosciences	560494	1:200
KDR	Human	APC	89106	BD Biosciences	560871	1:200
Vascular Endothelial Cadherin (VECAD/CD144)	Human	AF647	55-7H1	BD Biosciences	561567	1:100
Vascular Endothelial Cadherin (VECAD/CD144)	Human	PE	55-7H1	BD Biosciences	561714	1:100
Vascular Endothelial Cadherin (VECAD/CD144)	Human	Unconjugated	Polyclonal	R&D Systems	AF938	1:100
CD44	Human/Murine	BV711	IM7	Biolegend	103057	1:800
CD45	Human/Murine	Unconjugated	Polyclonal	Invitrogen	PIPA587427	1:100
Epithelial Cadherin (E-Cadherin)	Human/Murine	Unconjugated	DECMA-1	Santa Cruz Biotechnology	sc-59778	1:50
CD150	Murine	BV711	TC15-12F12.2	Biolegend	115941	1:400
CD41	Murine	BV421	MWReg30	Biolegend	133911	1:400
CD43	Murine	FITC	S11	Biolegend	143204	1:100
CD45	Murine	BUV395	30-F11	BD Biosciences	564279	1:200
CD48	Murine	BV605	HM48-1	Biolegend	103441	1:100
EPCR	Murine	APC	eBio1560	eBioscience	50-151-23	1:200
Kit	Murine	BV510	ACK2	Biolegend	135119	1:400
Kit	Murine	APC	2B8	Biolegend	105812	1:200
Lineage Cocktail	Murine	FITC	Cocktail	Invitrogen	22777072	1:5
Sca-1 (Ly-6A/E)	Murine	PE	D7	eBioscience	50-110-49	1:200
Vascular Endothelial Cadherin (VECAD/CD144)	Murine	Biotin	BV13	Biolegend	138008	1:200
Streptavidin	N/A	APC-Cy7	N/A	Biolegend	405208	1:200
Calcein Blue AM	Viability Dye	N/A	N/A	Invitrogen	C1429	1:1000
Live/Dead Fixable Blue	Viability Dye	N/A	N/A	Invitrogen	L34961	1:800

Table 1. Antibodies used for flow cytometry and immunofluorescent microscopy.

Single cell RNA sequencing

Adherent cells from days 4, 5 and 6 of explant cultures were released from Matrigel coated wells using Accutase. Collected cells were stained for VE-Cadherin-APC-Cy7 and resuspended in sort buffer (2% BSA in PBS) containing Calcein Blue AM (1:1000). Using a Beckman MoFlo Coulter Astrios, live-singlets and VECAD$^+$ events were sorted into sort buffer (2% BSA in PBS with 5mM EDTA). Cells counts and viability after sorting were confirmed by hemocytometer using trypan blue. Suspension cells were left unsorted as VECAD expression is lost gradually as hematopoietic cells differentiate post-EHT emergence. VECAD$^+$ sorted adherent cells and unsorted suspension cells were single cell captured using the 10X Genomics Chromium platform and prepared using the Single Cell 3' v3 kit. Library preparation and sequencing was done at the Boston University Microarray and Sequencing Resource (BUMSR) Core using the Illumina NextSeq 2000 instrument.

Bioinformatic analysis

Reads were demultiplexed and aligned to the mouse genome assembly (GRCm38, Ensembl) with the STARsolo pipeline[199]. Further analyses were done using Seurat v. 3.1.4[126]. After inspection of the quality control metrics, cells with more than 12% of mitochondrial content or less than 800 detected genes were excluded for downstream analyses. We normalized and scaled the UMI counts using the regularized negative binomial regression (SCTransform)[127]. Following the standard procedure in Seurat's pipeline, we performed linear dimensionality reduction (PCA), and used the top 20 principal components to compute both the UMAP[128] and the clusters (Louvain method[129]) which were computed at a range of resolutions from 1.5 to 0.05 (more to fewer clusters). Cell cycle scores and classifications were done using the Seurat method[130]. The cut-offs for independent filtering[132] prior to differential expression testing required genes: a) being detected in at least 10% of the cells of either population and b) having a natural log fold change of at least 0.25 between populations. The tests were performed using Seurat's wrapper for the MAST framework[133]. For a comparison on the performance of methods for single-cell differential expression see Soneson & Robinson et al.[134].

Statistical analysis

Significance for Enrichr based pathway enrichment was determined by Fisher exact test[135,136]. Significance for pairwise scRNA-Seq gene expression comparisons was determined using the MAST framework[133]. Significance for flow cytometry assays performed in biological triplicate was determined by student paired t-test.

RESULTS

Murine fetal lung explant cultures produce HSPCs

To assess the functional capacity of potential lung HECs to produce blood progenitors, cells isolated from murine E17 lungs were plated onto Matrigel coated plates in an adapted hematopoietic differentiation media, termed HSPC medium[200]. This serum-free media was formulated to support the final stages of specification of HECs into HSPCs. The primary rationale for choosing E17 was that (1) this is during the window that fetal breathing movements are occurring[194], and (2) E17 is a timepoint that is distant from the AGM EHT window (E8-11)[183], thus helping to minimize contamination from AGM-EHT derived progenitors.

In contrast to fetal liver explants where immediate expansion of floating cells is observed due to an expanding hematopoietic progenitor population, fetal lung explants initially developed a robust adherent layer. Discrete clusters of suspension cells are observed by day 3, which expand to robust colonies between days 4-6 (**Figure 3.1A**). To visually determine cell identity based on their morphology, Wright-Giemsa stains of cytospins of day 6 suspension cells were performed, which revealed cells with a progenitor-like morphology as well as various differentiated hematopoietic cells including macrophages/monocytes, neutrophils and megakaryocytes (**Figure 3.1B**). This diversity of hematopoietic cells suggests that hematopoietic progenitors are arising from these cultures. To examine this, suspension cells were functionally assessed for progenitor potential by MethoCult assay. Day 4-6 suspension cells showed similar potential to form all types of colony forming units (CFUs), but this potential was no longer detected at Day 8 (**Figure 3.1C**, **D**). Progenitor phenotyping was further assessed by flow cytometric assessment of the broad murine HSPC markers $Lin^-/Sca^+/Kit^+$ (LSK) and the SLAM markers CD48 and CD150. A greater fraction of $CD45^+$ hematopoietic cells isolated from the adherent cell layer were LSK-HSPCs and $CD48^-/CD150^+$ SLAM marker defined HSCs (**Figure 3.1E**). Collectively, these data suggest that the adherent layer of cells from fetal lung explants gave rise to HSPCs.

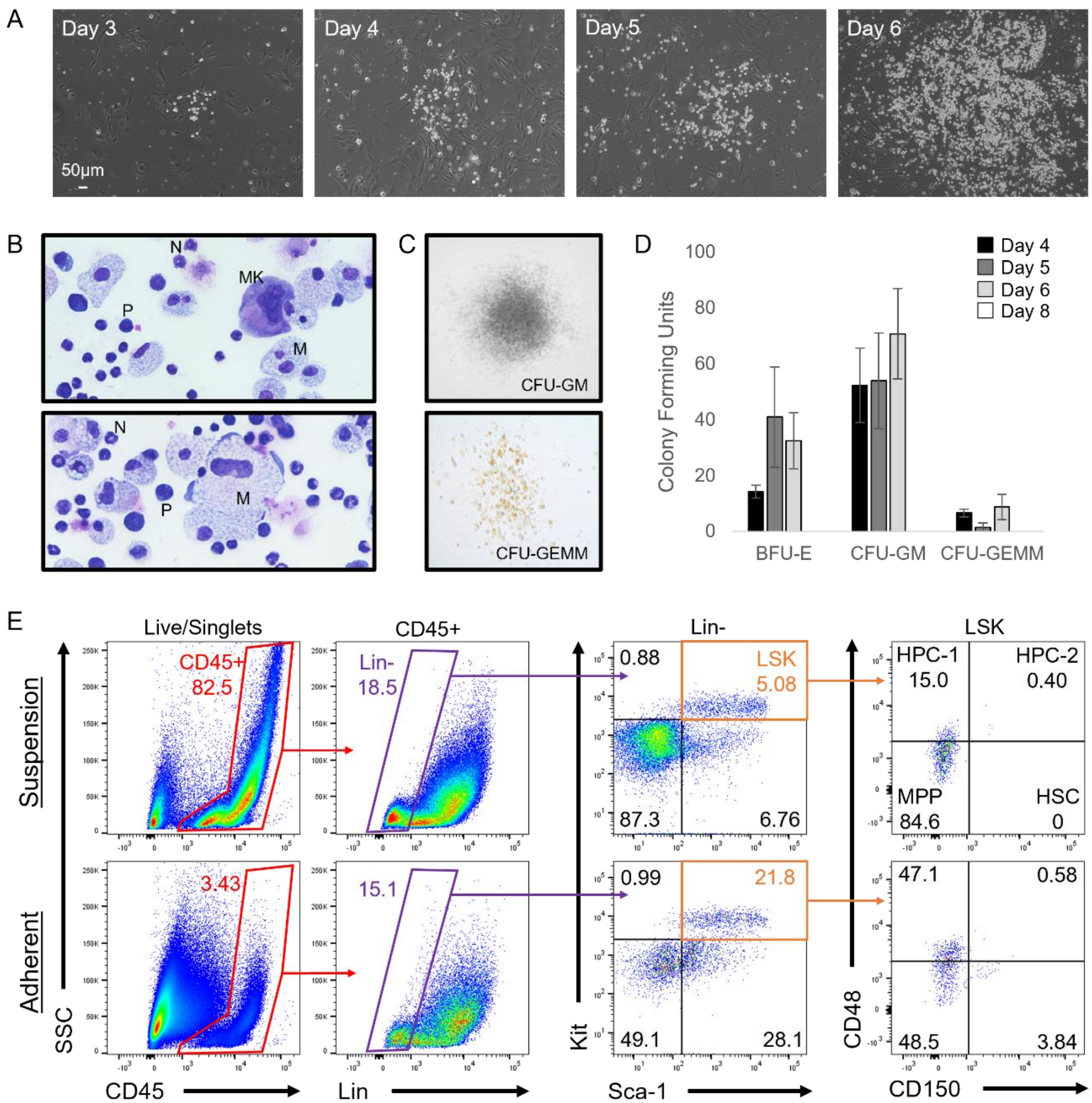

Figure 3.1. Murine fetal lung explant cultures produce HSPCs. (A) Images of a single position between days 3 to 6 of a murine fetal lung explant culture. (B) Cytospin of fetal lung derived suspension cells. Images are annotated for cell type: MK = Megakaryocyte, N = Neutrophil, M = Monocyte/Macrophage, P = Progenitor. (C) Images of representative colonies from a CFU assay. (D) Colony counts from CFU assays performed with day 4, 5, 6 and 8 suspension cells. (E) Representative plots of flow cytometric assessment of LSK and SLAM marker defined HSPC populations. Suspension represents cells that were floating in media, and Adherent represents cells that were collected post-treatment with Accutase. Error bars represent standard deviation.

Murine fetal lung explants exhibit the dynamics of EHT

Time-lapse capture of live explant cultures from days 5-6 showed adherent cells transitioning to suspension cells (data not shown). These observations closely mimic AGM explant cultures and in-vitro based hematopoietic differentiations showing the transition of HECs into hematopoietic cells[201–204]. The resultant pre-HSPCs that are birthed from AGM derived HECs retain some endothelial markers and are marked by co-expression of the endothelial marker vascular endothelial cadherin (VECAD) and the broad hematopoietic marker CD45[205]. Fetal Lung explants gave rise to $VECAD^+/CD45^+$ cells, and a gradual reduction in VECAD expression coincided with the expression of the more differentiated marker CD45 (**Figure 3.2A**). The fraction of $CD45^+$ cells that were $VECAD^+$ also decreased with successive days of culture (**Figure 3.2B**). Time matched fetal livers, which house HSPCs but not HECs[206], were cultured under the same conditions and did not result in the production of a population of $VECAD^+/CD45^+$ cells (**Figure 3.3A**). This suggests that fetal lung derived $VECAD^+/CD45^+$ pre-HSPCs are not resultant from the expansion of pre-existing progenitors. SLAM marker defined HSCs were predominantly present amongst the $VECAD^+$ suspension cells (**Figure 3.2C**). With time, a gradual reduction in the fraction of $VECAD^+$ HSCs was observed, which coincided with the expansion of the more lineage restricted hematopoietic progenitor cell 1 (HPC-1) and HPC-2 populations.

Beyond VECAD, successive staging from a pro-HSC to a pre-HSC phenotype is marked by the expression of CD41 and CD43, respectively[207]. EPCR and CD44 have also been previously demonstrated as markers of pre-HSPCs[207–209]. Fetal lung derived

VECAD$^+$/CD45$^+$ cells showed expression of CD41, CD43, CD44, and EPCR (**Figure 3.2D**). There was a notable reduction in CD41, CD43 and EPCR expression as these cells transitioned into a suspension state. Intensity of EPCR expression also decreased as VECAD$^+$/CD45$^-$ cells matured away from an endothelial signature (**Figure 3.3B**). In contrast, CD41 expression transiently peaked at the VECAD$^+$/CD45$^+$ pre-HSPC stage. Under these experimental conditions, however, no notable changes in CD44 expression were observed regardless of physical and maturational state. We also observed significantly less expression of pre-HSC markers on fetal liver VECAD$^+$/CD45$^+$ cells suggesting that in contrast to those from the fetal lung, these cells are likely not pre-HSPCs (**Figure 3.3A**).

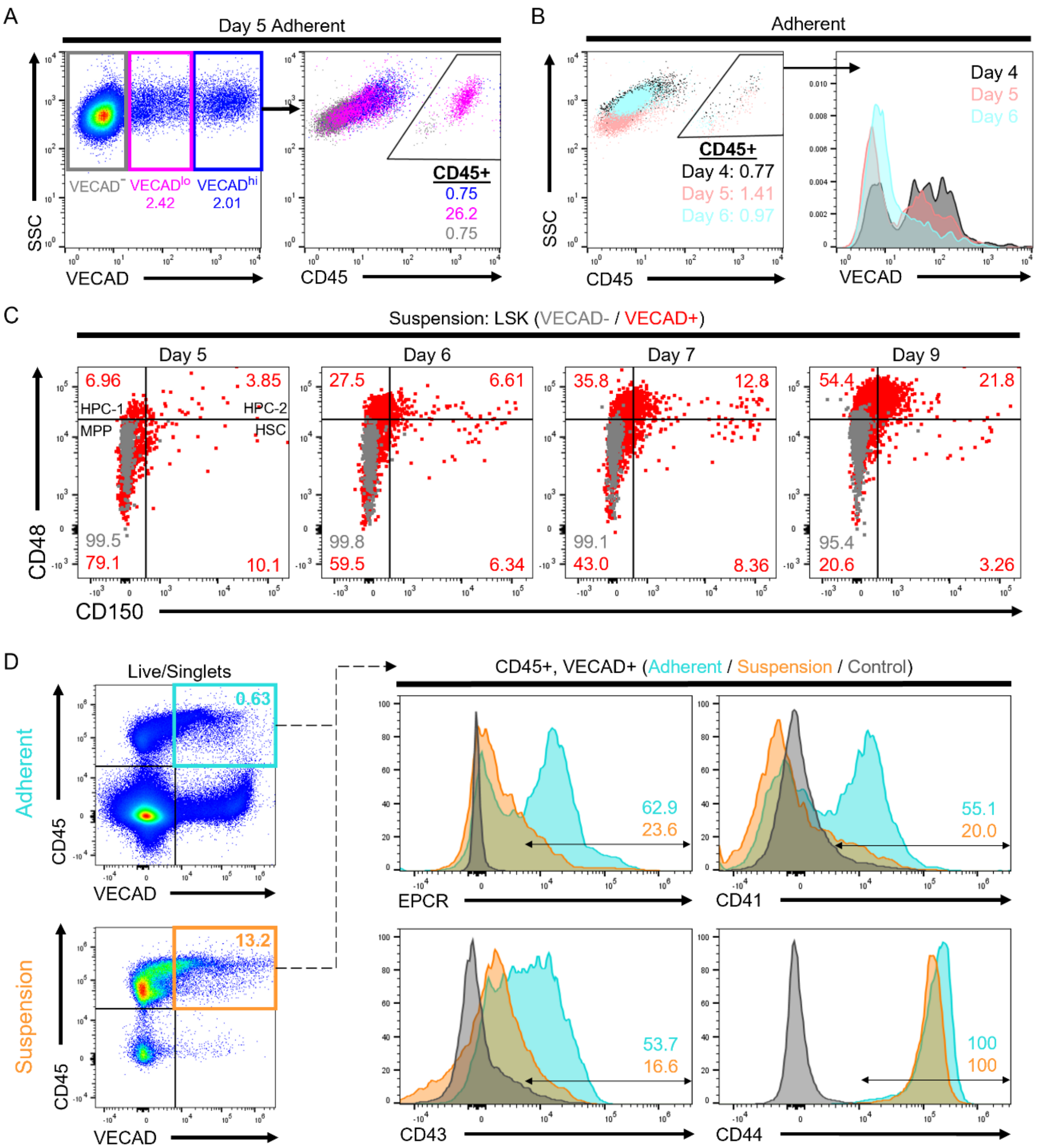

Figure 3.2. Murine fetal lung explants exhibit the dynamics of EHT. (A) Flow cytometric assessment of VECAD and CD45 expression on day 5 fetal lung explants. (B) CD45 and VECAD expression across days 4 to 6. VECAD expression is gradually lost as endothelial cells complete their transition to CD45+ hematopoietic cells, and this process diminishes across days 4-6 of culture. (C) Assessment of SLAM marker defined HSPC populations stratified by VECAD expression across multiple days in culture. (D) Assessment of pre-HSC and EHT markers on VECAD+/CD45+ defined progenitors and separated by adherent versus suspension cell populations.

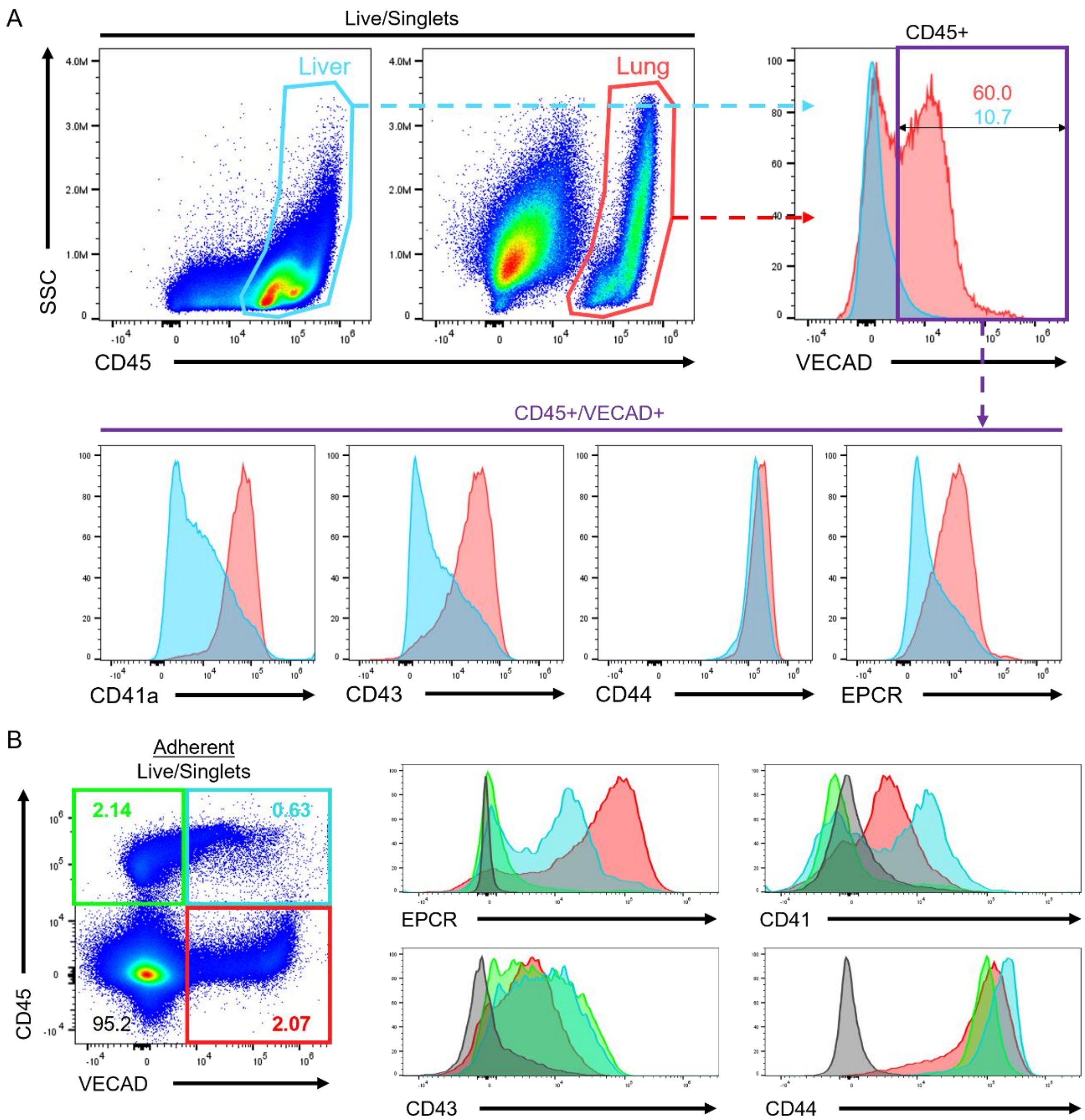

Figure 3.3. Assessment of EHT and pre-HSC markers on fetal liver and fetal lung explants. (A) Comparison of EHT and pre-HSC markers between fetal liver and fetal lung explants. (B) Comparison of EHT and pre-HSC markers between populations differentiated by VECAD and CD45 expression.

Human fetal lung explants undergo EHT to produce HSPCs

In an effort to understand if this phenomenon is conserved in humans, cells collected from human fetal lungs isolated from embryos aged between 19-24 weeks post-conception were cultured under the same conditions described above. Similar to murine fetal lung explants, human fetal lung explants initially developed an adherent layer and gave rise to suspension cells between days 7-10 (**Figure 3.4A**). Cytospins and flow cytometry of suspension cells showed progenitor-like cells and various differentiated cell types, including megakaryocytes, red blood cells, monocytes/macrophages and neutrophils (**Figure 3.4B**, **C**). Suspension cells assessed by Methocult assay also showed CFU capacity (**Figure 3.4D**). These data collectively suggest that human fetal lung explants are giving rise to HSPCs capable of multilineage differentiation.

To assess whether these suspension cells were derived via EHT, flow cytometric assessment of endothelial and HSPC markers was performed on human fetal lung explants (**Figure 3.4E**). Human HSPCs were broadly defined by co-expression of the progenitor marker CD34 and the hematopoietic marker CD45. The majority of fetal lung derived $CD34^+/CD45^+$ progenitors co-expressed VECAD, which was downregulated as these cells differentiated and lost expression of CD34. Additionally, fetal lung derived HSPCs expressed the HSPC markers KDR, GPI80, CD44 and EPCR. Reduction in the expression of these pre-HSPC/HSPC markers coincided with the loss of CD34 expression. Notably, human fetal lung derived HSPCs were enriched with a distinct CD44-high population, which others have reported is a marker of type II pre-HSPCs found within the intra-aortic hematopoietic clusters of the AGM[208].

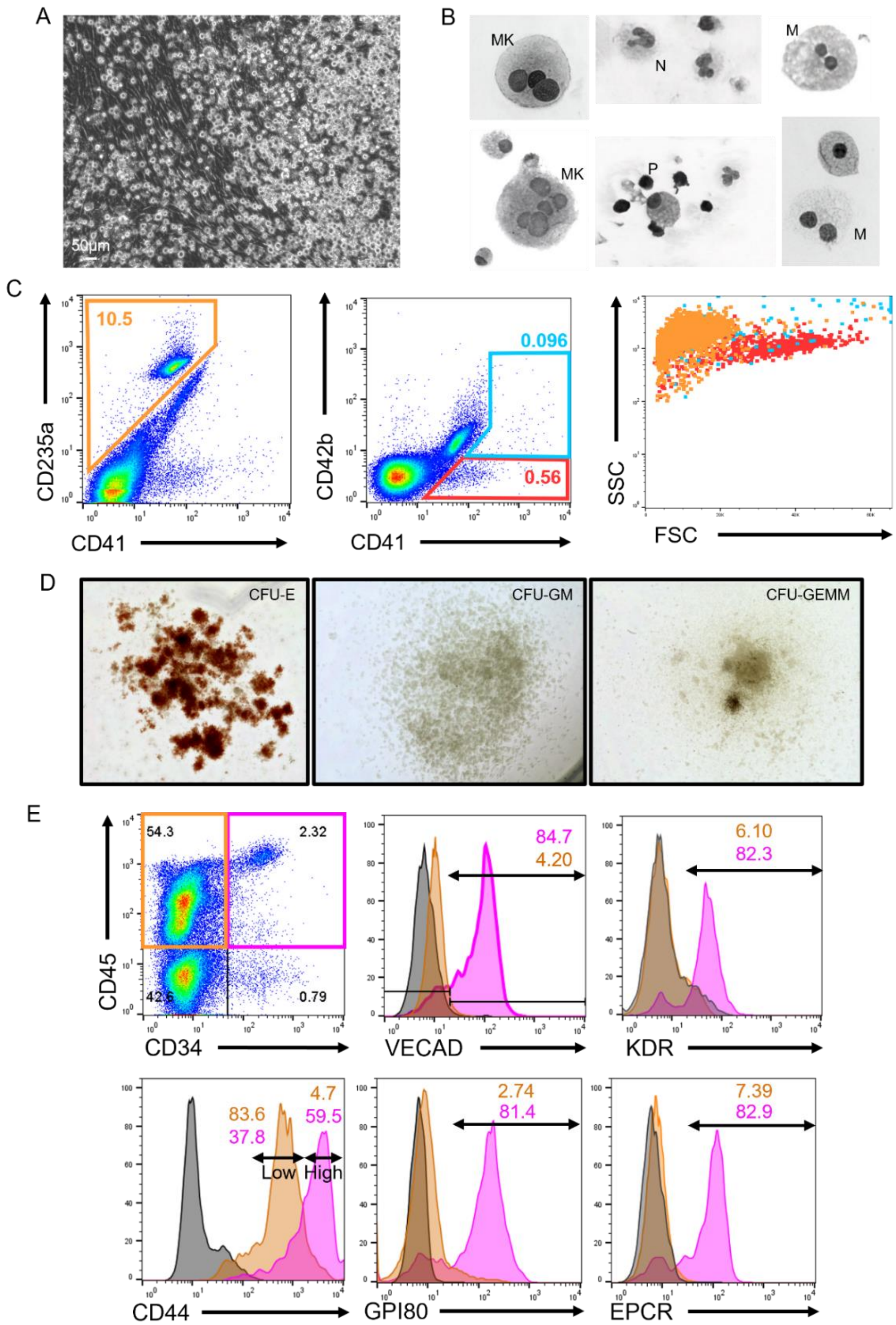

Figure 3.4. Human fetal lung explants undergo EHT to produce HSPCs. (A) Image of a human fetal lung explant culture showing a robust population of floating hematopoietic cells against a background of adherent cells. (B) Cytospin of human fetal lung suspension cells. (C) Flow cytometric assessment of differentiated erythrocyte and megakaryocyte populations. (D) Images of representative colonies from a CFU assay. (E) Assessment of pre-HSC and EHT markers on CD34+/CD45+ defined progenitors versus CD34-/CD45+ differentiated hematopoietic cells.

Hematopoietic clusters are a common histological hallmark of EHT occurring within the AGM and can be found in other organs that exhibit EHT including the placenta, and the umbilical and vitelline arteries[189]. To investigate whether fetal lung EHT can occur in-vivo we performed immunofluorescent staining of fixed-frozen human fetal lung sections. Immunofluorescent analysis revealed distinct regions of colocalized cells co-expressing the broad hematopoietic marker CD45, the endothelial marker VE-Cadherin, and the pre-HSC marker CD41a (**Figure 3.5A**). Additional staining for E-Cadherin suggests that these regions of EHT are not localized within the developing lung epithelium (**Figure 3.5B**).

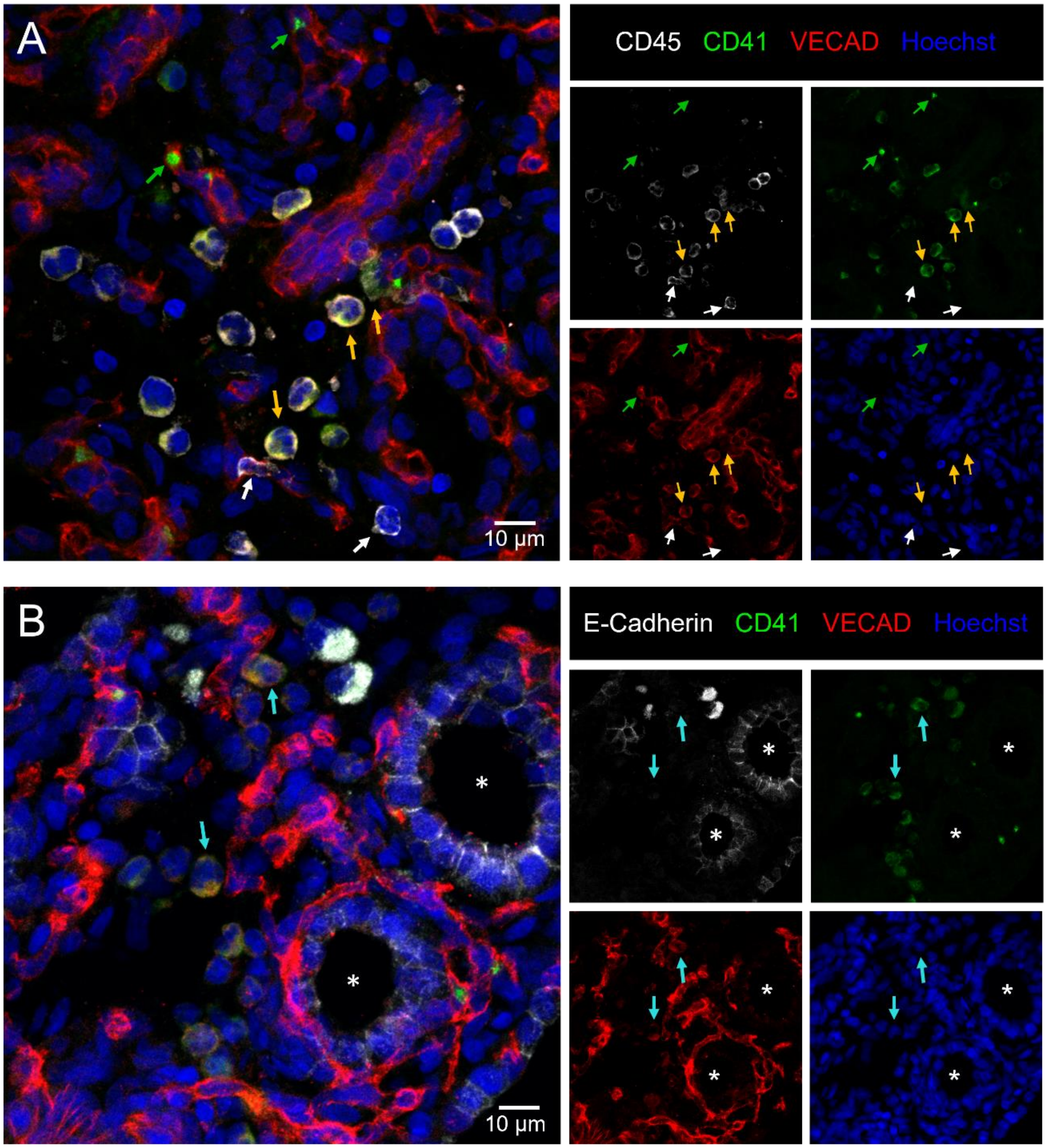

Figure 3.5. Immunofluorescent staining of in-situ fetal lung EHT. 12µm sections of a fixed frozen post-conception week 20 human fetal lung stained with the broad hematopoietic marker CD45, the EHT marker CD41, the endothelial marker VECAD, the epithelial cell marker E-Cadherin, and the nuclear stain Hoechst. (A) Cells co-expressing VECAD, CD41 and CD45 are highlighted with yellow arrows. Anucleate platelets single positive for CD41 are highlighted with green arrows. Differentiated hematopoietic cells only positive for CD45 are highlighted with white arrows. (B) Cells co-expressing VECAD and CD41 are highlighted with teal arrows, demonstrating they are not in developing E-Cadherin+ epithelial spaces, which are highlighted by a white asterisk.

Single cell transcriptomic mapping of murine fetal lung EHT

To map the developmental trajectory of cells produced in the murine fetal lung explant model system and to illustrate the repertoire of cells involved in the process, Single cell RNA sequencing (scRNA-Seq) was performed. The optimal time window for EHT in our model was determined to be from days 4-6 with the peak of $CD45^{+}/VECAD^{lo}$ cells on day 5 (**Figure 3.6A**). Since cells that have recently undergone EHT transiently retain expression of VECAD, adherent cells were collected into a single cell suspension and sorted for $VECAD^{+}$ to enrich for both endothelial cells and cells undergoing transition (**Figure 3.6B**). To ensure the capture of progenitor cells as well as differentiated cells that have downregulated VECAD post-EHT, suspension cells were collected for sequencing but left unsorted. The single cell capture and processing was performed using the Chromium 10x Genomics platform, and subsequently sequenced using the Illumina NextSeq 2000 platform. A schematic of the sequencing methodology as well as cell capture numbers and read depth can be found in **Figure 3.6C**, **D**.

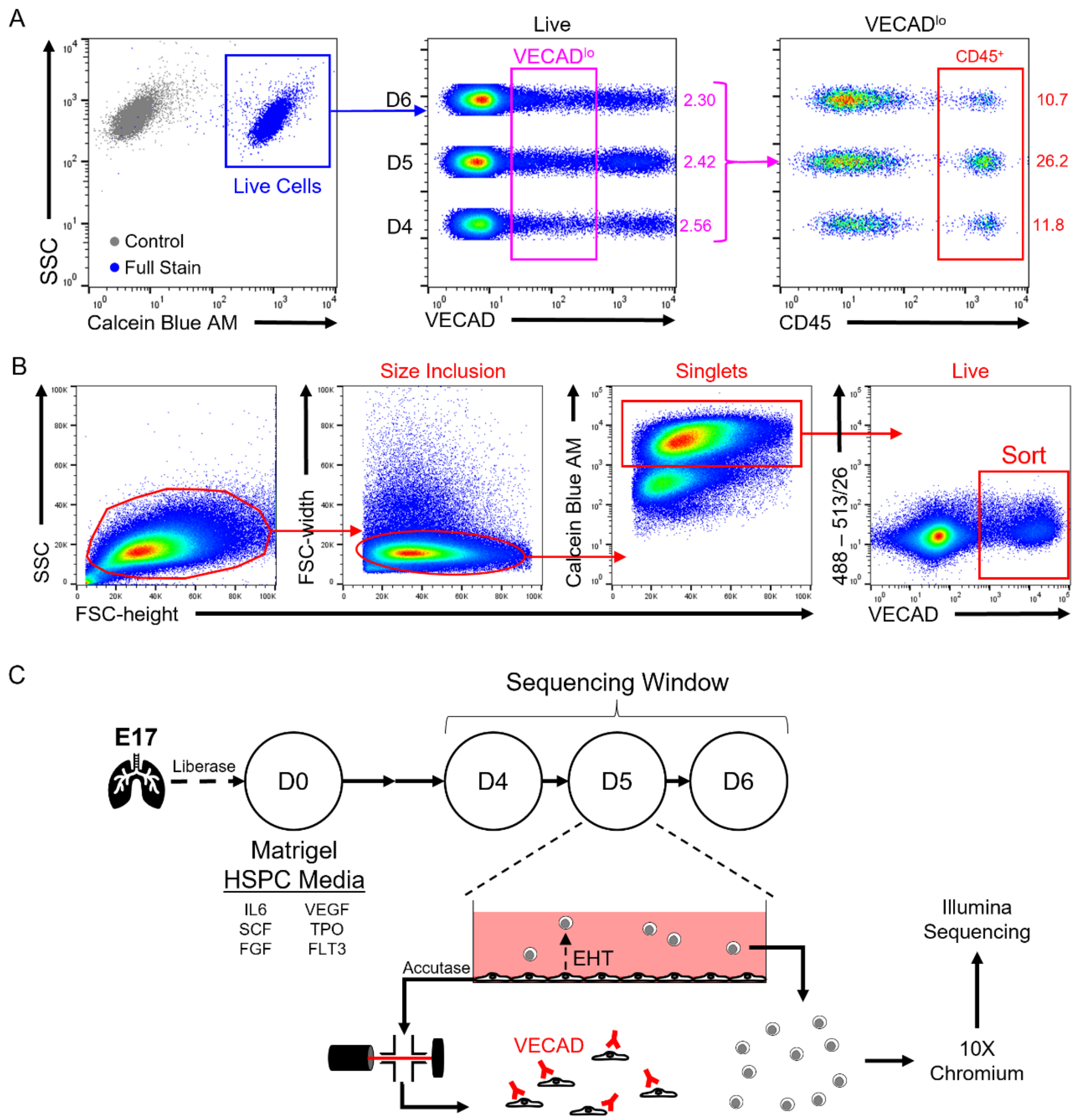

D

Metric	Day 4 Suspension	Day 4 Adherent	Day 5 Suspension	Day 5 Adherent	Day 6 Suspension	Day 6 Adherent
Estimated Number of Cells	2693	532	2497	1099	1398	1915
Mean Reads per Cell	16139	68754	17906	34019	39497	21106
Median Genes per Cell	2863	5681	2994	4098	3883	3162

Figure 3.6. Optimization of scRNA-Seq protocol and analysis. (A) Comparison of the fraction of VECADlo cells that are CD45+. (B) Sorting strategy for scRNA-Seq of adherent cells from fetal lung explants. (C) Schematic of scRNA-Seq procedure. (D) Table showing baseline metrics of scRNA-Seq analysis.

SPRING analysis revealed a trajectory of cells transitioning from an adherent to a suspension state through 3 distinct clusters: endothelial, transitional, and hematopoietic (**Figure 3.7A**, **B**). Supervised gene expression analyses of canonical endothelial markers showed robust expression and subsequent downregulation in the endothelial and transitional populations, respectively (**Figure 3.7C**). Analysis of genes previously described to be important during EHT, many of which were recently reviewed[185], highlighted the expression of these key markers at a discrete stage of EHT. For example, *Notch1*, *Jag1*, *Dll4*, and *Sox17* were largely isolated to the endothelial cell stage. In contrast, *Yap1* and *Tead1* demonstrated sustained expression through the transitional cell stage. These results are in agreement with other reports demonstrating that *Notch1* and *Sox17* are critical in the early patterning of HECs, but their continued expression throughout EHT can be restrictive[210,211]. In contrast, Yap was previously shown to be critical in the maintenance of EHT, but not its initiation[193]. Lastly, expression of *Lyve1* was predominantly expressed during the endothelial stage, which suggests the production of a definitive wave of hematopoiesis[212].

As cells transitioned to hematopoietic commitment, they began expressing key pre-HSPCs genes including *Cdca7*, *Myb*, *Gfi1* and *Spn* (CD43) (**Figure 3.7C**). Expression of *Cdca7* was previously demonstrated to be isolated to pre-HSC populations found within AGM intra-aortic hematopoietic clusters[213]. *Myb* is critical in HSC maintenance and proliferation[214], *Gfi1* is critical in mediating the loss of an endothelial identity[215], and *Spn* (CD43) is a known marker of early pre-HSCs[207,216]. Notably, expression of these genes was primarily isolated to early progenitor clusters and decreased along the trajectory of maturation (**Figure 3.8A**), which is in agreement with other reports showing that their downregulation is necessary to allow for competent differentiation.

Complementary to these supervised analyses, unsupervised analysis of the top 50 differentially expressed genes showed that transitional cells retain the expression of genes involved in the downregulation of angiogenesis as they differentiate away from an endothelial fate (**Figure 3.7D**, **Figure 3.8B**). This coincided with the upregulation of genes critical in extracellular matrix (ECM) organization as these cells undergo a physical transition from an adherent to a suspension state. In agreement with these findings, others have demonstrated that the emergence of hematopoietic cells from HECs relies on the *Runx1* mediated upregulation of genes involved in ECM organization, cell adhesion and cell migration[217]. Many of the same genes, including *Runx1*, were upregulated predominantly within the transitional cluster (**Figure 3.7C**, **D**).

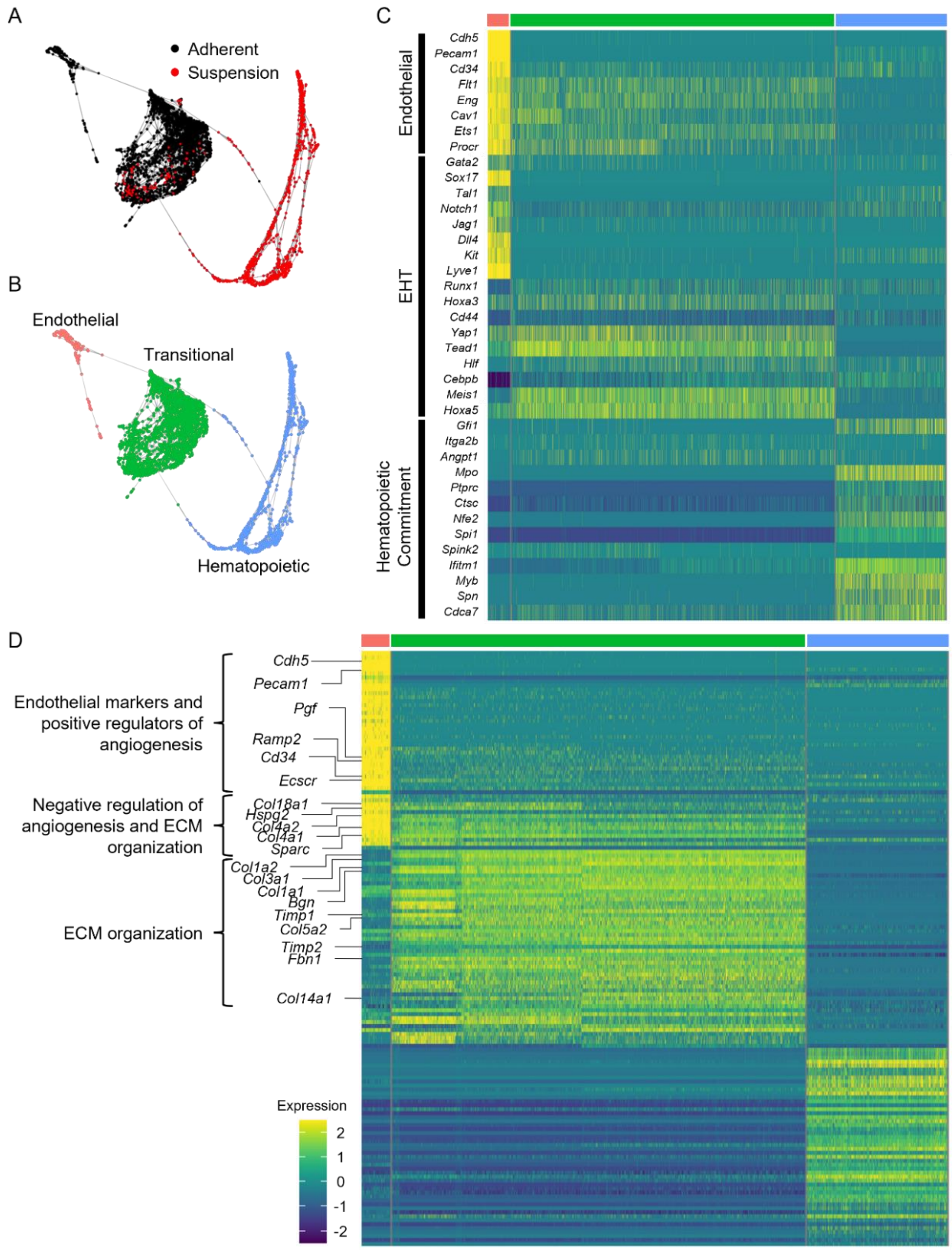

Figure 3.7. Single cell transcriptomic mapping of murine fetal lung EHT. (A, B) SPRING plot trajectory of EHT clusters. (C) Heatmap of supervised gene expression analysis of endothelial, EHT and hematopoietic commitment markers. (D) Heatmap of unsupervised analysis of the top 50 differentially expressed genes. Representative gene ontology analysis is highlighted here along with the associated genes enriched in these biological processes.

A

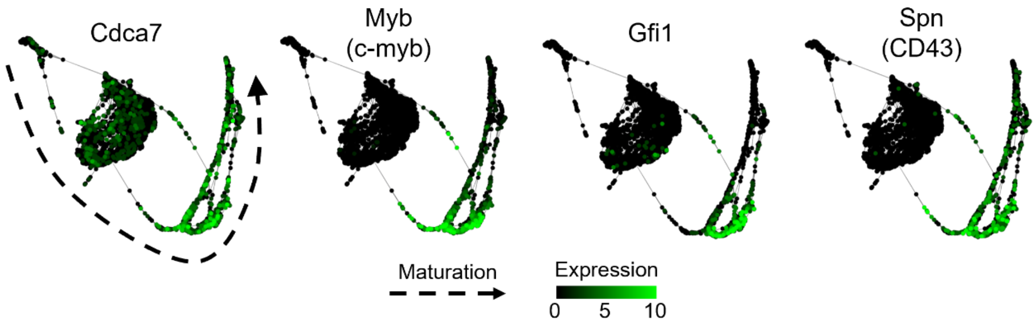

B

Cluster	Index	Name	p-value
Endothelial	1	regulation of angiogenesis (GO:0045765)	3.55E-08
	2	apical junction assembly (GO:0043297)	2.14E-06
	3	bicellular tight junction assembly (GO:0070830)	2.58E-05
	4	blood vessel morphogenesis (GO:0048514)	2.58E-05
	5	tight junction assembly (GO:0120192)	2.58E-05
	6	glomerulus vasculature development (GO:0072012)	2.58E-05
	7	cell-cell junction assembly (GO:0007043)	4.79E-05
	8	maintenance of blood-brain barrier (GO:0035633)	5.71E-05
	9	extracellular structure organization (GO:0043062)	5.71E-05
	10	external encapsulating structure organization (GO:0045229)	5.71E-05
Transitional	1	extracellular matrix organization (GO:0030198)	3.99E-05
	2	skin morphogenesis (GO:0043589)	0.000173
	3	muscle contraction (GO:0006936)	0.000173
	4	extracellular structure organization (GO:0043062)	0.000173
	5	external encapsulating structure organization (GO:0045229)	0.000173
	6	skin development (GO:0043588)	0.000222
	7	supramolecular fiber organization (GO:0097435)	2.69E-04
	8	collagen fibril organization (GO:0030199)	2.82E-04
	9	regulation of membrane protein ectodomain proteolysis (GO:0051043)	1.95E-03
	10	negative regulation of dendritic cell differentiation (GO:2001199)	4.07E-03
Hematopoietic	1	neutrophil degranulation (GO:0043312)	2.92E-13
	2	neutrophil activation involved in immune response (GO:0002283)	2.92E-13
	3	neutrophil mediated immunity (GO:0002446)	2.92E-13
	4	defense response to bacterium (GO:0042742)	2.61E-09
	5	leukocyte aggregation (GO:0070486)	0.000104
	6	defense response to Gram-negative bacterium (GO:0050829)	0.000112
	7	neutrophil migration (GO:1990266)	1.25E-04
	8	innate immune response (GO:0045087)	7.64E-04
	9	regulation of phagocytosis (GO:0050764)	8.85E-04
	10	myeloid cell activation involved in immune response (GO:0002275)	8.85E-04

Figure 3.8. SPRING and DGE analysis of fetal lung scRNA-Seq. (A) SPRING plots showing the expression of key hematopoietic commitment markers. The dotted arrow represents the trajectory of maturation. (B) Extended list of Gene Ontology biological processes enrichment analysis.

Fetal Lung EHT is functionally reliant on canonical developmental pathways

To functionally assess the dependence of fetal lung EHT on Notch signaling, the Notch inhibitor, Compound E, was applied to explant cultures. Application of Compound E led to a significant reduction in VECAD$^+$/CD45$^+$ pre-HSPCs (**Figure 3.9B**, **C**). This is in line with other reports demonstrating that in-vitro Notch inhibition and in-vivo transgenic knockout of Notch1 specifically blocks EHT, but the proliferation, differentiation, and maintenance of HSPCs is conserved[210,218].

In addition to the Notch family genes described previously, gene expression analysis demonstrated that fetal lung HECs exhibit the dynamic regulation of TGFβ/BMP pathways required for EHT. Similar to Notch, TGFβ/BMP pathways are important in the early patterning of HECs, but their subsequent inhibition is required for EHT[211,219–221]. Expression of key mediators of TGFβ/BMP signaling, including *Smad1*, *Smad5*, *Acvrl1* and *Tgfbr2*, peaked at the endothelial stage and was progressively downregulated throughout EHT (**Figure 3.9A**). Driving this downregulation was the concurrent upregulation of the TGFβ/BMP inhibitors *Smad7*, *Bmper* and *Ltbp1*.

To assess the dependence of TGFβ signaling in fetal lung EHT, the TGFβ receptor inhibitor, SB431542, and recombinant TGFβ2 were applied to explant cultures. Application of recombinant TGFβ2 led to a significant reduction in VECAD$^+$/CD45$^+$ pre-HSPCs (**Figure 3.9B**, **C**). In contrast, SB431542 did not significantly affect the production of VECAD$^+$/CD45$^+$ pre-HSPCs. However, SB431542 induced a significant increase in the intensity of VECAD expression, while TGFβ2 caused a reduction (**Figure 3.9D**, **E**). While others have shown that SB431542 treatment can enhance the production of HSPCs[211,222], these findings suggest that there is already sufficient inhibition from the upregulation of TGFβ/BMP inhibitors discussed previously.

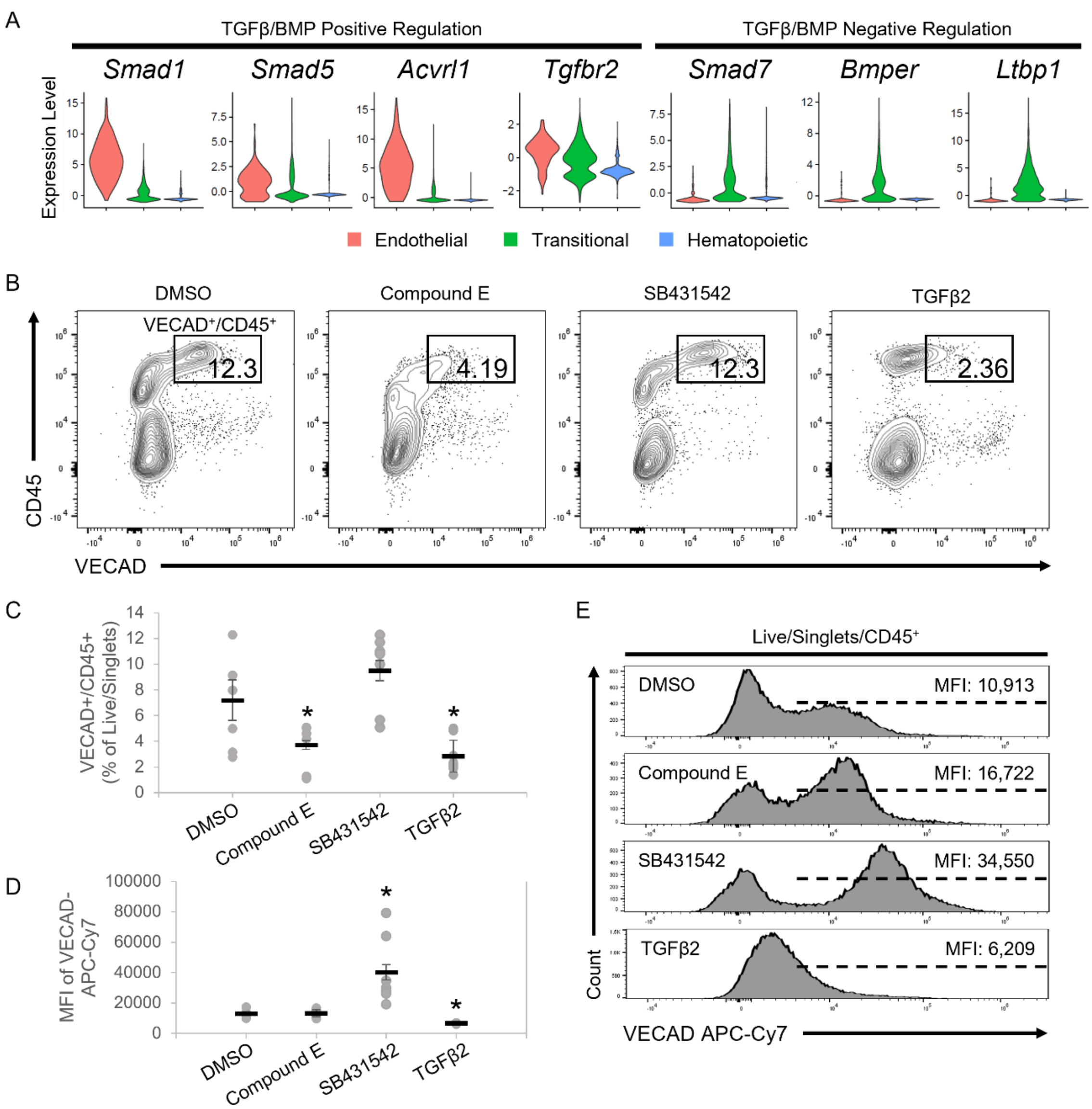

Figure 3.9. Fetal Lung EHT is functionally reliant on canonical developmental pathways. (A) Violin plots of expression of TGFβ/BMP pathways genes. (B) Representative flow cytometry plots demonstrating the change in CD45+/VECAD+ progenitors post-treatment with the Notch inhibitor Compound E, the TGFβ inhibitor SB431542, and recombinant TGFβ2. (C) Counts of CD45+/VECAD+ progenitors post-treatment. (D) Average MFI of VECAD expression post-treatment. (E) Representative histograms of VECAD expression post-treatment. Error bars represent standard deviation. *P < 0.01 compared to DMSO control.

DISCUSSION

Although not defined as a hematopoietic organ, the lung houses many resident blood cells that carry out both broad and tissue specific hematopoietic functions. Immune surveillance in the lung is carried out via unique resident immune cells, including dendritic cells, T-cells, B-cells, alveolar macrophages, interstitial macrophages, innate lymphoid cells and natural killer cells[66,76]. Supporting these classical immune cells are lung-resident megakaryocytes, which have a unique immune phenotype in addition to carrying out platelet biogenesis[223,224]. Lastly, the murine lung has been demonstrated to house HSPCs[55,83,192]. Complementary to these prior findings, we have demonstrated here that the murine and human fetal lungs are a source of functional HECs capable of giving rise to HSPCs. This suggests that the developing lung may have a more direct role in hematopoiesis than previously thought.

Although we have demonstrated the presence of fetal pulmonary HECs, the physiological significance of de-novo hematopoiesis occurring outside of the AGM and in the lung remains unclear. The potential need for the fetal lung to have an alternative source of blood may stem from the fact that most blood is shunted away from the fetal lung because oxygenation is provided via the mother. As a result, the developing murine lung only receives about 16% of total circulating blood[167]. The de-novo generation of blood in the fetal lung may act as an additional in-situ source of essential blood products for organogenesis. This is an important consideration when accounting for the role of macrophages and platelets in both organogenesis and angiogenesis[56,225–227]. Notably, the origins of many lung resident blood cells are not fully understood, but to date, the origins of resident macrophages are the most well studied.

Lung macrophages are derived from three distinct developmental waves originating from the yolk sac, fetal liver and BM[78]. Each wave persists into adulthood and occupies unique niches within the lung[72]. Recent work also suggests that such developmentally and phenotypically distinct subsets of macrophages may also extend to the heart, liver, kidney, and brain[80]. These findings demonstrate the complex diversity seen throughout hematopoietic development and how each phase individually makes significant physiological contributions. As such, the differentiation capacity of lung HECs requires further investigation to determine whether lung HECs contribute to the in-situ development of lung hematopoietic populations.

While often discussed as the precursor to HSCs, HECs also give rise to other blood progenitors. A subset of placental HECs lineage traced by *Hoxa13* preferentially form placental macrophages, termed Hofbauer cells, that remain solely in the placenta[228]. This finding also suggests that differentiation capacity and bias may already be predetermined at the HEC stage, which others have also proposed. THBS1 marks a subset of human embryonic stem cell derived endothelial cells that are biased towards megakaryopoiesis[28]. *Ly6a* versus *Tek* expression marks HECs with HSC versus EMP potential, respectively[229]. CXCR4 expression differentiates AGM derived HECs with HSC versus MPP potential[230].

Others have described the presence of functional HSCs in E16 murine fetal lungs. However, LSK progenitors only make up on average about 0.02% of the total fetal lung cell isolate, compared to 0.75% in the adult BM[83]. This low number of HSPCs suggests that the role of fetal lung HECs may not contribute significantly to the progenitor cell pool and instead are skewed towards the immediate production of differentiated cell populations.

While more in-vivo work is required to determine the developmental trajectory and potency of lung HECs, the contributions of hematopoiesis that are not reliant on long-term HSCs are important to consider. Indeed, the majority of embryonic hematopoiesis is maintained by a pool of yolk sac derived erythro-myeloid progenitors (EMPs) that reside in the fetal liver[231,232]. EMPs give rise to the majority of tissue resident macrophages that persist into adulthood[233], and embryonic erythrocyte production is sustained primarily from EMPs[234]. In addition to EMPs, transient HSCs that do not persist into adulthood have also been demonstrated to be involved in the establishment of the developing hematopoietic system. *Tie2*-Cre lineage tracing studies suggest that fetal HSCs that contribute to establishment of the developing hematopoietic system differentiate rapidly, which is in stark contrast to adult long term HSCs that are relatively quiescent[235]. Studies utilizing the

Flk2-Cre tracer model (FlkSwitch) also demonstrate the existence of a transient population of HSCs with a lymphoid bias[236,237]. Although fulfilling the classic definition of an HSC based on their capacity for long-term multi-lineage reconstitution, these transient HSCs are only present from E10.5 until P14.

Notably, the fetal lung HECs described here were isolated from E17 mice, which is outside of the window of EHT within the AGM (E9.5-11.5). Work from Yvernogeau et al. also suggests that EHT can occur beyond this AGM window within the perinatal bone marrow[191]. They noted that perinatal sources of hematopoiesis occur at a time when HSC expansion in the fetal liver has stopped (~E17) and the BM niche is still maturing in order to support the long-term residency of adult HSCs. Later stage EHT in the lung may thus aid in minimizing the need for long term HSC-dependent hematopoiesis during early development.

Niche interactions are another critical component of driving EHT[84,238]. Induction of key developmental pathways via secreted ligands is spatially organized within the AGM and influence the potency of resultant progenitors[198]. Replicating these conditions is thus critical in simulating EHT in an in-vitro setting. Most other employed methods of ex-vivo HEC cultures are reliant on the utilization of a supportive feeder cell layer, such as OP9 cells or immortalized AKT endothelial cells, to instruct EHT[218,239]. Notably, fetal lung explants undergo EHT without such feeders, which suggests that the lung independently has the cellular makeup to support EHT. However, further investigation is required to determine the cell-specific interactions of the in-vivo microenvironment where EHT would occur and how the lung niche instructs local HEC development.

Altogether, the findings described here demonstrate the existence of functionally validated HECs in the fetal lung, a population which is also conserved in humans. Given the diversity in HEC development and the significance of each distinct wave of hematopoiesis, the physiological influence of lung HEC development in-vivo needs further investigation. Expanding our overall understanding of HEC location and timing will also aid towards the goal of fully understanding the biological cues required for the development of functional HECs. Such findings can eventually be harnessed for the common goal of producing putative HSCs and functionally mature hematopoietic cells from pluripotent stem cells.

CHAPTER FOUR: SUMMARY AND FUTURE DIRECTIONS

Summary

We herein describe the characterization of the lung as a significant site of hematopoietic development. We first demonstrated the lung's role in the functionalization of a distinct lung MK population with a uniquely immune phenotype. Notably, the development of the immune lung-MK phenotype arises during embryogenesis when the lung microenvironment is sterile. This suggests that the cellular milieu specific to the lung is priming the local hematopoietic population for the eventual post-natal exposure to foreign antigens, which we and others have shown further matures MKs to develop more antigen presentation capacity[223]. The stage of megakaryopoiesis at which the immune programming initially occurs is not known. However, others have demonstrated that HSCs are preferentially primed towards megakaryopoiesis, and this MK priming may even be predetermined at the hemogenic endothelial stage[28,240]. This provides an important context for understanding the potential significance of the herein described fetal lung HECs. We have demonstrated that the fetal lung is a source of HECs with the capacity to undergo EHT to produce HSPCs with multi-lineage differentiation capacity, including megakaryopoiesis. This suggests the possible existence of a lung HEC to lung MK axis wherein local HEC development is directed to produce lung specific MKs. However, the lineage capacity of lung HECs and thus their overall contributions to pulmonary and hematopoietic physiology remains to be determined.

Future Directions

In our studies, explant cultures were the primary methodology employed to investigate lung HECs. This ex-vivo methodology removes these cells from their microenvironment, thus limiting our understanding of these cells in their native in-vivo context. Of note, we do not believe we have induced the direct conversion of endothelial cells as direct conversion involves the forced overexpression of select transcription factors to competently induce transdifferentiation[185]. However, this still leaves many questions about whether these cells under steady state conditions in-vivo will naturally undergo EHT and what their contributions are to hematopoietic development in the lung.

Lineage tracing would be very useful in this regard, but current models designed to trace endothelial and hematopoietic progenitor populations have significant limitations. While many lineage tracing models have been developed to trace either endothelial cell or HSPC populations individually, all models exhibit a significant amount of recombination events across both populations, especially during embryonic development[241]. As such, application of these methods would still not sufficiently answer such questions when considering the rarity of HECs and the existence of circulating HSPCs, especially during the embryonic migration of HSPCs exiting the fetal liver[242].

Combinatorial tracer models could potentially alleviate some of these concerns. GATA2 is a transcription factor that is critical during EHT. However, transgenic knockout of GATA2 does not impede the self-renewal and differentiation of HSCs[243,244]. Using a floxed GATA2 mouse crossed with an inducible VECAD-Cre-ERT2 mouse would allow for tamoxifen induced ablation of EHT post-AGM development. In theory, this would provide insight into how HEC populations outside of the AGM time window contribute to hematopoiesis. However, this model, as well as the majority of other Cre-based models, would still have the lingering issue of not being tissue specific.

An inducible barcoding model could potentially be utilized to allow for the tracing of hematopoietic progeny back to a tissue specific progenitor cell[245]. However, others have previously noted that EHT is not the result of asymmetric cell division[204]. As such, a parent endothelial cell to trace the resultant hematopoietic progeny back to would not exist and negates the utility of such a method. Development of novel combinatorial technologies to trace organ specific cell populations will greatly support these endeavors.

Organ specific tracing of lung MKs would also be an important avenue of investigation as the origin of platelet subsets is not known. Notably, subsets of platelets expressing more immune markers have been previously identified, and immune MKs have been described in both the lung and the BM[110]. However, of the 3 MK subsets found in the BM, immune MKs are the furthest away from the BM sinusoids and are unable to produce platelets ex-vivo[27]. This suggests that BM immune MKs may not significantly contribute to overall platelet mass. In contrast, work from ourselves and others have demonstrated that lung MKs have a more uniform phenotype, and ex-vivo assays demonstrate their ability to produce platelets[223]. This suggests that the bulk of immune platelets may be derived from lung MKs. The development of a lineage tracing model specific to lung MKs and/or the application of barcoding to lung MKs to trace what type(s) of platelets they produce would be essential in investigating the overall contributions of lung MKs to circulating platelet mass.

Future Applications

Understanding the developmental underpinnings of lung HECs and MKs has a wide range of potential applications. Emerging evidence suggests that in order to develop putative HECs imbued with the potential to produce engraftable HSCs requires a complete understanding of the patterning cues that precede the HEC stage[185]. This understanding is critical for applications involving the directed differentiation of pluripotent stem cells (PSCs) through critical developmental stages to produce in-vitro blood products. To this end, understanding how the lung mechanistically directs HEC development and EHT will further inform what developmental cues are necessary for this patterning to occur.

Beyond progenitor staging, patterning of MKs with in-vitro PSC based methodologies also has significant roadblocks. MK differentiations are currently very inefficient in producing PSC-derived MKs[246]. Novel methods have been developed to overcome these barriers and continue to evolve with time. For example, the Eto Lab developed a method of expanding PSC derived MK progenitors through the use of immortalization to produce what they termed imMKCLs that can be passaged for months[247]. However, these MKs still lack the maturity and diversity observed across in-vivo MKs. The subsequent in-vitro development of platelets from PSC derived MKs is also very limited. The most efficient method described to date involves a turbulent flow-based bioreactor developed by the Eto lab that can produce on average about 70-80 platelets per MK[160]. These two methods combined were a significant leap in efficiency, but still paled in comparison to the estimated 1,000 platelets produced per MK in-vivo[248].

Knowledge of how the cellular and physical architecture of the lung supports thrombogenesis could be applied towards developing more efficient methods of in-vitro platelet biogenesis. For example, a recent preprint publication suggests that the transfusion of MKs through an ex-vivo lung's vasculature may increase platelet yield to upwards of 1,000 platelets per MK[249]. They further suggest that healthy lung endothelium is an important component to the lung's capacity to efficiently support thrombopoiesis. As such, understanding the cell-cell mechanisms involved in the induction of lung thrombogenesis could be useful towards the further development of in-vitro based bioreactors. Understanding these cellular cues also has potential therapeutic applications. For example, local delivery of thrombopoiesis inducing small molecules to the lung via tools like a nebulizer could be a potential avenue for the rapid and minimally invasive treatment of thrombocytopenia.

Conclusion

Overall, findings from the studies described here expand on the important notion that hematopoietic development is a diverse, multifactorial process that involves many organs.

We describe newly defined roles for the lung in both adult and developmental hematopoiesis that suggests the lung may have a greater responsibility in blood development than was previously thought. Identifying ways to harness the hematopoietic potential of the lung will aid in the development of novel methods of in-vitro directed hematopoiesis that will significantly impact the future of cellular therapeutics.

BIBLIOGRAPHY

1. Schmitt, A., Guichard, J., Massé, J.-M., Debili, N. & Cramer, E. M. Of mice and men: Comparison of the ultrastructure of megakaryocytes and platelets. *Experimental Hematology* **29**, 1295–1302 (2001).
2. Lee, H. O., Davidson, J. M. & Duronio, R. J. Endoreplication: polyploidy with purpose. *Genes & Development* **23**, 2461–2477 (2009).
3. Mazzi, S., Lordier, L., Debili, N., Raslova, H. & Vainchenker, W. Megakaryocyte and polyploidization. *Experimental Hematology* **57**, 1–13 (2018).
4. Cosgrove, J., Hustin, L. S. P., Boer, R. J. de & Perié, L. Hematopoiesis in numbers. *Trends in Immunology* **0**, (2021).
5. Bleeker, J. S. & Hogan, W. J. Thrombocytosis: Diagnostic Evaluation, Thrombotic Risk Stratification, and Risk-Based Management Strategies. *Thrombosis* **2011**, 536062 (2011).
6. Trier, D. A. *et al.* Platelet Antistaphylococcal Responses Occur through P2X1 and P2Y12 Receptor-Induced Activation and Kinocidin Release. *Infection and Immunity* (2008) doi:10.1128/IAI.00935-08.
7. Gafter-Gvili, A. *et al.* Thrombocytopenia in Staphylococcus aureus bacteremia: risk factors and prognostic importance. *Mayo Clinic Proceedings* **86**, 389–396 (2011).
8. Vanderschueren, S. *et al.* Thrombocytopenia and prognosis in intensive care. *Critical Care Medicine* **28**, 1871–1876 (2000).
9. Gurung, A. M., Carr, B. & Smith, I. Thrombocytosis in intensive care. *British Journal of Anaesthesia* **87**, 926–928 (2001).

10. Eisinger, F., Patzelt, J. & Langer, H. F. The Platelet Response to Tissue Injury. *Frontiers in Medicine* **5**, (2018).

11. Gawaz, M. & Vogel, S. Platelets in tissue repair: control of apoptosis and interactions with regenerative cells. *Blood* **122**, 2550–2554 (2013).

12. Koupenova, M., Livada, A. C. & Morrell, C. N. Platelet and Megakaryocyte Roles in Innate and Adaptive Immunity. *Circulation Research* **130**, 288–308 (2022).

13. Lesyk, G. & Jurasz, P. Advances in Platelet Subpopulation Research. *Frontiers in Cardiovascular Medicine* **6**, (2019).

14. Karpatkin, S. & Charmatz, A. Heterogeneity of human Platelets: *I. Metabolic and kinetic evidence suggestive of young and old platelets*. *The Journal of Clinical Investigation* **48**, 1073–1082 (1969).

15. Polanowska-Grabowska, R., Raha, S. & Gear, A. R. L. Adhesion efficiency, platelet density and size. *British Journal of Haematology* **82**, 715–720 (1992).

16. Thompson, C. B., Eaton, K. A., Princiotta, S. M., Rushin, C. A. & Valeri, C. R. Size dependent platelet subpopulations: relationship of platelet volume to ultrastructure, enzymatic activity, and function. *British Journal of Haematology* **50**, 509–519 (1982).

17. Blair, T. A., Michelson, A. D. & Frelinger, A. L. Mass Cytometry Reveals Distinct Platelet Subtypes in Healthy Subjects and Novel Alterations in Surface Glycoproteins in Glanzmann Thrombasthenia. *Scientific Reports* **8**, 10300 (2018).

18. Chapman, L. M. *et al.* Platelets Present Antigen in the Context of MHC Class I. *The Journal of Immunology* **189**, 916–923 (2012).

19. Spurgeon, B. E. J. & Frelinger III, A. L. Comprehensive phenotyping of human platelets by single-cell cytometry. *Cytometry Part A* **n/a**,.

20. Hally, K., Fauteux-Daniel, S., Hamzeh-Cognasse, H., Larsen, P. & Cognasse, F. Revisiting Platelets and Toll-Like Receptors (TLRs): At the Interface of Vascular Immunity and Thrombosis. *International Journal of Molecular Sciences* **21**, 6150 (2020).

21. Gurses, K. M. *et al.* Enhanced Platelet Toll-like Receptor 2 and 4 Expression in Acute Coronary Syndrome and Stable Angina Pectoris. *The American Journal of Cardiology* **116**, 1666–1671 (2015).

22. Gurses, K. M. *et al.* Platelet Toll-like receptor and its ligand HMGB-1 expression is increased in the left atrium of atrial fibrillation patients. *Cytokine* **103**, 50–56 (2018).

23. Claushuis, T. A. M. *et al.* Platelet Toll-like receptor expression and activation induced by lipopolysaccharide and sepsis. *Platelets* **30**, 296–304 (2019).

24. Teruel-Montoya, R. *et al.* MicroRNA Expression Differences in Human Hematopoietic Cell Lineages Enable Regulated Transgene Expression. *PLOS ONE* **9**, e102259 (2014).

25. Olson, T. S. *et al.* Megakaryocytes promote murine osteoblastic HSC niche expansion and stem cell engraftment after radioablative conditioning. *Blood* **121**, 5238–5249 (2013).

26. Zhao, M. *et al.* Megakaryocytes maintain homeostatic quiescence and promote post-injury regeneration of hematopoietic stem cells. *Nature Medicine* **20**, 1321–1326 (2014).

27. Sun, S. *et al.* Single-cell analysis of ploidy and the transcriptome reveals functional and spatial divergency in murine megakaryopoiesis. *Blood* **138**, 1211–1224 (2021).

28. Wang, H. *et al.* Decoding Human Megakaryocyte Development. *Cell Stem Cell* **0**, (2020).

29. Italiano, J. E., Jr *et al.* Angiogenesis is regulated by a novel mechanism: pro- and antiangiogenic proteins are organized into separate platelet α granules and differentially released. *Blood* **111**, 1227–1233 (2008).

30. Sehgal, S. & Storrie, B. Evidence that differential packaging of the major platelet granule proteins von Willebrand factor and fibrinogen can support their differential release. *Journal of thrombosis and haemostasis: JTH* **5**, 2009–2016 (2007).

31. Battinelli, E. M. *et al.* Megakaryocytes package contents into separate α-granules that are differentially distributed in platelets. *Blood Advances* **3**, 3092–3098 (2019).

32. Zufferey, A. *et al.* Mature murine megakaryocytes present antigen-MHC class I molecules to T cells and transfer them to platelets. *Blood Advances* **1**, 1773–1785 (2017).

33. Cunin, P. & Nigrovic, P. A. Megakaryocyte emperipolesis: a new frontier in cell-in-cell interaction. *Platelets* **31**, 700–706 (2020).

34. Cunin, P. *et al.* Megakaryocyte emperipolesis mediates membrane transfer from intracytoplasmic neutrophils to platelets. *eLife* **8**, e44031 (2019).

35. Aschoff, L. Ueber capilläre Embolie von riesenkernhaltigen Zellen. *Archiv für pathologische Anatomie und Physiologie und für klinische Medicin* **134**, 11–25 (1893).

36. BRILL, R. & HALPERN, M. M. THE FREQUENCY OF MEGAKARYOCYTES IN AUTOPSY SECTIONS. *Blood* **3**, 286–291 (1948).

37. Orbison, J. L. & Laipply, T. C. Pneumococcal lobar pneumonia associated with megakaryocytic and leukoblastic hyperplasia. *Ohio State Medical Journal* 41:148 (1945).

38. Bunting, C. H. Blood platelets and megakaryocytes in Hodgkin's disease. *Johns Hopkins Bull.* 22:114 (1911).

39. Downey, H., Palmer, M. & Powell, L. The origin of the megakaryocytes in the spleen and liver in a case of atypical myelosis. *Folia haemat.* 41:55 (1930).

40. Medlar, E. M. & Sasano, K. T. The significance of lesions resembling Hodgkin's disease. *Am. J. Path.* 7:491 (1931).

41. Petri, S. Uber das intravaskulare Vorkommen der Megakaryozyten beim Menschen. *Folia haemat.* 37:129 (1931).

42. Abramson, N. & Melton, B. Leukocytosis: basics of clinical assessment. *American Family Physician* **62**, 2053–2060 (2000).

43. Aksu, K., Donmez, A. & Keser, G. Inflammation-induced thrombosis: mechanisms, disease associations and management. *Current Pharmaceutical Design* **18**, 1478–1493 (2012).

44. Howell, W. H. & Donahue, D. D. THE PRODUCTION OF BLOOD PLATELETS IN THE LUNGS. *The Journal of Experimental Medicine* **65**, 177–203 (1937).

45. Kaufman, R. M., Airo, R., Pollack, S., Crosby, W. H. & Doberneck, R. Origin of Pulmonary Megakaryocytes. *Blood* **25**, 767–775 (1965).

46. Kallinikos-Maniatis, A. Megakaryocytes and Platelets in Central Venous and Arterial Blood. *Acta Haematologica* **42**, 330–335 (1969).

47. KAUFMAN, R. M., CAPTAIN, AIRO, R., POLLACK, S. & CROSBY, W. H., COLONEL. Circulating Megakaryocytes and Platelet Release in the Lung. *Blood* **26**, 720–731 (1965).

48. Trowbridge, E. A., Martin, J. F. & Slater, D. N. Evidence for a theory of physical fragmentation of megakaryocytes, implying that all platelets are produced in the pulmonary circulation. *Thrombosis Research* **28**, 461–475 (1982).

49. Breslow, A., Kaufman, R. M. & Lawsky, A. R. The effect of surgery on the concentration of circulating megakaryocytes and platelets. *Blood* **32**, 393–401 (1968).

50. Levine, R. F. Isolation and Characterization of Normal Human Megakaryocytes. *British Journal of Haematology* **45**, 487–497 (1980).

51. Tomer, A., Harker, L. A. & Burstein, S. A. Purification of human megakaryocytes by fluorescence-activated cell sorting. *Blood* **70**, 1735–1742 (1987).

52. Tomer, A., Harker, L. A. & Burstein, S. A. Flow cytometric analysis of normal human megakaryocytes. *Blood* **71**, 1244–1252 (1988).

53. Huang, H. & Cantor, A. B. Common Features of Megakaryocytes and Hematopoietic Stem Cells: What's the Connection? *Journal of cellular biochemistry* **107**, 857–864 (2009).

54. Fischer, U. M. *et al.* Pulmonary passage is a major obstacle for intravenous stem cell delivery: the pulmonary first-pass effect. *Stem Cells and Development* **18**, 683–692 (2009).

55. Lefrançais, E. *et al.* The lung is a site of platelet biogenesis and a reservoir for haematopoietic progenitors. *Nature* **544**, 105–109 (2017).

56. Tsukiji, N. *et al.* Platelets play an essential role in murine lung development through Clec-2/podoplanin interaction. *Blood* **132**, 1167–1179 (2018).

57. Rafii, S. *et al.* Platelet-derived SDF1 primes pulmonary capillary vascular niche to drive lung alveolar regeneration. *Nature cell biology* **17**, 123–136 (2015).

58. Bain, W. *et al.* Platelets inhibit apoptotic lung epithelial cell death and protect mice against infection-induced lung injury. *Blood Advances* **3**, 432–445 (2019).

59. Bozza, F. A., Shah, A. M., Weyrich, A. S. & Zimmerman, G. A. Amicus or adversary: platelets in lung biology, acute injury, and inflammation. *American Journal of Respiratory Cell and Molecular Biology* **40**, 123–134 (2009).

60. Fein, A. M., Lippmann, M., Holtzman, H., Eliraz, A. & Goldberg, S. K. The risk factors, incidence, and prognosis of ARDS following septicemia. *Chest* **83**, 40–42 (1983).

61. Wang, T. *et al.* Thrombocytopenia is associated with acute respiratory distress syndrome mortality: an international study. *PloS One* **9**, e94124 (2014).

62. Brogly, N. *et al.* Impact of thrombocytopenia on outcome of patients admitted to ICU for severe community-acquired pneumonia. *The Journal of Infection* **55**, 136–140 (2007).

63. Branton, M. H. & Kopp, J. B. TGF-β and fibrosis. *Microbes and Infection* **1**, 1349–1365 (1999).

64. Linge, P., Fortin, P. R., Lood, C., Bengtsson, A. A. & Boilard, E. The non-haemostatic role of platelets in systemic lupus erythematosus. *Nature Reviews Rheumatology* **14**, 195- (2018).

65. Weyrich, A. S. & Zimmerman, G. A. Platelets in Lung Biology. *Annual Review of Physiology* **75**, 569–591 (2013).

66. Ardain, A., Marakalala, M. J. & Leslie, A. Tissue-resident innate immunity in the lung. *Immunology* **159**, 245–256 (2020).

67. Yoshida, M. & Whitsett, J. A. Interactions between pulmonary surfactant and alveolar macrophages in the pathogenesis of lung disease. *Cellular and Molecular Biology (Noisy-Le-Grand, France)* **50 Online Pub**, OL639-648 (2004).

68. Forbes, A. *et al.* Alveolar macrophage depletion is associated with increased surfactant pool sizes in adult rats. *Journal of Applied Physiology (Bethesda, Md.: 1985)* **103**, 637–645 (2007).

69. van Iwaarden, J. F., Claassen, E., Jeurissen, S. H. M., Haagsman, H. P. & Kraal, G. Alveolar Macrophages, Surfactant Lipids, and Surfactant Protein B Regulate the Induction of Immune Responses via the Airways. *American Journal of Respiratory Cell and Molecular Biology* **24**, 452–458 (2001).

70. Bedoret, D. *et al.* Lung interstitial macrophages alter dendritic cell functions to prevent airway allergy in mice. *The Journal of Clinical Investigation* **119**, 3723–3738 (2009).

71. Kawano, H. *et al.* IL-10-producing lung interstitial macrophages prevent neutrophilic asthma. *International Immunology* **28**, 489–501 (2016).

72. Chakarov, S. *et al.* Two distinct interstitial macrophage populations coexist across tissues in specific subtissular niches. *Science* (2019) doi:10.1126/science.aau0964.

73. Lai, D.-M., Shu, Q. & Fan, J. The origin and role of innate lymphoid cells in the lung. *Military Medical Research* **3**, 25 (2016).

74. Humphries, D. C. *et al.* Pulmonary-Resident Memory Lymphocytes: Pivotal Orchestrators of Local Immunity Against Respiratory Infections. *Frontiers in Immunology* **12**, (2021).

75. Snyder, M. E. & Farber, D. L. Human lung tissue resident memory T cells in health and disease. *Current Opinion in Immunology* **59**, 101–108 (2019).

76. Barker, K. A. *et al.* Lung-resident memory B cells protect against bacterial pneumonia. *The Journal of Clinical Investigation* **131**, (2021).

77. Allie, S. R. *et al.* The establishment of resident memory B cells in the lung requires local antigen encounter. *Nature Immunology* **20**, 97–108 (2019).

78. Tan, S. Y. S. & Krasnow, M. A. Developmental origin of lung macrophage diversity. *Development (Cambridge, England)* **143**, 1318–1327 (2016).

79. Epelman, S., Lavine, K. J. & Randolph, G. J. Origin and Functions of Tissue Macrophages. *Immunity* **41**, 21–35 (2014).

80. Dick, S. A. *et al.* Three tissue resident macrophage subsets coexist across organs with conserved origins and life cycles. *Science Immunology* (2022) doi:10.1126/sciimmunol.abf7777.

81. Gasteiger, G., Fan, X., Dikiy, S., Lee, S. Y. & Rudensky, A. Y. Tissue residency of innate lymphoid cells in lymphoid and nonlymphoid organs. *Science* **350**, 981–985 (2015).

82. Hoffmann, F. *et al.* Origin, Localization, and Immunoregulatory Properties of Pulmonary Phagocytes in Allergic Asthma. *Frontiers in Immunology* **7**, (2016).

83. Hillel-Karniel, C. *et al.* Multi-lineage Lung Regeneration by Stem Cell Transplantation across Major Genetic Barriers. *Cell Reports* **30**, 807-819.e4 (2020).

84. Heck, A. M., Ishida, T. & Hadland, B. Location, Location, Location: How Vascular Specialization Influences Hematopoietic Fates During Development. *Frontiers in Cell and Developmental Biology* **8**, 602617 (2020).

85. Borges, I. *et al.* Lung as a Niche for Hematopoietic Progenitors. *Stem cell reviews* **13**, 567–574 (2017).

86. Hirakawa, H., Lee, Y. & Ding, L. The Fetal Hematopoietic Niche: Components and Mechanisms for Hematopoietic Stem Cell Emergence and Expansion. *Current Stem Cell Reports* (2022) doi:10.1007/s40778-021-00202-9.

87. Cunin, P. & Nigrovic, P. A. Megakaryocytes as immune cells. *Journal of Leukocyte Biology* (2019) doi:10.1002/JLB.MR0718-261RR.

88. Xu, X. R. *et al.* Platelets are versatile cells: New discoveries in hemostasis, thrombosis, immune responses, tumor metastasis and beyond. *Critical Reviews in Clinical Laboratory Sciences* **53**, 409–430 (2016).

89. Olumuyiwa-Akeredolu, O., Page, M. J., Soma, P. & Pretorius, E. Platelets: emerging facilitators of cellular crosstalk in rheumatoid arthritis. *Nature Reviews Rheumatology* (2019) doi:10.1038/s41584-019-0187-9.

90. Machlus, K. R. & Italiano, J. E. The incredible journey: From megakaryocyte development to platelet formation. *J Cell Biol* **201**, 785–796 (2013).

91. Lefrançais, E. & Looney, M. R. Platelet Biogenesis in the Lung Circulation. *Physiology* **34**, 392–401 (2019).

92. Levine, R. F. *et al.* Circulating megakaryocytes: Delivery of large numbers of intact, mature megakaryocytes to the lungs. *European Journal of Haematology* **51**, 233–246 (1993).

93. Pedersen, N. T. Occurrence of megakaryocytes in various vessels and their retention in the pulmonary capillaries in man. *Scandinavian Journal of Haematology* **21**, 369–375 (1978).

94. Zucker-Franklin, D. & Philipp, C. S. Platelet production in the pulmonary capillary bed: new ultrastructural evidence for an old concept. *The American Journal of Pathology* **157**, 69–74 (2000).

95. Sharma, G. K. & Talbot, I. C. Pulmonary megakaryocytes: ‘missing link’ between cardiovascular and respiratory disease? *Journal of Clinical Pathology* **39**, 969–976 (1986).

96. Slater, D. N., Trowbridge, E. A. & Martin, J. F. The megakaryocyte in thrombocytopenia: a microscopic study which supports the theory that platelets are produced in the pulmonary circulation. *Thrombosis Research* **31**, 163–176 (1983).

97. Dhanjal, T. S. *et al.* A novel role for PECAM-1 in megakaryocytokinesis and recovery of platelet counts in thrombocytopenic mice. *Blood* **109**, 4237–4244 (2007).

98. Kacena, M. A., Gundberg, C. M. & Horowitz, M. C. A reciprocal regulatory interaction between megakaryocytes, bone cells, and hematopoietic stem cells. *Bone* **39**, 978–984 (2006).

99. Avecilla, S. T. *et al.* Chemokine-mediated interaction of hematopoietic progenitors with the bone marrow vascular niche is required for thrombopoiesis. *Nature Medicine* **10**, 64–71 (2004).

100. Rafii, S. *et al.* Human bone marrow microvascular endothelial cells support long-term proliferation and differentiation of myeloid and megakaryocytic progenitors. *Blood* **86**, 3353–3363 (1995).

101. Ciovacco, W. A., Cheng, Y.-H., Horowitz, M. C. & Kacena, M. A. Immature and mature megakaryocytes enhance osteoblast proliferation and inhibit osteoclast formation. *Journal of Cellular Biochemistry* **109**, 774–781 (2010).

102. Lemieux, J. M., Horowitz, M. C. & Kacena, M. A. Involvement of integrins alpha(3)beta(1) and alpha(5)beta(1) and glycoprotein IIb in megakaryocyte-induced osteoblast proliferation. *Journal of Cellular Biochemistry* **109**, 927–932 (2010).

103. Kacena, M. A. *et al.* Megakaryocyte-mediated inhibition of osteoclast development. *Bone* **39**, 991–999 (2006).

104. Wang, J. F., Liu, Z. Y. & Groopman, J. E. The alpha-chemokine receptor CXCR4 is expressed on the megakaryocytic lineage from progenitor to platelets and modulates migration and adhesion. *Blood* **92**, 756–764 (1998).

105. Hamada, T. *et al.* Transendothelial migration of megakaryocytes in response to stromal cell-derived factor 1 (SDF-1) enhances platelet formation. *The Journal of Experimental Medicine* **188**, 539–548 (1998).

106. Malara, A. *et al.* The secret life of a megakaryocyte: emerging roles in bone marrow homeostasis control. *Cellular and molecular life sciences : CMLS* **72**, 1517–1536 (2015).

107. Campbell, R. A. *et al.* Human megakaryocytes possess intrinsic anti-viral immunity through regulated induction of IFITM3. *Blood* blood-2018-09-873984 (2019) doi:10.1182/blood-2018-09-873984.

108. Middleton, E. A., Weyrich, A. S. & Zimmerman, G. A. Platelets in Pulmonary Immune Responses and Inflammatory Lung Diseases. *Physiological Reviews* **96**, 1211–1259 (2016).

109. Koupenova Milka, Clancy Lauren, Corkrey Heather A., & Freedman Jane E. Circulating Platelets as Mediators of Immunity, Inflammation, and Thrombosis. *Circulation Research* **122**, 337–351 (2018).

110. Semple, J. W., Italiano, J. E. & Freedman, J. Platelets and the immune continuum. *Nature Reviews Immunology* **11**, 264–274 (2011).

111. Freishtat, R. J. *et al.* Sepsis Alters the Megakaryocyte–Platelet Transcriptional Axis Resulting in Granzyme B–mediated Lymphotoxicity. *American Journal of Respiratory and Critical Care Medicine* **179**, 467–473 (2009).

112. Frydman, G. H. *et al.* Megakaryocytes contain extranuclear histones and may be a source of platelet-associated histones during sepsis. *Scientific Reports* **10**, 4621 (2020).

113. Boilard, E. & Flamand, L. The role of the megakaryocyte in immunity has gone viral. *Blood* **133**, 2001–2002 (2019).

114. Zhou, Y. *et al.* Megakaryocytes participate in the occurrence of bleomycin-induced pulmonary fibrosis. *Cell Death & Disease* **10**, 1–14 (2019).

115. Mikkola, H. K. A., Fujiwara, Y., Schlaeger, T. M., Traver, D. & Orkin, S. H. Expression of CD41 marks the initiation of definitive hematopoiesis in the mouse embryo. *Blood* **101**, 508–516 (2003).

116. Mitjavila-Garcia, M. T. *et al.* Expression of CD41 on hematopoietic progenitors derived from embryonic hematopoietic cells. *Development* **129**, 2003–2013 (2002).

117. Rybtsov, S. *et al.* Tracing the Origin of the HSC Hierarchy Reveals an SCF-Dependent, IL-3-Independent CD43− Embryonic Precursor. *Stem Cell Reports* **3**, 489–501 (2014).

118. Nagy, Z. *et al.* The Gp1ba-Cre transgenic mouse: a new model to delineate platelet and leukocyte functions. *Blood* **133**, 331–343 (2019).

119. Gollomp, K. & Poncz, M. Gp1ba-Cre or Pf4-Cre: pick your poison. *Blood* **133**, 287–288 (2019).

120. Murphy, G. J. & Leavitt, A. D. A model for studying megakaryocyte development and biology. *Proceedings of the National Academy of Sciences* **96**, 3065–3070 (1999).

121. Mikkola, H. K. A. & Orkin, S. H. The journey of developing hematopoietic stem cells. *Development* **133**, 3733–3744 (2006).

122. Levine, R. F., Hazzard, K. C. & Lamberg, J. D. The significance of megakaryocyte size. *Blood* **60**, 1122–1131 (1982).

123. Lo Celso, C. & Scadden, D. Isolation and Transplantation of Hematopoietic Stem Cells (HSCs). *Journal of Visualized Experiments : JoVE* (2007) doi:10.3791/157.

124. Vijey, P., Posorske, B. & Machlus, K. R. In vitro culture of murine megakaryocytes from fetal liver-derived hematopoietic stem cells. *Platelets* **29**, 583–588 (2018).

125. Smith, B. W. *et al.* The aryl hydrocarbon receptor directs hematopoietic progenitor cell expansion and differentiation. *Blood* **122**, 376–385 (2013).

126. Stuart, T. *et al.* Comprehensive Integration of Single-Cell Data. *Cell* **177**, 1888-1902.e21 (2019).

127. Hafemeister, C. & Satija, R. Normalization and variance stabilization of single-cell RNA-seq data using regularized negative binomial regression. *Genome Biology* **20**, 296 (2019).

128. McInnes, L., Healy, J. & Melville, J. UMAP: Uniform Manifold Approximation and Projection for Dimension Reduction. *arXiv:1802.03426 [cs, stat]* (2018).

129. Blondel, V. D., Guillaume, J.-L., Lambiotte, R. & Lefebvre, E. Fast unfolding of communities in large networks. *Journal of Statistical Mechanics: Theory and Experiment* **2008**, P10008 (2008).

130. Tirosh, I. *et al.* Dissecting the multicellular ecosystem of metastatic melanoma by single-cell RNA-seq. *Science* **352**, 189–196 (2016).

131. Popescu, D.-M. *et al.* Decoding human fetal liver haematopoiesis. *Nature* **574**, 365–371 (2019).

132. Bourgon, R., Gentleman, R. & Huber, W. Independent filtering increases detection power for high-throughput experiments. *Proceedings of the National Academy of Sciences* **107**, 9546–9551 (2010).

133. Finak, G. *et al.* MAST: a flexible statistical framework for assessing transcriptional changes and characterizing heterogeneity in single-cell RNA sequencing data. *Genome Biology* **16**, 278 (2015).

134. Soneson, C. & Robinson, M. D. Bias, robustness and scalability in single-cell differential expression analysis. *Nature Methods* **15**, 255–261 (2018).

135. Kuleshov, M. V. *et al.* Enrichr: a comprehensive gene set enrichment analysis web server 2016 update. *Nucleic Acids Research* **44**, W90-97 (2016).

136. Chen, E. Y. *et al.* Enrichr: interactive and collaborative HTML5 gene list enrichment analysis tool. *BMC bioinformatics* **14**, 128 (2013).

137. McGowan, S. E. The Formation of Pulmonary Alveoli. in *The Lung* 65–84 (Elsevier, 2014). doi:10.1016/B978-0-12-799941-8.00004-3.

138. Orkin, S. H. & Zon, L. I. Hematopoiesis: An Evolving Paradigm for Stem Cell Biology. *Cell* **132**, 631–644 (2008).

139. Herriges, M. & Morrisey, E. E. Lung development: orchestrating the generation and regeneration of a complex organ. *Development (Cambridge, England)* **141**, 502–513 (2014).

140. Robin, C., Ottersbach, K., Boisset, J.-C., Oziemlak, A. & Dzierzak, E. CD41 is developmentally regulated and differentially expressed on mouse hematopoietic stem cells. *Blood* **117**, 5088–5091 (2011).

141. Seo, H. *et al.* A β1-tubulin–based megakaryocyte maturation reporter system identifies novel drugs that promote platelet production. *Blood Advances* **2**, 2262–2272 (2018).

142. Tomer, A. Human marrow megakaryocyte differentiation: multiparameter correlative analysis identifies von Willebrand factor as a sensitive and distinctive marker for early (2N and 4N) megakaryocytes. *Blood* **104**, 2722–2727 (2004).

143. Sim, X. *et al.* Identifying and enriching platelet-producing human stem cell–derived megakaryocytes using factor V uptake. *Blood* **130**, 192–204 (2017).

144. Zhu, F. *et al.* Screening for genes that regulate the differentiation of human megakaryocytic lineage cells. *Proceedings of the National Academy of Sciences* **115**, E9308–E9316 (2018).

145. Seita, J. *et al.* Gene Expression Commons: an open platform for absolute gene expression profiling. *PloS One* **7**, e40321 (2012).

146. Weinreb, C., Wolock, S. & Klein, A. M. SPRING: a kinetic interface for visualizing high dimensional single-cell expression data. *Bioinformatics* **34**, 1246–1248 (2018).

147. Choudry, F. A. *et al.* Single cell transcriptional characterization of human megakaryocyte lineage commitment and maturation. *bioRxiv* 2020.02.20.957936 (2020) doi:10.1101/2020.02.20.957936.

148. Coppinger, J. A. *et al.* Characterization of the proteins released from activated platelets leads to localization of novel platelet proteins in human atherosclerotic lesions. *Blood* **103**, 2096–2104 (2004).

149. De Jong, J. S. M. & Dekker, L. R. C. M. Platelets and Cardiac Arrhythmia. *Frontiers in Physiology* **1**, (2010).

150. Jenne, C. N., Urrutia, R. & Kubes, P. Platelets: bridging hemostasis, inflammation, and immunity. *International Journal of Laboratory Hematology* **35**, 254–261 (2013).

151. Miller, A. J. *et al.* Basal stem cell fate specification is mediated by SMAD signaling in the developing human lung. *bioRxiv* 461103 (2018) doi:10.1101/461103.

152. Epaud, R. *et al.* Knockout of Insulin-Like Growth Factor-1 Receptor Impairs Distal Lung Morphogenesis. *PLOS ONE* **7**, e48071 (2012).

153. Gläser, S. *et al.* Association between Serum Insulin-Like Growth Factor (IGF) I and IGF Binding Protein-3 and Lung Function. *The Journal of Clinical Endocrinology & Metabolism* **94**, 2452–2458 (2009).

154. Machlus, K. R., Thon, J. N. & Italiano, J. E. Interpreting the developmental dance of the megakaryocyte: a review of the cellular and molecular processes mediating platelet formation. *British Journal of Haematology* **165**, 227–236 (2014).

155. Noetzli Leila J., French Shauna L., & Machlus Kellie R. New Insights Into the Differentiation of Megakaryocytes From Hematopoietic Progenitors. *Arteriosclerosis, Thrombosis, and Vascular Biology* **39**, 1288–1300 (2019).

156. Levin, J. *et al.* Pathophysiology of Thrombocytopenia and Anemia in Mice Lacking Transcription Factor NF-E2. *Blood* **94**, 3037–3047 (1999).

157. Shivdasani, R. A., Zucker-Franklin, D., Jackson, C. W., Hunt, P. & Orkint, S. H. Transcription Factor NF-E2 Is Required for Platelet Formation Independent of the Actions of Thrombopoietin/ MGDF in Megakaryocyte Development. 10.

158. Kuvardina, O. N. *et al.* RUNX1 represses the erythroid gene expression program during megakaryocytic differentiation. *Blood* **125**, 3570–3579 (2015).

159. Zimmet, J. & Ravid, K. Polyploidy: Occurrence in nature, mechanisms, and significance for the megakaryocyte-platelet system. *Experimental Hematology* **28**, 3–16 (2000).

160. Ito, Y. *et al.* Turbulence Activates Platelet Biogenesis to Enable Clinical Scale Ex Vivo Production. *Cell* **174**, 636-648.e18 (2018).

161. Wendel, D. P., Taylor, D. G., Albertine, K. H., Keating, M. T. & Li, D. Y. Impaired distal airway development in mice lacking elastin. *American Journal of Respiratory Cell and Molecular Biology* **23**, 320–326 (2000).

162. Boström, H. *et al.* PDGF-A signaling is a critical event in lung alveolar myofibroblast development and alveogenesis. *Cell* **85**, 863–873 (1996).

163. Bartram, U. & Speer, C. P. The Role of Transforming Growth Factor β in Lung Development and Disease. *CHEST* **125**, 754–765 (2004).

164. Hakuno, F. & Takahashi, S.-I. 40 YEARS OF IGF1: IGF1 receptor signaling pathways. *Journal of Molecular Endocrinology* **61**, T69–T86 (2018).

165. Roback, E. W. *et al.* An infant with deletion of the distal long arm of chromosome 15 (q26.1→qter) and loss of insulin-like growth factor 1 receptor gene. *American Journal of Medical Genetics* **38**, 74–79 (1991).

166. Woods, K. A., Camacho-Hübner, C., Savage, M. O. & Clark, A. J. L. Intrauterine Growth Retardation and Postnatal Growth Failure Associated with Deletion of the Insulin-Like Growth Factor I Gene. *New England Journal of Medicine* **335**, 1363–1367 (1996).

167. Zhou, Y.-Q. *et al.* Assessment of flow distribution in the mouse fetal circulation at late gestation by high-frequency Doppler ultrasound. *Physiological Genomics* **46**, 602–614 (2014).

168. Perez-Muñoz, M. E., Arrieta, M.-C., Ramer-Tait, A. E. & Walter, J. A critical assessment of the "sterile womb" and "in utero colonization" hypotheses: implications for research on the pioneer infant microbiome. *Microbiome* **5**, (2017).

169. de Goffau, M. C. *et al.* Human placenta has no microbiome but can contain potential pathogens. *Nature* **572**, 329–334 (2019).

170. Pariser, D. N. *et al.* Lung megakaryocytes are immune modulatory cells. *The Journal of Clinical Investigation* (2020) doi:10.1172/JCI137377.

171. Crooks, M. G., Fahim, A., Naseem, K. M., Morice, A. H. & Hart, S. P. Increased Platelet Reactivity in Idiopathic Pulmonary Fibrosis Is Mediated by a Plasma Factor. *PLoS ONE* **9**, (2014).

172. Yadav, H. & Kor, D. J. Platelets in the pathogenesis of acute respiratory distress syndrome. *American Journal of Physiology - Lung Cellular and Molecular Physiology* **309**, L915–L923 (2015).

173. Liu, L., Lin, F., Ma, X., Chen, Z. & Yu, J. Tumor-educated platelet as liquid biopsy in lung cancer patients. *Critical Reviews in Oncology/Hematology* 102863 (2020) doi:10.1016/j.critrevonc.2020.102863.

174. Zheng, W., Zhang, H., Zhao, D., Zhang, J. & Pollard, J. W. Lung Mammary Metastases but Not Primary Tumors Induce Accumulation of Atypical Large Platelets and Their Chemokine Expression. *Cell Reports* **29**, 1747-1755.e4 (2019).

175. Oxley, T. J. *et al.* Large-Vessel Stroke as a Presenting Feature of Covid-19 in the Young. *New England Journal of Medicine* **0**, e60 (2020).

176. Zhang, Y. *et al.* Coagulopathy and Antiphospholipid Antibodies in Patients with Covid-19. *New England Journal of Medicine* **382**, e38 (2020).

177. Helms, J. *et al.* Neurologic Features in Severe SARS-CoV-2 Infection. *New England Journal of Medicine* **0**, null (2020).

178. Li, H. *et al.* SARS-CoV-2 and viral sepsis: observations and hypotheses. *The Lancet* **395**, 1517–1520 (2020).

179. Xiang-hua, Y. *et al.* Severe Acute Respiratory Syndrome and Venous Thromboembolism in Multiple Organs. *American Journal of Respiratory and Critical Care Medicine* **182**, 436–437 (2010).

180. Oudkerk, M. *et al.* Diagnosis, Prevention, and Treatment of Thromboembolic Complications in COVID-19: Report of the National Institute for Public Health of the Netherlands. *Radiology* 201629 (2020) doi:10.1148/radiol.2020201629.

181. Rapkiewicz, A. V. *et al.* Megakaryocytes and platelet-fibrin thrombi characterize multi-organ thrombosis at autopsy in COVID-19: A case series. *EClinicalMedicine* **0**, (2020).

182. A, N. D.-N. *et al.* Pulmonary and systemic involvement of COVID-19 assessed by ultrasound-guided minimally invasive autopsy. *Histopathology* (2020) doi:10.1111/his.14160.

183. Wu, Y. & Hirschi, K. K. Regulation of Hemogenic Endothelial Cell Development and Function. *Annual Review of Physiology* **83**, 17–37 (2021).

184. Tavian, M. *et al.* Aorta-Associated CD34+ Hematopoietic Cells in the Early Human Embryo. 6.

185. Lange, L., Morgan, M. & Schambach, A. The hemogenic endothelium: a critical source for the generation of PSC-derived hematopoietic stem and progenitor cells. *Cellular and Molecular Life Sciences* (2021) doi:10.1007/s00018-021-03777-y.

186. Li, W., Ferkowicz, M. J., Johnson, S. A., Shelley, W. C. & Yoder, M. C. Endothelial cells in the early murine yolk sac give rise to CD41-expressing hematopoietic cells. *Stem Cells and Development* **14**, 44–54 (2005).

187. Chen, M. J., Yokomizo, T., Zeigler, B., Dzierzak, E. & Speck, N. A. Runx1 is required for the endothelial to hematopoietic cell transition but not thereafter. *Nature* **457**, 887–891 (2009).

188. Rhodes, K. E. *et al.* The Emergence of Hematopoietic Stem Cells is Initiated in the Placental Vasculature in the Absence of Circulation. *Cell stem cell* **2**, 252–263 (2008).

189. Yzaguirre, A. D. & Speck, N. A. Insights into blood cell formation from hemogenic endothelium in lesser-known anatomic sites. *Developmental Dynamics* **245**, 1011–1028 (2016).

190. Li, Z. *et al.* Mouse Embryonic Head as a Site for Hematopoietic Stem Cell Development. *Cell Stem Cell* **11**, 663–675 (2012).

191. Yvernogeau, L. *et al.* In vivo generation of haematopoietic stem/progenitor cells from bone marrow-derived haemogenic endothelium. *Nature Cell Biology* **21**, 1334–1345 (2019).

192. Summer, R. *et al.* Embryonic Lung Side Population Cells Are Hematopoietic and Vascular Precursors. *American Journal of Respiratory Cell and Molecular Biology* **33**, 32–40 (2005).

193. Lundin, V. *et al.* YAP Regulates Hematopoietic Stem Cell Formation in Response to the Biomechanical Forces of Blood Flow. *Developmental Cell* **52**, 446-460.e5 (2020).

194. Niblock, M. M. *et al.* In utero development of fetal breathing movements in C57BL6 mice. *Respiratory Physiology & Neurobiology* **271**, 103288 (2020).

195. Tang, Z. *et al.* Mechanical Forces Program the Orientation of Cell Division during Airway Tube Morphogenesis. *Developmental Cell* **44**, 313-325.e5 (2018).

196. Li, J. *et al.* The Strength of Mechanical Forces Determines the Differentiation of Alveolar Epithelial Cells. *Developmental Cell* **44**, 297-312.e5 (2018).

197. Canu, G. & Ruhrberg, C. First blood: the endothelial origins of hematopoietic progenitors. *Angiogenesis* **24**, 199–211 (2021).

198. Souilhol, C. *et al.* Inductive interactions mediated by interplay of asymmetric signalling underlie development of adult haematopoietic stem cells. *Nature Communications* **7**, 10784 (2016).

199. Kaminow, B., Yunusov, D. & Dobin, A. *STARsolo: accurate, fast and versatile mapping/quantification of single-cell and single-nucleus RNA-seq data*. http://biorxiv.org/lookup/doi/10.1101/2021.05.05.442755 (2021) doi:10.1101/2021.05.05.442755.

200. Leung, A. *et al.* Notch and Aryl Hydrocarbon Receptor Signaling Impact Definitive Hematopoiesis from Human Pluripotent Stem Cells: Definitive Hematopoiesis in Pluripotent Stem Cells. *STEM CELLS* **36**, 1004–1019 (2018).

201. Yvernogeau, L. *et al.* An in vitro model of hemogenic endothelium commitment and hematopoietic production. *Development* **143**, 1302–1312 (2016).

202. Ohta, R., Sugimura, R., Niwa, A. & Saito, M. K. Hemogenic Endothelium Differentiation from Human Pluripotent Stem Cells in A Feeder- and Xeno-free Defined Condition. *JoVE (Journal of Visualized Experiments)* e59823 (2019) doi:10.3791/59823.

203. Boisset, J.-C. *et al.* In vivo imaging of haematopoietic cells emerging from the mouse aortic endothelium. *Nature* **464**, 116–120 (2010).

204. Eilken, H. M., Nishikawa, S.-I. & Schroeder, T. Continuous single-cell imaging of blood generation from haemogenic endothelium. *Nature* **457**, 896–900 (2009).

205. Taoudi, S. *et al.* Extensive Hematopoietic Stem Cell Generation in the AGM Region via Maturation of VE-Cadherin+CD45+ Pre-Definitive HSCs. *Cell Stem Cell* **3**, 99–108 (2008).

206. Fantin, A. *et al.* KIT Is Required for Fetal Liver Hematopoiesis. *Frontiers in Cell and Developmental Biology* **9**, (2021).

207. Ottersbach, K. Endothelial-to-haematopoietic transition: an update on the process of making blood. *Biochemical Society Transactions* **47**, 591–601 (2019).

208. Oatley, M. *et al.* Single-cell transcriptomics identifies CD44 as a marker and regulator of endothelial to haematopoietic transition. *Nature Communications* **11**, 1–18 (2020).

209. Fidanza, A. *et al.* Single-cell analyses and machine learning define hematopoietic progenitor and HSC-like cells derived from human PSCs. *Blood* **136**, 2893–2904 (2020).

210. Kumano, K. *et al.* Notch1 but Not Notch2 Is Essential for Generating Hematopoietic Stem Cells from Endothelial Cells. *Immunity* **18**, 699–711 (2003).

211. Vargel, Ö. *et al.* Activation of the TGFβ pathway impairs endothelial to haematopoietic transition. *Scientific Reports* **6**, 21518 (2016).

212. Lee, L. K. *et al.* LYVE1 Marks the Divergence of Yolk Sac Definitive Hemogenic Endothelium from the Primitive Erythroid Lineage. *Cell reports* **17**, 2286–2298 (2016).

213. Guiu, J. *et al.* Identification of Cdca7 as a novel Notch transcriptional target involved in hematopoietic stem cell emergence. *Journal of Experimental Medicine* **211**, 2411–2423 (2014).

214. Greig, K. T., Carotta, S. & Nutt, S. L. Critical roles for c-Myb in hematopoietic progenitor cells. *Seminars in Immunology* **20**, 247–256 (2008).

215. Lancrin, C. *et al.* GFI1 and GFI1B control the loss of endothelial identity of hemogenic endothelium during hematopoietic commitment. *Blood* **120**, 314–322 (2012).

216. Vodyanik, M. A., Thomson, J. A. & Slukvin, I. I. Leukosialin (CD43) defines hematopoietic progenitors in human embryonic stem cell differentiation cultures. *Blood* **108**, 2095–2105 (2006).

217. Lie-A-Ling, M. *et al.* RUNX1 positively regulates a cell adhesion and migration program in murine hemogenic endothelium prior to blood emergence. *Blood* **124**, e11–e20 (2014).

218. Hadland, B. K. *et al.* Endothelium and NOTCH specify and amplify aorta-gonad-mesonephros–derived hematopoietic stem cells. *The Journal of Clinical Investigation* **125**, 2032–2045 (2015).

219. Zhang, C. *et al.* Inhibition of endothelial ERK signalling by Smad1/5 is essential for haematopoietic stem cell emergence. *Nature Communications* **5**, 3431 (2014).

220. Monteiro, R. *et al.* Transforming Growth Factor β Drives Hemogenic Endothelium Programming and the Transition to Hematopoietic Stem Cells. *Developmental Cell* **38**, 358–370 (2016).

221. McGarvey, A. C. *et al.* A molecular roadmap of the AGM region reveals BMPER as a novel regulator of HSC maturation. *Journal of Experimental Medicine* **214**, 3731–3751 (2017).

222. Wang, C. *et al.* TGFβ inhibition enhances the generation of hematopoietic progenitors from human ES cell-derived hemogenic endothelial cells using a stepwise strategy. *Cell Research* **22**, 194–207 (2012).

223. Pariser, D. N. *et al.* Lung megakaryocytes are immune modulatory cells. https://www.jci.org/articles/view/137377/pdf (2020) doi:10.1172/JCI137377.

224. Yeung, A. K., Villacorta-Martin, C., Hon, S., Rock, J. R. & Murphy, G. J. Lung megakaryocytes display distinct transcriptional and phenotypic properties. *Blood Advances* **4**, 6204–6217 (2020).

225. Neo, W. H., Lie-A-Ling, M., Fadlullah, M. Z. H. & Lacaud, G. Contributions of Embryonic HSC-Independent Hematopoiesis to Organogenesis and the Adult Hematopoietic System. *Frontiers in Cell and Developmental Biology* **9**, (2021).

226. Bertozzi, C. C. *et al.* Platelets regulate lymphatic vascular development through CLEC-2–SLP-76 signaling. *Blood* **116**, 661–670 (2010).

227. Battinelli, E. M. 24 - The Role of Platelets in Angiogenesis. in *Platelets (Fourth Edition)* (ed. Michelson, A. D.) 433–441 (Academic Press, 2019). doi:10.1016/B978-0-12-813456-6.00024-2.

228. Liang, G. *et al.* De novo generation of macrophage from placenta-derived hemogenic endothelium. *Developmental Cell* **56**, 2121-2133.e6 (2021).

229. Chen, M. J. *et al.* Erythroid/Myeloid Progenitors and Hematopoietic Stem Cells Originate from Distinct Populations of Endothelial Cells. *Cell Stem Cell* **9**, 541–552 (2011).

230. Dignum, T. *et al.* Multipotent progenitors and hematopoietic stem cells arise independently from hemogenic endothelium in the mouse embryo. *Cell Reports* **36**, 109675 (2021).

231. Dzierzak, E. & Bigas, A. Blood Development: Hematopoietic Stem Cell Dependence and Independence. *Cell Stem Cell* **22**, 639–651 (2018).

232. Frame, J. M., McGrath, K. E. & Palis, J. Erythro-Myeloid Progenitors: “definitive” hematopoiesis in the conceptus prior to the emergence of hematopoietic stem cells. *Blood cells, molecules & diseases* **51**, 10.1016/j.bcmd.2013.09.006 (2013).

233. Ghosn, E., Yoshimoto, M., Nakauchi, H., Weissman, I. L. & Herzenberg, L. A. Hematopoietic stem cell-independent hematopoiesis and the origins of innate-like B lymphocytes. *Development* **146**, dev170571 (2019).

234. Soares-da-Silva, F. *et al.* Yolk sac, but not hematopoietic stem cell–derived progenitors, sustain erythropoiesis throughout murine embryonic life. *Journal of Experimental Medicine* **218**, (2021).

235. Busch, K. *et al.* Fundamental properties of unperturbed haematopoiesis from stem cells in vivo. *Nature* **518**, 542–546 (2015).

236. Beaudin, A. E. *et al.* A transient developmental hematopoietic stem cell gives rise to innate-like B and T cells. *Cell stem cell* **19**, 768–783 (2016).

237. Waas, B. & Maillard, I. Fetal hematopoietic stem cells are making waves. *Stem Cell Investigation* **4**, 25 (2017).

238. Taoudi, S. & Medvinsky, A. Functional identification of the hematopoietic stem cell niche in the ventral domain of the embryonic dorsal aorta. *Proceedings of the National Academy of Sciences of the United States of America* **104**, 9399–9403 (2007).

239. Rybtsov, S. *et al.* Hierarchical organization and early hematopoietic specification of the developing HSC lineage in the AGM region. *Journal of Experimental Medicine* **208**, 1305–1315 (2011).

240. Rodriguez-Fraticelli, A. E. *et al.* Clonal analysis of lineage fate in native haematopoiesis. *Nature* **553**, 212–216 (2018).

241. Joseph, C. *et al.* Deciphering Hematopoietic Stem Cells in Their Niches: A Critical Appraisal of Genetic Models, Lineage Tracing, and Imaging Strategies. *Cell Stem Cell* **13**, 520–533 (2013).

242. Wright, D. E., Wagers, A. J., Gulati, A. P., Johnson, F. L. & Weissman, I. L. Physiological migration of hematopoietic stem and progenitor cells. *Science (New York, N.Y.)* **294**, 1933–1936 (2001).

243. de Pater, E. *et al.* Gata2 is required for HSC generation and survival. *Journal of Experimental Medicine* **210**, 2843–2850 (2013).

244. Kang, H. *et al.* GATA2 Is Dispensable for Specification of Hemogenic Endothelium but Promotes Endothelial-to-Hematopoietic Transition. *Stem Cell Reports* **11**, 197–211 (2018).

245. Bowling, S. *et al.* An Engineered CRISPR-Cas9 Mouse Line for Simultaneous Readout of Lineage Histories and Gene Expression Profiles in Single Cells. *Cell* **181**, 1410-1422.e27 (2020).

246. Smith, B. W. & Murphy, G. J. Stem cells, megakaryocytes, and platelets: *Current Opinion in Hematology* **21**, 430–437 (2014).

247. Nakamura, S. *et al.* Expandable Megakaryocyte Cell Lines Enable Clinically Applicable Generation of Platelets from Human Induced Pluripotent Stem Cells. *Cell Stem Cell* **14**, 535–548 (2014).

248. Patel, S. R., Hartwig, J. H. & Italiano, J. E. The biogenesis of platelets from megakaryocyte proplatelets. *Journal of Clinical Investigation* **115**, 3348–3354 (2005).

249. Zhao, X. *et al. Platelet generation from circulating megakaryocytes is triggered in the lung vasculature*. 2021.11.01.466743 https://www.biorxiv.org/content/10.1101/2021.11.01.466743v1 (2021) doi:10.1101/2021.11.01.466743.

[redacted]

[redacted]

[redacted]

[redacted]

[redacted]